Analytical Pyrolysis

Edited by Peter Kusch

Analytical Pyrolysis

Edited by Peter Kusch

IntechOpen

Supporting open minds since 2005

Notice
Statements and opinions expressed in the chapters are these of the individual contributors and not necessarily those of the editors or publisher. No responsibility is accepted for the accuracy of information contained in the published chapters. The publisher assumes no responsibility for any damage or injury to persons or property arising out of the use of any materials, instructions, methods or ideas contained in the book.

We are IntechOpen,
the world's leading publisher of Open Access books
Built by scientists, for scientists

4,000+
Open access books available

116,000+
International authors and editors

120M+
Downloads

151
Countries delivered to

Our authors are among the
Top 1%
most cited scientists

12.2%
Contributors from top 500 universities

Interested in publishing with us?
Contact book.department@intechopen.com

Numbers displayed above are based on latest data collected.
For more information visit www.intechopen.com

Meet the editor

Dr. Peter Kusch studied chemistry at the Pedagogical University in Opole and received a doctorate in Organic Chemical Technology at the Poznań University of Technology, Poland. From 1977 to 1988 he worked as an analytical chemist and adjunct at the Institute of Heavy Organic Synthesis "Blachownia" (Kędzierzyn-Koźle, Poland). After moving with his family to Germany, he worked for several years in the Fischer Labor- und Verfahrenstechnik GmbH company (Meckenheim/Bonn, Germany) as a laboratory manager and specialist in analytical pyrolysis and gas chromatography. Since 1998 until his retirement in 2018 he was a scientific coworker at the Department of Applied Natural Sciences of the Bonn-Rhein-Sieg University of Applied Sciences in Rheinbach, Germany. He has been author/coauthor of over 90 scientific publications, one book, 13 invited book chapters, and 11 patents in the area of chromatography, mass spectrometry, analytical pyrolysis, and chemical technology. Dr. Kusch is a reviewer for several international journals in the area of analytical chemistry. He is the Editorial Board Member of the journals *Polymer Testing* and *Heliyon* (Elsevier).

Contents

Preface

The word *pyrolysis*, translated from the original Greek *pyros = fire* and *lyso = decomposition*, means a chemical transformation of a sample when heated at a temperature higher than ambient in an inert atmosphere in the absence of oxygen. Pyrolysis can be divided into two types: applied pyrolysis and analytical pyrolysis. Applied pyrolysis is concerned with the production of chemicals. When performed on a large scale, pyrolysis is involved in industrial processes such as the manufacture of coke from coal and the conversion of biomass into biofuels. In contrast, analytical pyrolysis is a laboratory procedure in which small amounts of organic materials undergo thermal treatment. Analytical pyrolysis deals with the structural identification and quantitation of pyrolysis products with the ultimate aim of establishing the identity of the original material and the mechanisms of its thermal decomposition. Pyrolysis temperatures of 550–1400°C are high enough to break molecular bonds in macromolecules, thereby forming smaller, simpler volatile compounds. The pyrolytic process is carried out in a pyrolysis unit (pyrolyzer) interfaced with analytical instrumentation such as gas chromatography (GC), mass spectrometry (MS), gas chromatography coupled with mass spectrometry (GC/MS), or with Fourier-transform infrared spectroscopy (GC/FTIR). By measurement and identification of the pyrolysis products with the help of these techniques, the molecular composition of the original sample can often be reconstructed.

Applications of analytical pyrolysis range from research and development of new materials, characterization and competitor product evaluation, medicine, biology and biotechnology, geology, airspace, environmental analysis (microplastics) for forensic purposes or conservation, and restoration of cultural heritage. These applications cover analysis and identification of synthetic polymers/copolymers and biopolymers. Analytical pyrolysis allows the confirmation of the source of a failed product, the identification of contaminants causing failure, competitive analysis, as well as overcoming a problem in product development or quality control. This technique is often used for wood studies due to its ability to provide details of the molecular structure of lignocellulose.

This book is the outcome of contributions by experts in the field of pyrolysis. Chapters 1 and 2 include applications of analytical pyrolysis coupled with MS to characterize the structure of synthetic organic polymers and lignocellulosic materials as well as cellulosic pulps and isolated lignins. In Chapter 3 the pyrolysis characteristics of solid wood, waste particle board, and bio-oil are investigated. The pyrolysis products were identified by GC/MS. Chapter 4 presents a thermal degradation study of cellulose and biomass, examined by scanning electron micrography, FTIR spectroscopy, thermogravimetry, differential thermal analysis, and TG/MS. Finally, Chapter 5 describes the calorimetric determination of high heating values of different raw biomass, plastic waste, and biomass-plastic waste mixtures and their by-products resulting from pyrolysis.

The editor would like to thank all the authors of these chapters for their contribution and commitment, which made the publication of this book possible. All the help and advice from Ms. Dolores Kuzelj, the Author Service Manager, is also gratefully acknowledged.

Dr. Peter Kusch
Department of Applied Natural Sciences,
Bonn-Rhein-Sieg University of Applied Sciences,
Rheinbach, Germany

Section 1

Pyrolysis - GC/MS(FID)

Chapter 1

Introductory Chapter: Analytical Pyrolysis-Gas Chromatography/ Mass Spectrometry of Polymeric Materials

Peter Kusch

1. Analytical pyrolysis

According to the International Union of Pure and Applied Chemistry (IUPAC) recommendation, analytical pyrolysis (Py) is defined as the characterization in an inert atmosphere of a material or a chemical process by a chemical degradation reaction(s) induced by thermal energy [1]. Thermal degradation under controlled conditions is often used as a part of an analytical procedure, either to render a sample into a suitable form for subsequent analysis by gas chromatography (GC), mass spectrometry (MS), gas chromatography coupled with the mass spectrometry (GC/ MS), with the Fourier-transform infrared spectroscopy (GC/FTIR), or by direct monitoring as an analytical technique in its own right [2]. Analytical pyrolysis deals with the structural identification and quantitation of pyrolysis products with the ultimate aim of establishing the identity of the original material and the mechanisms of its thermal decomposition. The pyrolysis temperatures of 550–1400°C are high enough to actually break molecular bonds in the molecules of the solid sample, thereby forming smaller, simpler volatile compounds. Depending on the amount of energy supplied, the bonds in each molecule break in a predictable manner [3]. By the measurement and identification of the fragments, the molecular composition of the original sample can often be reconstructed [4].

Analytical pyrolysis technique hyphenated to GC/MS has extended the range of possible tools for the characterization of synthetic polymers and copolymers. This technique has been used extensively over the last 30 years as a complementary analytical tool used to characterize the structure of synthetic organic polymers and copolymers, polymer blends, biopolymers, and natural resins. Pyrolysis-GC/MS is a destructive analytical technique. Typical fields of interest and application are polymer identification by comparison of pyrograms and mass spectra with known references, qualitative analysis and structural characterization of copolymers, determination of the microstructure of polymers, determination of the polymers steric structure, investigation of thermal stability of polymers and copolymers, determination of residual monomers and solvents, volatile organic compounds (VOCs) as well as additives in polymers [5].

Pyrolysis method allows for the direct analysis of very small solid or liquid polymer/copolymer sample amounts (5–200 μg) and eliminates the need for time-consuming sample preparation (pretreatment) by performing analyses directly on the sample. The essential requirements for the apparatus in analytical pyrolysis are reproducibility of the pyrolysis temperature, rapid temperature rise, and accurate

temperature control. Depending upon the heating mechanism, pyrolysis systems have been classified into two groups: the continuous-mode pyrolyzer (furnace pyrolyzer) and pulse-mode pyrolyzer (flash pyrolyzer), such as the heated filament, Curie-point, and laser pyrolyzer. The pyrolysis unit (pyrolyzer) is connected directly to the injector port of a gas chromatograph.

Once the polymer/copolymer sample has been pyrolyzed, volatile fragments are swept from the heated pyrolysis unit by the carrier gas (helium) into the gas chromatograph. The volatile pyrolysis products (pyrolyzate) are chromatographically separated by using a fused silica capillary column, according to the boiling points and the affinity of analytes to the stationary phase (internal capillary column wall coating). The detection technique of the separated compounds is typically mass spectrometry (MS). The substances detected by the mass spectrometry are subsequently identified by the interpretation of the obtained mass spectra, by using mass spectra libraries (e.g., NIST/EPA/NIH, Wiley, MPW, Norman Mass Bank, m/z Cloud), or by using reference substances.

Pyrolysis-GC/MS can be applied to research and development of new materials, quality control, characterization and competitor product evaluation, medicine, biology, and biotechnology, geology, airspace, and environmental analysis to forensic purposes or conservation and restoration of cultural heritage. These applications cover analysis and identification of polymers/copolymers and additives in components of automobiles, tires, packaging materials, textile fibers, coatings, adhesives, half-finished products for electronics, paints or varnishes, lacquers, leather, paper or wood products, food, pharmaceuticals, surfactants, and fragrances.

2. Example of application: characterization of poly(vinyl alcohol) by pyrolysis-GC/MS

Poly(vinyl alcohol) (PVA) was first prepared by Hermann and Haehnel in 1924 by hydrolyzing poly(vinyl acetate) in ethanol with potassium hydroxide [6]. PVA is produced commercially from poly(vinyl acetate), usually by a continuous process. The acetate groups are hydrolyzed by ester interchange with methanol in the presence of anhydrous sodium methylate or aqueous sodium hydroxide. PVA is an odorless and tasteless, translucent, white- or cream-colored granular powder. It is soluble in water, slightly soluble in ethanol, but insoluble in other organic solvents. PVA is divided into two classes—partially hydrolyzed PVA and fully hydrolyzed PVA. Partially hydrolyzed PVA is used in food as a moisture barrier film, for food supplement tablets, and for dry food with inclusions that need to be protected from moisture uptake. Poly(vinyl alcohol) has various applications in the food industries as a binding and coating agent. PVA protects the active ingredients from moisture, oxygen, and other environmental components while simultaneously masking their taste and odor. This polymer is used as a water-soluble film useful for packaging. An example is the envelope containing laundry detergent in "liqui-tabs." PVA is used also as packaging material for dishwasher tabs.

2.1 Experimental

Approximately, 200 μg of poly(vinyl alcohol) sample was cut out with a scalpel and inserted into the bore of the pyrolysis solids-injector, without any further preparation, and then placed on the quartz wool of the quartz tube of the furnace pyrolyzer *Pyrojector II™* (SGE Analytical Science, Melbourne, Australia) with the plunger. The pyrolyzer was operated at a constant temperature of 700°C. The pressure of helium (99.999 v/v%) carrier gas at the inlet to the furnace was 95 kPa.
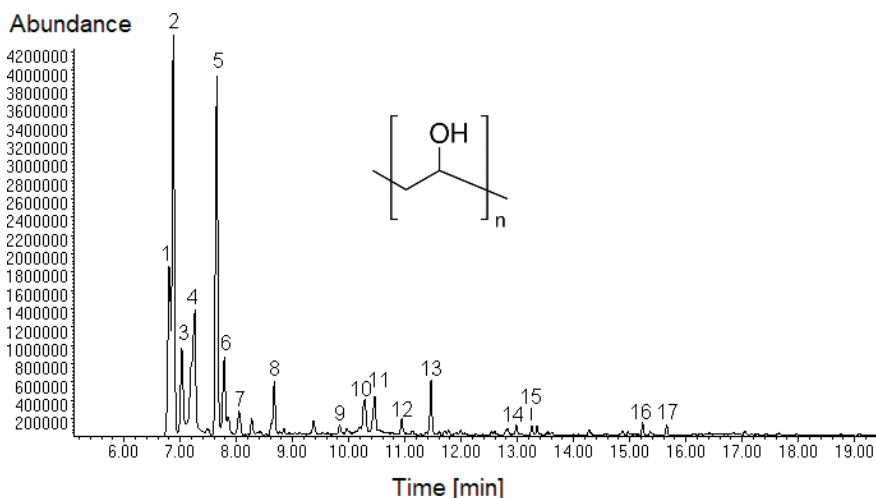
Figure 1.
Pyrolysis-GC/MS chromatogram of PVA at 700°C. For the analytical conditions, see experimental and reference [5].

Peak No.	Retention time t_R (min)	Pyrolysis product
1	6.81	Cyclopropane
2	6.88	Acetaldehyde
3	7.00	Methylbutene
4	7.26	Acetic acid
5	7.65	2-Butenal (crotonaldehyde)
6	7.78	Benzene
7	8.05	Acetic acid anhydride
8	8.68	Toluene
9	9.84	Ethylbenzene
10	10.28	Styrene
11	10.46	2,4-Hexadienal
12	10.95	2-Cyclohexen-1-one
13	11.47	Benzaldehyde
14	13.00	Propenylbenzene
15	13.26	Acetophenone
16	15.23	Dihydronaphthalene
17	15.68	Naphthalene

For the analytical conditions, see experimental and reference [5].

Table 1.
Pyrolysis products of PVA at 700°C.

The pyrolyzer was connected to a *7890A* gas chromatograph with a series *5975C* quadrupole mass spectrometer (Agilent Technologies Inc., Santa Clara, CA, USA) operated in electron impact ionization (EI) mode. The fused silica capillary column 60 m long, 0.25 mm I.D. with DB 5-MS stationary phase, film thickness 0.25 μm was used (J&W Scientific, Folsom, CA, USA). The GC/MS analytical conditions were described in detail in another publication of the author [5]. GC/MS data were

processed with the *ChemStation* software (Agilent Technologies) and the *NIST 05* mass spectra library.

2.2 Results and discussion

Figure 1 shows the pyrolysis-GC/MS chromatogram of PVA at 700°C. The pyrolysis products identified by using the *NIST 05* mass spectra library are summarized in **Table 1**.

As shown in **Figure 1** and **Table 1**, pyrolysis of poly(vinyl alcohol) produces a series of aldehydes (acetaldehyde, crotonaldehyde, 2,4-hexadienal, benzaldehyde) and aromatic hydrocarbons. This is the result of the formation of double bonds by the elimination of H_2O from the PVA macromolecules (dehydration), followed by the breaking of the carbon chain with or without cyclization. The side-group scission occurs when the side groups attached to the backbone are broken away, resulting in the backbone becoming polyunsaturated. A two-step degradation mechanism begins with the elimination of H_2O from the polymer chain leaving a polyunsaturated backbone that, upon further heating, produces the characteristic aromatics. This is similar to the degradation mechanism seen in poly(vinyl chloride) (PVC), in which hydrogen chloride (HCl) is first stripped from the polymer, which creates multiple double bonds, eventually producing aromatics [7].

3. Conclusion

Analytical pyrolysis-GC/MS proved to be a valuable hyphenated technique for the analysis and identification of synthetic organic polymeric materials. This technique allows the direct analysis of very small sample amounts (5–200 µg) without the need of time-consuming sample preparation. Pyrolysis-GC/MS can be applied to research and development of new materials, quality control, as well as characterization and competitor product evaluation. Pyrolysis-GC/MS allows the confirmation of the source of a failed product, the identification of contaminants causing failure, the competitive analysis, as well as overcoming a problem in product development or quality control [5].

Author details

Peter Kusch
Department of Applied Natural Sciences, Bonn-Rhein-Sieg University of Applied Sciences, Rheinbach, Germany

*Address all correspondence to: ptrkusch@arcor.de

IntechOpen

References

[1] Uden PC. Nomenclature and terminology for analytical pyrolysis, IUPAC recommendations 1993. Pure and Applied Chemistry. 1993;**65**(11):2405-2409

[2] Bruce Sitholé B. Pyrolysis in the pulp and paper industry. In: Meyers RA, editor. Encyclopedia of Analytical Chemistry. Chichester, UK: John Wiley & Sons Ltd.; 2000. pp. 8443-8481

[3] Majors RE. Sample Preparation Fundamentals for Chromatography. Wilmington, DE, USA: Agilent Technologies Inc.; 2013

[4] Tsuge S, Ohtani H. Pyrolysis-gas chromatography. In: Dettmer-Wilde K, Engewald W, editors. Practical Gas Chromatography. Berlin, Heidelberg, Germany: Springer-Verlag; 2014. pp. 829-847

[5] Kusch P. Pyrolysis-Gas Chromatography/Mass Spectrometry of Polymeric Materials. London, UK: World Scientific Europe; 2018

[6] Saxena SK. Chemical and Technical Assessment, Polyvinyl Alcohol, 61st JECFA: FAO; 2004

[7] Moldoveanu SC. Analytical Pyrolysis of Synthetic Organic Polymers. Amsterdam, The Netherlands: Elsevier; 2005. pp. 282-283

Chapter 2

Chemical Characterization of Lignocellulosic Materials by Analytical Pyrolysis

Ana Lourenço, Jorge Gominho and Helena Pereira

Abstract

Analytical pyrolysis is used to chemically study complex molecular materials and is applied in a wide range of fields. Pyrolysis is a thermochemical process associated to the breaking of chemical bonds using thermal energy, transforming a nonvolatile compound into a volatile degradation mixture. This chapter refers to analytical pyrolysis of lignocellulosic materials, i.e., when pyrolysis is used for chemical characterization, applied to samples with small particle sizes, at 500–650°C, and with short residence times. The reactions that occur during pyrolysis of the structural components are discussed regarding the mechanisms and the pyrolysis products obtained from cellulose, hemicelluloses, and lignin. A compilation of data is made on the characterization of lignocellulosic materials using Py-GC/FID(MS) or Py-GC/MS as analytical tools including woods and barks of several species. The pyrogram profiles and important parameters on lignin chemical composition such as the H:G:S relation and the S/G ratio are summarized. Analytical pyrolysis is a versatile methodology that may be applied to characterize the lignin directly on the lignocellulosic material or after isolation from the cell wall matrix (e.g., as MWL or dioxane lignin) or from pulps or spent liquors. It is therefore an excellent tool to study lignin compositional variability in different materials and along various processing pathways.

Keywords: Py-GC/MS, wood, barks, lignin, cellulose, H:G:S relation, S/G ratio

1. Introduction

Analytical pyrolysis has been used to study complex molecular materials covering a wide range of fields. A search in *Scopus*® for "analytical pyrolysis" found a total of 756 publications within the subject areas of chemistry, chemical engineering, environmental science, agricultural and biological sciences, materials science, earth and planetary sciences, energy, and engineering. This clearly shows the amplitude of application of this analytical technique, highlighting its importance for the scientific community.

Pyrolysis may be defined based on the occurring chemical reactions, e.g., "the transformation of a nonvolatile compound into a volatile degradation mixture by heat, in the absence of oxygen" [1] or "the breaking of chemical bonds using thermal energy" [2], as well as on its potential applications, e.g., "the basic thermochemical process for converting biomass to a more useful fuel" [3].

The word pyrolysis is derived from *pyro* = fire and *lysis* = separation and is inherently associated with reaction pathways of combustion and coal formation. The production of wood charcoal was the first application example of pyrolysis under controlled conditions, followed by wood distillation to produce methanol, and later by the petrochemical industry where heavy crude oil fractions are transformed into light fuels.

During pyrolysis, the biomass is heated at temperatures of 400–1000°C, in an atmosphere without oxygen, for a short period of time (0.5 s to 5 min), generating bio-oil (liquid), charcoal (solid), and fuel gas products [4–6]. When pyrolysis is used for the chemical characterization of complex polymers, it is denominated *analytical pyrolysis*. This chapter only refers to procedures of analytical pyrolysis, where the sample has small particle sizes (<1 mm or <0.5 mm) and is heated at temperatures from 500 to 650°C with short residence times (10 s to 1 min).

The analysis is performed in a pyrolysis unit linked to an analytical instrument for the separation and measurement of the pyrolysis products, usually a gas chromatograph (GC). The pyrolysis unit comprises a controller (that provides the electrical energy for heating) and the pyrolyzer itself (e.g., a coil) that is heated at high temperatures. The pyrolysis units can be of several types, depending on the heating technique: (i) microfurnaces that provide constant heating, and the samples are introduced by a syringe or a small cup; (ii) Curie-point pyrolyzers, in which the sample is rapidly heated by magnetic induction; or (iii) filament style pyrolyzers that use a resistant metal for filament construction, usually platinum, that is heated following a temperature program, with the sample placed in a quartz boat if using a coil probe or placed directly into a ribbon probe [7]. Other possibilities include laser and plasma pyrolyzers [4]: the laser pyrolyzer allows the analysis directly on the solid matter with no need for sample preparation or pretreatment; the plasma pyrolyzer has a high gas productivity but is seldom used since it requires considerable electrical power consumption [4].

Pyrolysis linked to GC is a powerful combination for the characterization of complex materials: pyrolysis produces a mixture of volatile compounds that flows through a capillary column carried by an inert gas (usually helium) where the compounds are separated due to different retention times and are subsequently identified by mass spectrometry (MS) or/and quantified by a flame ionization detector (FID). An MS detector is frequently used associated with pyrolysis due to advantages in relation to speed, specificity, and sensitivity: the pyrolysis product is identified based on the selective fragmentation by electron impact and, even if a molecular ion is not found, the fragmentation pattern together with the retention time on the GC column and comparison with spectra in data bases can identify the compound [4]. The FID detector is sensitive and reliable giving nearly the same response for different organic compounds and therefore is preferred for quantification once the compounds have been identified [8].

The advantage of pyrolysis is that a wide range of macromolecules and materials (from plant materials to textiles, synthetic polymers, and many others) may be studied since they are thermally fragmented into volatile compounds that can be subsequently separated, identified, and quantified. The reactions that occur during pyrolysis of the structural components of plants—cellulose, hemicelluloses, and lignin—will be discussed in the following subsection.

The aim of this chapter is to present a compilation of data regarding the characterization of lignocellulosic materials using Py-GC/FID(MS) or Py-GC/MS as analytical tools.

1.1 Broad features of pyrolysis reactions

During pyrolysis, the molecules are degraded by the breaking of chemical bonds through homolitic scissions with formation of free radicals that further react by recombination, rearrangements, or elimination of radicals and hydrogen [2]. Any radical is instable and will react as soon as possible with other radicals or molecules. The pyrolysate composition will depend on the stability of the produced radicals or molecules, e.g., a tertiary radical is more stable than a secondary radical and is consequently produced in higher proportion.

The pyrolysis products depend on the original chemical composition of the raw material. Therefore, the pyrolysis of lignocellulosic materials will produce pyrolysis products from their main components: cellulose, hemicelluloses, and lignin. **Figure 1** presents a pyrogram of *Eucalyptus globulus* wood as an example of the complex mixture of volatile compounds that is obtained. The peaks corresponding to the fragmentation of lignin and polysaccharides are numerous, and most may be assigned as derivatives from either carbohydrates or lignin, including differentiation between the monomeric moieties of lignin.

Pyrolysis of the lignocellulosic components involves complex reactions and mechanisms that depend on pyrolysis conditions (heating rate, pressure, and temperature) and on biomass particle size [5]. The study of the thermolytic break-down of model compounds helps to explain the global mechanisms of pyrolysis, while kinetic models are helpful to characterize the degradation steps and to predict product distribution [9–12].

1.1.1 Lignin

The lignin polymer undergoes a number of degradation reactions that include depolymerization, hydrolysis, oxidation, dehydration, and decarboxylation [13]. The thermal decomposition of the lignin polymer starts with the cleavage of the weak bonds (α-ether and β-ether bonds), releasing a mixture of phenol-, guaiacyl-, and syringyl-type derivatives, which maintain their substituents in the aromatic ring [10, 11, 14]. This enables making their correspondence with the original lignin moieties of *p*-hydroxyphenyl, guaiacyl, and syringyl moieties [1, 15]. **Figure 2** shows a few of the compounds formed during lignin pyrolysis that can be assigned to specific original moieties: H units (phenol (1) and 4-methylphenol (*p*-cresol, 4)), G units (guaiacol (2) and 4-methylguaiacol (5)), and S units (syringol (3) and 4-methylsyringol (6)).
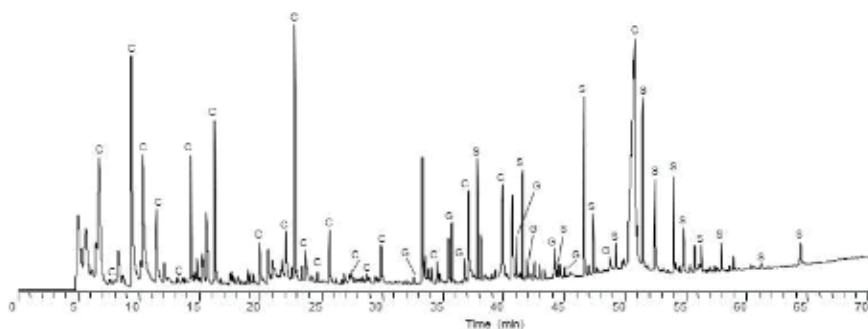
Figure 1.
Pyrogram of Eucalyptus globulus wood obtained by Py-GC/FID. The peaks are assigned to carbohydrates (C) and from lignin, distinguished in guaiacyl (G) and syringyl moieties (S).
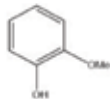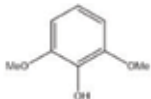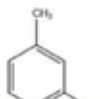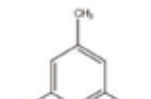
phenol (1)	guaiacol (2)	syringol (3)
4-methylphenol (4)	4-methylguaiacol (5)	4-methylsyringol (6)
H-units	**G-units**	**S-units**

Figure 2.
Some examples of the compounds obtained from lignin pyrolysis.
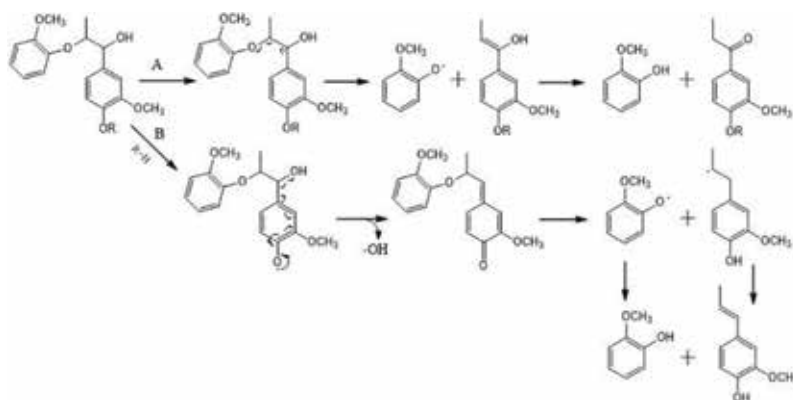
Figure 3.
Proposed radical mechanism for the formation of guaiacol (redrawn from Kawamoto [17]).

In the case of softwoods, more guaiacyl units are released during pyrolysis, while hardwoods will produce both types of compounds, in relation with the original monomeric composition of lignin [16]. Kawamoto [17] proposed two pathways for the degradation of lignin by the cleavage of ether bonds and formation of guaiacol (**Figure 3**). *Pathway A* starts with the formation of C_α radical by the liberation of hydrogen from C_α-H, followed by the cleavage of the β-ether bonds, forming $C_\alpha{=}O$ monomers and guaiacol. *Pathway B* starts with the formation of phenoxy radicals through the liberation of the phenolic OH, followed by the homolytic cleavage of the β-ether bond in the quinone methide intermediate.

The liberated compounds will further react by two possible ways: homolytic cleavage of the $O-CH_3$-producing catechols and pyrogallols or by radical rearrangement reactions producing cresols and xylenols [18, 19]. Recently, Kawamoto [17] presented an update on the state of art of the pathways and mechanisms involved in the lignin pyrolysis and focused upon the influence of temperature on the pyrolysis products. Pyrolysis primary reactions occur at 200–400°C, leading to the formation of 4-substituted guaiacols and 4-substituted syringols (in case of SG lignin), with the main side chains constituted by unsaturated alkyl groups and, in less extent, saturated alkyls groups [17]. The increase of temperature leads to secondary reactions, and guaiacols/syringols are degraded to catechols and cresols [17].
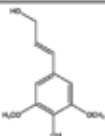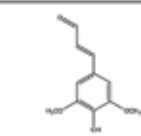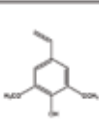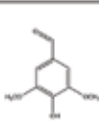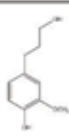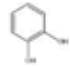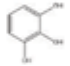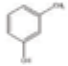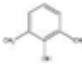
Temperature = 200–400°C				
Side-chain: unsaturated alkyl groups				Saturated alkyl groups
sinapyl alcohol (Ar-CH=CH-CH₂OH)	*trans*-sinapaldehyde (Ar-CH=CH-CHO)	4-vinylsyringol (Ar-CH=CH₂)	syringaldehyde (Ar-CHO)	dihydrosinapyl alcohol (Ar-CH₂=CH₂-CH₂OH)
Temperature => 400°C				
catechol	pyrogallol	cresol	xylenol	

Figure 4.
Influence of the pyrolysis temperature on the aromatic side chain of an S type lignin.

Figure 4 shows the lignin degradative products from S units that are produced during the primary and secondary reactions.

Other compounds with low molecular mass are also produced during pyrolysis, such as formaldehyde, methanol, acetic acid, acetaldehyde, and water as well as gases (CO, CO_2, and CH_4) that are assumed to be liberated from the methoxy group [20, 21].

1.1.2 Carbohydrates

The degradation of cellulose and hemicelluloses by pyrolysis occurs by heterolytic cleavage of the glycosidic C-O bonds [17] and involves complex reactions and several pathways [22]. First, cellulose breaks into lower molecular mass compounds and forms the so-called "activated cellulose" that can be decomposed by two competitive reactions, generating volatiles (anhydrosugars) or char and gases [3]. Volatiles are composed by the cellulose monomeric units including levoglucosan (7, **Figure 5**), levoglucosenone, and 1,4:3,6-dianhydro-α-D-glucopyranose [23, 24]. Levoglucosan is produced by the cleavage of the 1,4-glycosidic linkages followed by dehydration (**Figure 6**) [25]. The yield is influenced by the cellulose characteristics (purity and physical properties), by the pyrolysis conditions [22, 26], and also by the presence of inorganic compounds [27].

Cellulose pyrolysis produces also some compounds with low molecular mass (**Figure 5**), such as hydroxyacetaldehyde (8), 1-hydroxypropan-2-one (9), 1-hydroxybutan-2-one, and 2-furaldehyde (10) [3]. Hydroxyacetaldehyde is obtained by cleavage of a C-C linkage followed by ring opening, while 1-hydroxy-2-propan-2-one is formed by dehydration and decarboxylation reactions [28], where both compounds compete with levoglucosan formation [29].

The degradation of hemicelluloses involves pathways that are similar to those of cellulose and produces the same type of compounds [30]. For instance, xylan pyrolysis produces 1,4-anhydroxylopyranose, 1,5-anhydro-4-deoxy-pent-1-en-3-ulose [31], 4-hydroxy-5,6-dihydro-(2H)-pyran-2-one (11, **Figure 5**), a xylan marker [32], and 2-furaldehyde [28, 31], but not levoglucosan [30].

Other compounds, such as 2-furaldehyde and acetic acid, can be produced by either hemicelluloses or cellulose [28]. For instance, two chemical pathways lead to formation of 2-furaldehyde from xylan: (i) depolymerization of xylan by cleavage of the hemiacetal bond (between C1 and oxygen on the pyran ring) with ring opening, followed by dehydration between OH in C2 and C5 positions; (ii) cleavage of the 1,2-glycosidic bond between the 4-O-methyl-glucuronic acid unit and the xylan
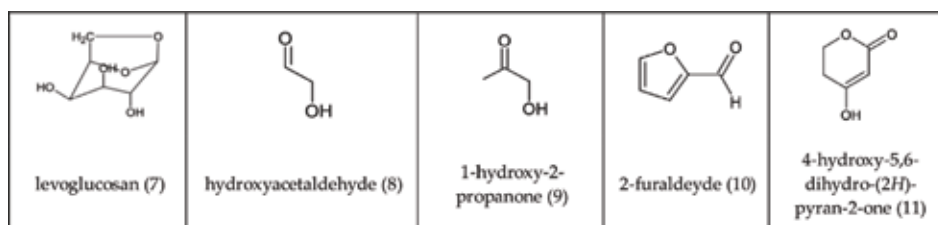
Figure 5.
Compounds obtained by the pyrolysis of carbohydrates.
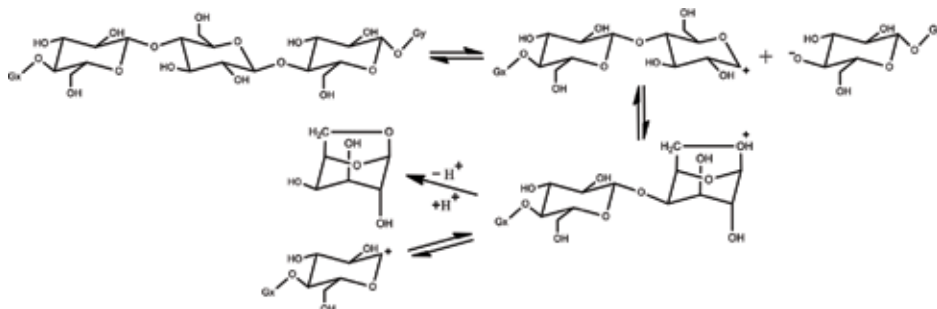
Figure 6.
Mechanism of levoglucosan formation (redrawn from Patwardhan et al. [24]).

unit, followed by ring opening and rearrangement of the 4-O-methyl-glucuronic acid after elimination of the methanol and CO_2 [33]. Acetic acid may also be formed by two possible pathways: (i) by elimination of acetyl groups linked to C2 in the xylan chain and (ii) elimination of the carbonyl and O-methyl groups [33].

Thus, the pyrolysis of polysaccharides has a particular aspect that is the production of the same compounds by thermal degradation of both cellulose and hemicelluloses, e.g., furans and pyrans have distinct molecular ions, but both can be obtained either from cellulose (hexose-based) or from hemicelluloses (hexose- and pentose-based) [34]. This fact contributes for the difficulty of distinguishing the origin of a polysaccharide-derived pyrolysis compound. Overall, carbohydrate-derived pyrolysis products are considerably more difficult to identify by mass spectrometry when compared to lignin-derived products for several reasons [35]: (i) the mass spectra of the carbohydrates are less specific since they are easily fragmented; (ii) there are several structural isomers with identical mass spectra; and (iii) the presence of inorganic compounds has a catalytic effect on the pyrolytic degradation of polysaccharides. Analytical pyrolysis is therefore less suitable for the determination of carbohydrates composition, e.g., the quantification of pentoses and hexoses.

1.2 Factors affecting pyrolysis reactions

Pyrolysis yields and product composition can be influenced by several factors:

i. The feedstock and its chemical composition, where different materials will produce, by pyrolysis, different types of compounds [3, 36].

ii. The presence of inorganic salts increases the formation of small molecules [37, 38], thereby reducing the proportion of large molecules that provide better structural information [39], and contributes for the production of levoglucosan [38].

iii. The sample components can interact during pyrolysis, e.g., the interaction between cellulose and hemicelluloses promotes the formation of furans and inhibits the formation of levoglucosan [40], while the presence of pyrolysis vapors from cellulose and lignin induces the secondary degradation of levoglucosan [41].

iv. The particle size influences the heating rate of the material: if the sample is composed of fine particles, the heating rate is uniform, and less interaction will occur between the produced primary compounds, thereby limiting secondary reactions [42].

v. The operating temperature influences the compounds produced [9, 43]: increase of temperature rises the yield of smaller products and gases, while it induces more secondary reactions. For example, the formation of levoglucosan occurs above 260°C, but in the range from 450 to 500°C, degradation products such as hydroxyacetaldehyde start to be formed [9]. Also, to degrade suberin (a cell wall polymer of barks) into volatiles, higher temperatures (above 650°C) are required as discussed by Marques and Pereira [44].

1.3 Advantages and disadvantages of analytical pyrolysis

Pyrolysis can be used to study complex molecular structures, covering wide and diversified fields: fibers and textiles, forensic materials, wood and paper, art materials, synthetic polymers [2]. Analytical pyrolysis presents some advantages over other chemical techniques to characterize lignocellulosic materials:

i. It is a rapid technique when compared with others, as it involves a simple sample preparation (extraction and milling), and data acquisition only takes from a few minutes to 1.5 h [1].

ii. It requires only a small sample size (1–100 μg) [45].

iii. It presents good reproducibility [46], provided that the sample is consistent in size [4] and distribution, for example, in a quartz boat.

iv. It does not require pre-isolation of the compounds to be studied [1]; for example, the lignin content in the sample can be determined without isolation as required in wet chemistry procedures.

v. The lignin and phenolic acid compounds are easily identified by mass spectrometry [15], because they maintain the ring substitution patterns from the lignin polymer and therefore can be identified as being derived from the *p*-hydroxyphenyl (H), guaiacyl (G), or syringyl (S) units of lignin [1].

vi. It provides information about S, G, and H lignin units [1, 47], enabling the calculation of the S/G ratio; this is a valuable parameter, for example, to determine the quality of pulpwood materials.

Nevertheless, pyrolysis also presents a few disadvantages:

i. It has limitations when analyzing samples constituted of carbohydrates, since during pyrolysis, their derivatives can originate either from hexoses or pentoses [34].

ii. The pyrolysis results are highly influenced by the methodology used, i.e., the conditions applied, such as time, temperature, and type of GC column, which can result in discrepancies when comparing results obtained by different authors.

iii. Attention must be paid when analyzing barks rich in suberin, for which the adequate temperature range to determine the H:G:S relation is 550–600°C, and higher temperatures should be applied if suberin composition is the target of the analysis [48].

2. Characterization of lignocellulosic materials

Analytical pyrolysis is an important tool for the chemical characterization of several lignocellulosic materials such as wood (softwoods and hardwoods), barks, pulps, and lignins and is an essential instrument to support the objective of potentiating their use as raw materials for different applications.

Table 1 makes a synthesis of results obtained by analytical pyrolysis for different lignocellulosic materials. Most wood species were studied due to their economic importance as pulping raw materials such as spruce and pine (softwoods) and birch and eucalypt (hardwoods), while herbaceous species are increasingly considered as fiber and energy sources. In addition, barks are important industrial residues with potential for added-value products under the biorefinery context in a circular economy.

An analysis of the available information regarding determination of lignin composition and content by analytical pyrolysis is made subsequently. Some studies applied analytical pyrolysis directly to the extractive-free material, while others studied isolated lignins, e.g., as MWL. This will be specified for each case.

2.1 Wood from gymnosperms

2.1.1 Picea abies

Lignin content in spruce determined by analytical pyrolysis was near the values obtained by wet chemical analysis as Klason lignin (21.6–25.7% of extractive-free dry wood) [49, 50]. Spruce presented more G lignin units (21.9% of identified compounds) and less H units (1.0%). The main pyrolysis products derived from G units were 4-vinylguaiacol (2.5%), 4-methylguaiacol (2.6%), coniferyl aldehyde (2.4%), and guaiacol (1.6%), while only phenol and cresol isomers were derived from H lignin [49]. The carbohydrates represented around 77% (of identified compounds), where levoglucosan was 11.1%, followed by hydroxyacetaldehyde (13.1%), and propanal-2-one (7.3%). The ratio between carbohydrates and lignin (C/L) was 3.4 [49]. The pyrolysis of spruce milled wood lignin (MWL) with addition of TMAH (tetramethylammonium hydroxide) and under different temperatures (310–710°C) showed that the lowest temperature (310°C) produced the highest yield of lignin monomers with intact propane side chain and minimized the production of unmethylated lignin monomers such as phenols and methoxyphenols [51].

2.1.2 Pinus pinaster

The lignin content of maritime pine wood determined by pyrolysis was well correlated with the Klason values determined by wet chemical analysis (23.0–29.6%

Species	Component	Lignin content (%)*	S/G	H/G	H:G:S	C/L	Ref.
SOFTWOODS							
Pinus pinaster	Wood	23.0-29.6	-	0.041-0.113	1:16:0	2.95	[49, 50]
Picea abies	Wood	21.6-25.7	-	0.034-0.118	1:23:0	3.36	[49, 50]
Pseudotsuga menziesii	Cork	-	0.1	-	1:7:0.8	-	[80]
HARDWOODS							
Eucalyptus globulus	Wood Pulps	23.0/23.7** 2.2/2.3**	1.9-5.4 0.58/ 0.51*	- -	1:8:29/ 1:11:39** 1:2:1**	3.2/ 3.1** 2.7-44.3	[55, 56]
Paulownia fortunei	Wood***	-	0.67	-	1:59:40	-	[67]
Tectona grandis	Sapwood Heartwood Bark	35.4 37.3 28.0	0.7 0.8 0.8	- - -	1:34:24 1:29:23 1:11:9	0.89 0.85 0.91	[69]
Quercus suber	Wood*** Phloem*** Cork***	- - -	1.2 0.7 0.1; 0.03	- - -	- - 1:11:0.3	- - -	[68, 75]
Quercus cerris	Wood Cork	- -	0.71 0.01	- -	1:52:37 1:38:1	- -	[48]
Betula pendula	Wood Cork	- -	1.5 0.14	- -	1:26:40 1:36:5	- -	[48]
MONOCOTYLEDONS							
Ensete ventricosum	Fibers Stalks	6.1 4.6	1.1 0.5	- -	1:0.7:0.8 1:0.4:0.2	11.0 13.4	[77]
Saccharum ssp.	Straw*** Bagasse***	- -	0.4 1.6	- -	1:17:7 1:19:30	- -	[76]

*% of lignin-derived peaks in the total chromatographic area;
**sapwood and heartwood respectively;
****Björkman lignin.

Table 1.
Chemical characterization by analytical pyrolysis of lignin in biomass components of different species.

of extractive-free dry wood) [49, 50]. Lignin was constituted predominantly by G units (23.7% of identified area) and less H units (1.6%) in accordance with soft-wood lignin literature compositional data [52]. The main compounds obtained were 4-vinylguaiacol (2.9%), 4-methylguaiacol (2.7%), coniferyl aldehyde (2.5%), and guaiacol (2.1%) [49]. The pyrolysis compounds derived from carbohydrates repre-sented 75% (of the total identified compounds), where levoglucosan was the main compound (12.5%) followed by hydroxyacetaldehyde (11.6%) and propanal-2-one (7.4%). The C/L ratio was 2.9 [49]. Alves et al. [53] showed that analytical pyrolysis conjugated with PCA analysis may be a potent tool for lignin origin discrimination, e.g., pine, spruce, and larch wood samples could be separated and, in the case of maritime pine, it was also possible to separate samples from two sites and between reaction wood and normal wood.

2.1.3 Pinus sylvestris

Scots pine wood pyrolysis produced a high amount of lignin-derived products from guaiacyl units (vanillin, homovanillin, acetaldehyde, coniferyl aldehyde, and coniferyl alcohols), and the highest peaks from carbohydrate-derived products were 5-hydroxymethyl-2-tetraydrofuraldehyde-3-one, 5-hydroxymethyl-2-furalde-hyde, and levoglucosan [54].

2.2 Wood from angiosperms

2.2.1 Eucalyptus globulus

Sapwood and heartwood samples were characterized by a similar content in lignin, respectively, 23.0 and 23.7%, in extractive-free base [55, 56]. The main lignin products were 4-vinylsyringol (12.0 *vs*. 11.4% of total area), 4-propenylsyringol (10.3 *vs*. 10.4%), syringol (10.0 *vs*. 7.0%), syringaldehyde (7.5 *vs*. 7.4%), 4-methyl-syringol (5.4 *vs*. 6.5%), and 4-allysyringol (4.0 *vs*. 3.8%). Sapwood presented the highest value of S/G ratio comparatively to heartwood (3.63 *vs*. 3.45), with an H:G:S relation of 1:8:29 and 1:11:39 [55]. Carbohydrates represented 49.2% (sapwood) and 43.3% (heartwood) of total chromatographic area, and their pyrolysis produced mainly levoglucosan (22.7 *vs*. 27.5%), hydroxyacetaldehyde (12.7 *vs*. 12.4%), oxo-propanal (10.5 *vs*. 10.1%), acetic acid (9.3 *vs*. 8.0%), and in minor amounts 4-hydroxy-5,6-dihydro-2H-pyran-2-one, 2-furaldehyde, and 3-hydroxypropanal in percentages between 5.1 and 2.5%. No great differences were attained between the carbohydrate-to-lignin ratio (C/L) with values of 3.2 and 3.1 [56].

Eucalypt wood was characterized by different authors in relation to the syringyl-to-guaiacyl (S/G) ratio, and a large variation range was observed: 5.4 [57], 4.3 [58], 4.1 [59], and 1.9–2.3 [60]. Such differences may derive from the tree origin [61] and the lignin heterogeneity as discussed by Yokoi et al. [62]. Eucalypt MWL isolated by the Björkman method had an S/G ratio of 3.0 [63], while eucalypt dioxane lignin was characterized with an S/G ratio of 5.6 and an H:G:S relation of 1:30:169 [64].

Other eucalypts, such as *Eucalyptus camaldulensis* trees presented S/G ratios ranging from 1.5 to 2.2 depending on the seed origin. The pyrograms profile regarding the distribution of the lignin-derived compounds showed a similar tendency: vinylsyringol, syringol, guaiacol, trans-coniferyl alcohol, and *trans*-sinapyl alcohol were the main pyrolyzates [62].

2.2.2 Fagus sylvatica

Beech MWL had a monomeric composition with more syringyl units (56.8% of the total lignin-derived compounds) over guaiacyl units (37.2%) and phenol groups (1.2–1.8%) showing that beech wood has an SG type of lignin. The lignin pyrogram showed a predominance of alcohol compounds such as coniferyl alcohol (13%) and sinapyl alcohol (10%), and less guaiacol (4.7%) and syringol lignin units (9.0%) [65]. Choi et al. [66] observed in the pyrograms of beech MWL other synapyl-derived compounds such as sinapaldehyde (12.4%), followed by syringol, 4-vinylsyringol, and syringaldehyde with 8.7%, and 4-methylsyringol (7.7%), and guaiacyl-derived compounds such as 4-vinylguaiacol (6.0%), guaiacol (4.6%), and 4-methylguaiacol (4.2%).

2.2.3 Paulownia fortune

The MWL pyrograms presented a predominance of guaiacyl over syringyl units and only small amounts of *p*-hydroxycinnamyl units (~1%), corresponding to an

H:G:S relation of 1:59:40 and an S/G ratio of 0.7 [67]. The main lignin-derived compounds released during pyrolysis were in molar % of the total peaks: guaiacol (9.0%), 4-vinylguaiacol (8.3%), 4-methylguaiacol (6.8%), syringaldehyde (5.3%), syringol (7.5%), vanillin (4.8%), *trans*-isoeugenol (4.8%), *trans*-coniferaldehyde (4.7%) *trans*-coniferyl alcohol (4.3%), 4-vinylsyringol (4.2%), 4-methylsyringol (4.1%), *trans*-4-propenylsyringol (3.0%), and *trans*-sinapaldehyde (4.0%) [67].

2.2.4 Quercus suber

Lourenço et al. [68] recently studied the wood from cork oak trees. The milled wood lignin was characterized with more syringyl lignin units, where the pyrolysis products were mainly 4-methylsyringol (15.9 *vs*. 8.9% in relative molar %), syringol (14 *vs*. 12.3%), 4-methylsyringol (10.0 *vs*. 15.8%), 4-vinylsyringol (4.5 *vs*. 11.6%), and guaiacol (7.3 *vs*. 13.1%). Marques and Pereira [48] reported for wood lignin a H:G:S relation of 1:25:24 and an S/G ratio of 0.9.

2.2.5 Tectona grandis

Teak sapwood and heartwood presented a similar lignin content of, respectively, 35.4 and 37.3% (extractive-free material), with a composition predominantly of guaiacyl units (57.6 and 54.4% of total lignin units), lower syringyl units (40.6 and 43.8%), and only 1.8% of *p*-hydroxyphenyl units [69]. The main lignin-derived compounds in the pyrolysis products were 4-vinylsyringol (6.3 and 6.9% of total chromatographic area), *trans*-coniferyl alcohol (4.5 and 4.4%), coniferaldehyde (2.0% in both), 4-vinylguaiacol (1.6%), 4-methylguaiacol (1.6%), and vanillin (1.5%). Therefore, teakwood lignin is a GS type of lignin with an H:G:S relation of 1:34:24 (sapwood) and 1:29:23 (heartwood) and an S/G ratio of 0.7 and 0.8, respectively. Carbohydrates represented 31.6% in sapwood and 31.6% in heartwood (% of total area), with a predominance of levoglucosan (15.2 and 14.4%), 2-hydroxymethyl-5-hydroxy-2,3-dihydro-4H-pyran-4-one (3.6%), and around 1.5% of furfural, 4-hydroxy-5,6-dihydro-2H-pyran-2-one and 5-hydroxymethyl-2-furaldehyde. The carbohydrate-to-lignin ratio was 0.89 and 0.85 in, respectively, sapwood and heartwood [69].

2.2.6 Betula pendula

Birch wood lignin has a monomeric composition with an H:G:S relation of 1:26:40 and an S/G ratio of 1.5 [48]. Ghalibaf et al. [70] studied untreated and treated (with hot-water-extracted) birch samples by Py-GC/MS under different temperatures (500–700°C) and reported an enhanced production of furan derivatives at 500°C and an increase of aromatic compounds when the temperature rises from 500 to 700°C. The carbohydrates-to-lignin ratio was 2.2 (untreated) and 1.4 (treated).

2.2.7 Cynara cardunculus

Cardoon stalks were separated in pith and depithed samples and characterized by Py-GC/MS(FID). The lignin content in stalks was in average 22.9%, ranged in pith from 18.8 to 24.6% and in depithed stalks from 22.7 to 25.5% [71]. The monomeric composition was slightly different between pith and depithed stalks: guaiacyl units predominated in depithed stalks (40 *vs*. 29% of total chromatographic area), syringyl units were predominant in pith (64 *vs*. 53%), and the same amount of H units was found in both (7%). The distribution of the main lignin products of cardoon pyrolysis

was: 4-vinylsyringol (in average 2.9% of total area), 4-propenylsyringol (2.0%), sinapinaldehyde (1.4%), *trans*-sinapyl alcohol (1.3%), syringol (1.0%), and *trans*-coniferyl alcohol (1.0%). In lower amounts (ca. 1%) were obtained: 4-methylguaiacol (0.9%), syringaldehyde (0.9%), 4-propylguaiacol (0.8%), and 4-vinylguaiacol (0.7%). The lignin monomeric composition presented an H:G:S relation of 1:4:9 (pith) and 1:6:8 (depithed), corresponding to an S/G ratio of 2.2 and 1.3 [71]. Cardoon lignin is an SG type of lignin, with more syringyl units compared to guaiacyl and less content of hydroxyphenyl units. Carbohydrates represented in average 21.8% in pith and 23.9% in depithed stalks (% of total chromatographic area). The carbohydrate pyrolysis products were levoglucosan as the main compound (7.6%), followed by 4-hydroxy-5,6-dihydro-2H-pyran-2-one (3.6%), furfural (2.3%), 2-hydroxymethyl-5-hydroxy-2,3-dihydro-4H-pyran-4-one (1.5%), and 3H-pyran-2,6-dione (1.3%).

The lignin present in the whole stalks was studied after isolation by the Björkman method (MCyL) and characterized by Py-GC/MS [72]. In general, there was a similar distribution of the lignin-derived compounds formed during pyrolysis of MCyL comparatively to depithed and pith samples pyrolysis, and the G units were released in higher abundances than the respective S units, attaining an S/G molar ratio 0.3.

2.2.8 Linum usitatissimum

Flax fibers and shives were studied regarding its lignin composition, after isolation by Björkman procedure [73]. The lignin-derived compounds released by pyrolysis were guaiacol, 4-methylguaiacol, 4-ethylguaiacol, 4-vinylguaiacol, vanillin, syringol, *trans*-isoeugenol, and 4-methylsyringol. Flax shive lignin also released high amounts of *trans*-coniferaldehyde and *trans*-coniferyl alcohol contrasting to the minor compounds produced by flax fiber lignin. Milled lignins presented significant differences in respect to H:G:S molar ratio of 1:6:1 (fibers) and 1:17:2 (shives), and the values of the S/G ratios were low in both lignins, with a ratio of 0.2 (fibers) and 0.1 (shives).

2.3 Monocotyledons

2.3.1 Miscanthus

Py-GC/MS was used to examine genotype and harvest influence upon the chemical composition [74]. The most abundant compounds were acetic acid, 4-ethenylphenol, and levoglucosenone. The effect of harvest time upon the relative amount of pyrolysis compounds was small, but the samples collected during February produced higher amounts of 2-propenoic acid methyl ester, 3-hydroxypropanal, (2H)-furan-3-one, 2-hydroxy-3-oxobutanal, and 1,5-anhydro-β-D-xylofuranose.

2.3.2 Bamboo

Milled lignin presented a lignin composition rich in G units (68% of identified lignin compounds), followed by S units (21%), and H units (11%) and included *p*-coumaric acids as degradation products [75]. Therefore, the correspondent H:G:S relation was 1:6:2 and the S/G ratio 0.3.

2.3.3 Saccharum ssp.

Sugarcane straw and bagasse presented differences regarding lignin composition. The isolated lignin from bagasse is rich in syringyl units, with an H:G:S

relation of 1:19:30 and an S/G ratio of 1.6. Straw lignin is rich in guaiacyl units, with an H:G:S relation 1:17:7 and an S/G ratio of 0.4 [76].

2.3.4 Ensete ventricosum

Enset or false banana fibers and inflorescence stalks were characterized by Py-GC/MS by a low amount of lignin (6 and 5% of total pyrogram area). The fibers presented a similar content in H units, but more G and S units when compared to stalks. Therefore, the H:G:S relation was 1:0.7:0.8 and 1:0.4:0.2,respectively. The S/G ratio values were 1.1 (fibers) and 0.5 (stalks). The fibers and the stalks presented a great amount of carbohydrates (67 *vs*. 62% of total pyrogram area), where levoglucosan was the main compound (17.1 *vs*. 5.4%), followed by 2-hydroxy-2-cyclopenten-1-one (1.4 *vs*. 3.1%), 2-hydroxymethyl-5-hydroxy-2,3-dihydro-(4H)-pyran-4-one (1.1 *vs*. 0.7%), and 4-hydroxy-5,6-dihydro-(2H)-pyran-2-one (1.2 *vs*. 0.3%) [77].

2.4 Barks

Barks are structurally heterogeneous and include phloem and periderm, and often a rhytidome with several superposed periderms [78]. Periderm contains cork (phellem), a tissue that differs chemically from wood and phloem by the presence of suberin as one of the cell wall structural polymers. The extent of cork proportion varies between species and some have cork-rich barks [79]. When chemically characterizing barks, it is therefore important to specify if the whole bark is analyzed or if the components are separated, i.e., in cork and phloem, for instance.

2.4.1 Pseudotsuga menziesii

Douglas-fir cork was separated from the whole bark and used for analysis. Cork was constituted by a lignin content of 60% (% total pyrogram) and carbohydrates content of 40% [80]. Cork pyrolysis products were mainly G units (~81% of lignin units): 4-vinylguaiacol (13%), 4-methylguaiacol (9%), guaiacol (6%), vanillin (5%), and eugenol, while the H units represented 11%, with phenol and dimethylphenol isomers as main derivatives, respectively, 1 and 4%. The S units were minority (~9%), mainly represented by syringol (2%) and 4-methylsyringol (2%) [80]. The H:G:S was 1:7:0.8 and the S/G ratio was 0.1. Some differences were found when Björkman lignin was isolated from saponified cork: the H:G:S relation was 1:40:1, while the S/G ratio was 0.02, revealing an enrichment of guaiacyl units and a decrease in H units with the isolation.

2.4.2 Quercus suber

The cork lignin represented 60.7%, with a predominance of guaiacyl units (84.7% of total lignin units), followed by *p*-hydroxyphenyl units (12.8%), and with a minor percentage of S units (2.5%); thus the H:G:S was 1:6.6:0.2 and the S/G ratio was 0.02 [75]. The prevalent degradation products from the G moieties in lignin were guaiacol, 4-methylguaiacol, 4-vinylguaiacol, isoeugenol, vanillin, and coniferyl alcohol and those from the S units were syringol and 4-methylsyringol [48, 75]. Cork pyrolysis produced a total carbohydrate of 39.3%, where hexoses represented 57% and pentoses 43% [75]. Björkman lignin was isolated from cork, and the results showed a predominance of guaiacyl units (~90% of lignin units), a decrease of H and S units, contributing for an H:G:S relation of 1:11:0.3 and an S/G ratio of 0.03 [75]. The milled lignin isolated from phloem tissue presented an S/G ratio of 0.62 [68].

2.4.3 Quercus cerris

The cork of *Q. cerris* was manually separated from bark and characterized by Py-GC/MS(FID). Cork presented a lignin content of 31.8% (% of total area), 8.5% of carbohydrates, with aliphatic compounds derived from suberin representing 18.4%. Lignin had a monomeric composition largely of G units (93.7%), with a low proportion of S and H units, respectively, 2.7 and 3.6%, which corresponds to an S/G ratio of 0.01 [48].

2.4.4 Betula pendula

The cork from birch bark is constituted predominantly by guaiacyl units (85.7% of total lignin) with a minor proportion of syringyl units (11.9%) and *p*-hydroxy-phenyl (2.4%), corresponding to an H:G:S relation of 1:36:5 and an S/G of 0.14 [48].

2.4.5 Tectona grandis

The whole teak bark was characterized with a lignin content of 28.0% determined by analytical pyrolysis (PY-GC/MS(FID)) [69]. The main pyrolysis compounds were 4-vinylsyringol and *trans*-coniferyl alcohol with, respectively, 1.4 and 2.7%. Teak bark has a GS type of lignin, with G units reaching 53.3% of the total lignin units, followed by S units with 42.1%, and a minor amount of H units (4.6%). The relation H:G:S was 1:11:9, and the S/G ratio was 0.8 [69].

3. Characterization of cellulosic pulps and isolated lignins

3.1 Cellulosic pulps

The lignin monomeric composition evaluated by the S/G ratio is a valuable parameter to estimate the aptitude of a raw material for pulping by predicting the ability of the material for delignification, the chemical consumption, and in some cases pulp yield, given the different reactivity of the lignin moieties in the pulping liquor. Some works used analytical pyrolysis to characterize the pulps in respect to lignin and, in some cases, to carbohydrates.

Ohra-aho and coworkers [81] characterized kraft pulps from *Pinus sylvestris* wood before and after bleaching. The hydroxyphenyl lignin units (phenol, 2-methylphenol, and 4-methylphenol) were highly enriched in the unbleached and bleached pulps: the proportion of hydroxyphenyl structures in the fully bleached pulp was threefold in comparison to the unbleached pulp, while in wood chips the proportion of hydroxy-phenyl structures was less than 1%. This enrichment in hydroxyphenyl structures is a documented fact, but the reason for the phenomenon has been unclear.

As regards *Eucalyptus globulus* wood, a correlation between pulp yield and the lignin monomeric composition of the starting material was shown, with woods with high S/G ratios (4.0–6.4) producing kraft pulps with higher pulp yields (46.6–59.6%) [46]. Lourenço et al. [55, 56] studied the kraft pulping behavior of sapwood and heartwood of eucalypt wood along delignification (from 1 to 180 min) and at different temperatures (130, 150, and 170°C). The residual lignin in the pulps was different from that of the initial wood and differed with time, i.e., the pulps were enriched in G and H units along delignification. The kinetics of the process showed that only small differences were found between S and G units reactivity during the bulk phase, while the higher reactivity of S over G units was better expressed in the later pulping stage. The S/G ratio ranged between 3 and 4.5 when the pulp residual

lignin was higher than 10% but decreased rapidly to less than 1 in the more delignified pulps [82]. The C/L values were the same in heartwood and sapwood (3.2) and remained constant during the first pulping times until a loss of 60% in lignin and 15–25% in carbohydrates occurred; after that, the ratio increased severely until 44, corresponding to the removal of 95% of lignin and 25–35% of carbohydrates [56].

3.2 Isolated lignin from cellulosic pulps and liquors

Residual lignin from *Picea abies* pulps was isolated and characterized by pyrolysis. The lignins presented an H:G relation of 1:47, 1:17, 1:12, and 1:42, respectively, for the kraft, sulfite, ASAM, and soda/AQ/MeOH pulps [66]. Overall, the main lignin-derived compounds were the same in all the isolated lignins but were produced in different percentages depending on the pulp. For example, guaiacol was the major lignin-derived pyrolysis product from kraft and soda/AQ/MeOH pulps (23.8 and 23.6% of the total lignin peaks), while 4-vinylguaiacol was the main lignin-derived compound in the lignin from ASAM pulp (22.6%) [66].

Ibarra and coworkers [63] isolated the lignin from the pulping liquor and from the pulp of *Eucalyptus globulus*: (i) after acidic precipitation from the kraft liquors and (ii) after enzymatic hydrolysis of the kraft pulps (unbleached, delignified with oxygen, and bleached with peroxide). Kraft lignin recovered from the liquor was characterized mainly with syringol (23.7 molar relative abundance), 4-methylsyringol (16.7), 4-vinylsyringol (10.5), guaiacol (6.1), 4-vinylguaiacol (6.2), *trans*-isoeugenol (3.3), and the S/G ratio reported was 5.2, showing a preferential solubility of syringyl units during pulping, as discussed by Lourenço et al. [82]. In the case of the lignin isolated from the pulps, the main compounds produced were the same mentioned for kraft lignin but were formed in minor amounts as shown by the S/G of 3.0, 3.0, and 3.9, respectively, for unbleached, bleached with oxygen, and bleached with peroxide [63]. These values are closer to the reported for eucalypt MWL, indicating that the lignin modified during pulping was released to the liquor and the pulps retained a residual lignin with features near to those of native lignin.

The lignins isolated enzymatically from pulps produced with beech wood (*Fagus sylvatica*), with different delignification processes, were characterized by an H:G:S relation of 1:20:14, 1:7:6, 1:78:88, and 1:20:13 for, respectively, kraft, sulfite, ASAM, and soda/AQ/MeOH pulps, while the corresponding S/G ratio values were 0.68, 0.77, 1.12, and 0.66 [66]. The main lignin-derived compounds produced by pyrolysis were 4-vinylsyringol (17.5% of total lignin) in lignin from sulfite pulp, and syringol (16.8, 17.4, and 21.5%) in, respectively, ASAM, kraft, and soda/AQ/MeOH pulps.

4. Concluding remarks

Analytical pyrolysis has proved to be an important tool for chemical characterization of lignocellulosic materials, including woods and barks, in particular to evaluate the lignin monomeric composition and its composition during delignification and bleaching process for the production of cellulosic pulps. Analytical pyrolysis is a versatile methodology that may be applied to characterize the lignin directly on the lignocellulosic material or after isolation from the cell wall matrix (e.g., as MWL or dioxane lignin) or from spent liquors.

Pyrolysis presents several advantages, such as the small sample size, easy preparation, and is a rapid technique with good reproducibility, although it has constraints regarding the influence that the analysis conditions have on the obtained

pyrolysis products and the little information given regarding carbohydrates profile. It is, however, an excellent methodology with a high potential to study lignin compositional variability in different materials and along various processing pathways.

Acknowledgments

Author details

Ana Lourenço*, Jorge Gominho and Helena Pereira
Forest Research Center, School of Agriculture, University of Lisbon, Lisbon, Portugal

*Address all correspondence to: analourenco@isa.ulisboa.pt

IntechOpen

References

[1] Meier D, Faix O. Pyrolysis-gas-chromatography-mass spectroscopy. In: Lin SY, Dence CW, editors. Methods in Lignin Chemistry. New York: Springer Series in Wood Science; 1992. pp. 177-199

[2] Wampler TP. Analytical pyrolysis: An overview. In: Wampler TP, editor. Applied Pyrolysis Handbook. 2nd ed. New York: Taylor Francis Group; 2007. p. 288

[3] Demirbas A. Pyrolysis mechanisms of biomass materials. Energy Sources, Part A: Recovery, Utilization, and Environmental Effects. 2009;**31**(13):1186-1193

[4] Bahng M, Mukarakate C, Robichaud DJ, Nimlos MR. Current technologies for analysis of biomass thermochemical processing: A review. Analytica Chimica Acta. 2009;**651**:117-138

[5] Demirbas A, Arin G. An overview of biomass pyrolysis. Energy Sources. 2002;**24**:471-482

[6] Dong C, Zhang Z, Lu Q, Yang Y. Characteristics and mechanism study of analytical fast pyrolysis of poplar wood. Energy Conversion and Management. 2012;**57**:49-59

[7] Wampler TP. Review. Introduction to pyrolysis-capillary gas chromatography. Journal of Chromatography A. 1999;**842**:207-220

[8] Holmbom B. Extractives. In: Timell TE, editor. Analytical Methods in Wood Chemistry Pulping and Papermaking. Springer-Verlag: Berlin; 1999. pp. 125-148

[9] Ranzi E, Cuoci A, Faravelli T, Frassoldati A, Migliavacca G, Pierucci S, et al. Chemical kinetics of biomass pyrolysis. Energy & Fuels. 2008;**22**:4292-4300

[10] Kawamoto H, Horigoshi S, Saka S. Pyrolysis reactions of various lignin model dimers. Journal of Wood Science. 2007;**53**:168-174

[11] Kawamoto H, Ryoritani M, Saka S. Different pyrolytic cleavage mechanisms of b-ether bond depending on the side-chain structure of lignin dimers. Journal of Analytical and Applied Pyrolysis. 2008;**81**:88-94

[12] Akazawa M, Kojima Y, Kato Y. Effect of pyrolysis temperature on the pyrolytic degradation mechanism of β-aryl ether linkages. Journal of Analytical and Applied Pyrolysis. 2016;**118**:164-174

[13] Brebu M, Vasile C. Thermal degradation of lignin—A review. Cellulose Chemistry and Technology. 2010;**44**(9):353-363

[14] Asmadi M, Kawamoto S, Saka S. Thermal reactions of guaiacol and syringol as lignin model aromatic nuclei. Journal of Analytical and Applied Pyrolysis. 2011;**92**:88-98

[15] Ralph J, Hatfield RD. Pyrolysis-GC-MS characterization of forage materials. Journal of Agricultural and Food Chemistry. 1991;**39**:1426-1437

[16] Hu J, Wu S, Jiang X, Xiao R. Structure-reactivity relationship in fast pyrolysis of lignin into monomeric phenolic compounds. Energy & Fuels. 2018;**32**:1843-1850

[17] Kawamoto H. Lignin pyrolysis reactions. Journal of Wood Science. 2017;**63**:117-132

[18] Stefanidis SD, Kalogiannis KG, Iliopoulou EF, Michailof CM, Pilavachi PA, Lappas AA. A study of lignocellulosic biomass pyrolysis via the pyrolysis of cellulose, hemicellulose and lignin. Journal of

Analytical and Applied Pyrolysis. 2014;**105**:143-150

[19] Asmadi M, Kawamoto H, Saka S. Thermal reactivities of catechols/pyrogallols and cresols/xylenols as lignin pyrolysis intermediates. Journal of Analytical and Applied Pyrolysis. 2011;**92**:76-87

[20] Shen DK, Gu S, Luo KH, Wang SR, Fang MX. The pyrolytic degradation of wood-derived lignin from pulping process. Bioresource Technology. 2010;**101**:6136-6146

[21] Yang H, Yan R, Chen H, Lee DH, Zheng C. Characteristics of hemicellulose, cellulose and lignin pyrolysis. Fuel. 2007;**86**:1781-1788

[22] Lu Q, Yang X, Dong C, Zhang Z, Zang X, Zhu X. Influence of pyrolysis temperature and time on the cellulose fast pyrolysis products: Analytical Py-GC/MS study. Journal of Analytical and Applied Pyrolysis. 2011;**92**:430-438

[23] Pouwels AD, Eijkel GB, Boon JJ. Curie-point pyrolysis-capillary gas chromatography-high-resolution mass spectrometry of microcrystalline cellulose. Journal of Analytical and Applied Pyrolysis. 1989;**14**(4):237-280

[24] Patwardhan P, Satrio JA, Brown RC, Shanks BH. Product distribution from fast pyrolysis of glucose-based carbohydrates. Journal of Analytical and Applied Pyrolysis. 2009;**86**:323-330

[25] Dobele G, Rossinskaja G, Telysheva G, Meier D, Faix O. Cellulose dehydration and depolymerization reactions during pyrolysis in the presence of phosphoric acid. Journal of Analytical and Applied Pyrolysis. 1999;**449**:307-317

[26] Li S, Lyons-Hart J, Banyasz J, Shafer K. Real-time evolved gas analysis by FTIR method: An experimental study of cellulose pyrolysis. Fuel. 2001;**80**:1809-1817

[27] Dobele G, Rossinskaja G, Dizhbite T, Telysheva G, Meier D, Faix O. Application of catalysts for obtaining 1,6-anhydrosaccharides from cellulose and wood by fast pyrolysis. Journal of Analytical and Applied Pyrolysis. 2005;**74**:401-405

[28] Shen DK, Gu S, Bridgwater AV. The thermal performance of the polysaccharides extracted from hardwood: Cellulose and hemicellulose. Carbohydrate Polymers. 2010;**82**:39-45

[29] Luo Z, Wang S, Liao Y, Cen K. Mechanism study of cellulose rapid pyrolysis. Industrial and Engineering Chemistry Research. 2004;**43**:5605-5610

[30] Zhu X, Lu Q. Production of chemicals from selective fast pyrolysis of biomass. In: Momba M, Bux F, editors. Biomass. Croatia: Sciyo; 2010. pp. 147-164

[31] Ponder GR, Richards GN. Thermal synthesis and pyrolysis of a xylan. Carbohydrate Research. 1991;**218**:143-155

[32] Kleen M, Gellerstedt G. Characterization of chemical and mechanical pulps by pyrolysis-gas chromatography/mass spectrometry. Journal of Analytical and Applied Pyrolysis. 1991;**19**:139-152

[33] Shen D, Jin W, Hu J, Xiao R, Luo K. An overview on fast pyrolysis of the main constituents in lignocellulosic biomass to value-added chemicals: Structures, pathways and interactions. Renewable and Sustainable Energy Reviews. 2015;**51**:761-774

[34] Faix O, Fortman I, Bremer J, Meier D. Thermal degradation products of wood. Gas chromatographic separation and mass spectrometric characterization of polysaccharide

derived products. Holz als Roh-und Werkstoff. 1991;**49**:213-219

[35] Faix O, Fortman I, Bremer J, Meier D. Thermal degradation products of wood. A collection of electron-impact (EI) mass spectra of polysaccharide derived products. Holz als Roh-und Werkstoff. 1991;**49**:299-304

[36] Dobele D, Dizhbite T, Rossinskaja G, Telysheva G, Meier D, Radtke S, et al. Pre-treatment of biomass with phosphoric acid prior to fast pyrolysis. A promising method for obtaining 1,6-anhydrosaccharides in high yields. Journal of Analytical and Applied Pyrolysis. 2003;**68-69**:197-211

[37] Müller-Hagedorn M, Bockhorn H, Krebs L, Müller U. A comparative kinetic study on the pyrolysis of three different wood species. Journal of Analytical and Applied Pyrolysis. 2003;**68-69**:231-249

[38] Patwardhan PR, Satrio JA, Brown RC, Shanks BH. Influence of inorganic salts on the primary pyrolysis products of cellulose. Bioresource Technology. 2010;**101**:4646-4655

[39] Moldoveanu SC. Analytical pyrolysis of natural organic polymers. In: Techniques and Instrumentation in Analytical Chemistry. Vol. 20. Amsterdam: Elsevier; 1998. 496 p

[40] Wang S, Guo X, Wang K, Luo Z. Influence of the interaction of components on the pyrolysis behavior of biomass. Journal of Analytical and Applied Pyrolysis. 2011;**91**:183-189

[41] Kawamoto H, Morisaki H, Saka S. Secondary decomposition of levoglucosan in pyrolytic production from cellulosic biomass. Journal of Analytical and Applied Pyrolysis. 2009;**85**:247-251

[42] Neves D, Thunman H, Matos A, Tarelho L, Gómez-Barea A.

Characterization and prediction of biomass pyrolysis products. Progress in Energy and Combustion Science. 2011;**37**:611-630

[43] Amen-Chen C, Pakdel H, Roy C. Production of monomeric phenols by thermochemical conversion of biomass: A review. Bioresource Technology. 2001;**79**:277-299

[44] Marques AV, Pereira H. Aliphatic bio-oils from corks: A Py-GC/MS study. Journal of Analytical and Applied Pyrolysis. 2014;**109**:29-40

[45] Brunow G, Lundquist K, Gellersted G. Lignin. In: Sjöström E, Alén R, editors. Analytical Methods in Wood Chemistry, Pulping, and Papermaking. New York: Springer Series in Wood Science; 1998. pp. 77-124

[46] del Río JC, Gutiérrez A, Hernando M, Landín P, Romero J, Martínez AT. Determining the influence of eucalypt lignin composition in paper pulp yield using Py-GC/MS. Journal of Analytical and Applied Pyrolysis. 2005;**74**:110-115

[47] del Rio JC, Gutiérrez A, Romero J, Martínez MJ, Martínez AT. Identification of residual lignin markers in eucalypt kraft pulps by Py-GC/MS. Journal of Analytical and Applied Pyrolysis. 2001;**58-59**:425-439

[48] Marques AV, Pereira H. Lignin monomeric composition of corks from the barks of *Betula pendula*, *Quercus suber* and *Quercus cerris* determined by Py-GC-MS/FID. Journal of Analytical and Applied Pyrolysis. 2013;**100**:88-94

[49] Alves A, Schwanninger M, Pereira H, Rodrigues J. Analytical pyrolysis as a direct method to determine the lignin content in wood—Part 1: Comparison of pyrolysis lignin with Klason lignin. Journal of Analytical and Applied Pyrolysis. 2006;**76**:209-213

[50] Alves A, Rodrigues J, Wimmer R, Schwanninger M. Analytical pyrolysis as a direct method to determine the lignin content in wood. Part 2: Evaluation of the common model and the influence of compression wood. Journal of Analytical and Applied Pyrolysis. 2008;**81**:167-172

[51] Klinberg A, Odermatt J, Meier D. Influence of parameters on pyrolysis-GC/MS of lignin in the presence of tetramethylammonium hydroxide. Journal of Analytical and Applied Pyrolysis. 2005;**74**:104-109

[52] Rowell RM, Pettersen R, Han JS, Rowell JS, Tshabalala MA. Cell wall chemistry. Part 1. Structure and chemistry. In: Rowell RM, editor. Handbook of Chemistry and Wood Composites. Florida: Taylor Francis; 2005

[53] Alves A, Gierlinger N, Schwanninger M, Rodrigues J. Analytical pyrolysis as a direct method to determine the lignin content in wood. Part 3. Evaluation of species-specific and tissue-specific differences in softwood lignin composition using principal component analysis. Journal of Analytical and Applied Pyrolysis. 2009;**85**:30-37

[54] Ohra-aho T, Linnekoski J. Catalytic pyrolysis of lignin by using analytical pyrolysis-GC-MS. Journal of Analytical and Applied Pyrolysis. 2015;**113**:186-192

[55] Lourenço A, Gominho J, Marques AV, Pereira H. Variation of lignin monomeric composition during kraft delignification of *Eucalyptus globulus* heartwood and sapwood. Journal of Wood Chemistry and Technology. 2013;**33**:1-18

[56] Lourenço A, Gominho J, Marques AV, Pereira H. Py-GC/MS(FID) assessed polysaccharides behavior during kraft delignification of *Eucalyptus globulus* heartwood and sapwood. Journal of

Analytical and Applied Pyrolysis. 2013;**101**:142-149

[57] del Río JC, Martínez AT, Gutiérrez A. Presence of 5-hydroxyguaiacyl units as native lignin constituents in plant as seen by Py-GC/MS. Journal of Analytical and Applied Pyrolysis. 2007;**79**:33-38

[58] Oudia A, Mészaros E, Jakab E, Simões R, Queiroz J, Ragauskas A, et al. Analytical pyrolysis study of biodelignification of cloned *Eucalyptus globulus* (EG) clone and *Pinus pinaster* Aiton kraft pulp and residual lignins. Journal of Analytical and Applied Pyrolysis. 2009;**85**:19-29

[59] Rencoret J, Gutierrez A, del Río JC. Lipid and lignin composition of woods from different eucalypt species. Holzforschung. 2007;**61**:165-174

[60] Rodrigues J, Graça J, Pereira H. Influence of tree eccentric growth on syringyl/guaiacyl ratio of *Eucalyptus globulus* wood lignin accessed by analytical pyrolysis. Journal of Analytical and Applied Pyrolysis. 2001;**58-59**:481-489

[61] Yokoi H, Nakase T, Ishida Y, Ohtani H, Tsuge S, Sonoda T, Ona T. Discriminative analysis of *Eucalyptus camaldulensis* grown from seeds of various origins based on lignin components measured by pyrolysis-gas chromatography. Journal of Analytical and Applied Pyrolysis. 2001;**57**:145-152.

[62] Yokoi H, Ishida Y, Ohtani H, Tsuge S, Sonoda T, Ona T. Characterization of within-tree variation of lignin components in *Eucalyptus camaldulensis* by pyrolysis-gas chromatography. The Analyst. 1999;**124**:669-674

[63] Ibarra D, Chávez MI, Rencoret J, del Río JC, Gutiérrez A, Romero J, et al. Lignin modification during *Eucalyptus globulus* kraft pulping followed by totally chlorine-free

bleaching: A two-dimensional nuclear magnetic resonance, Fourier transformed infrared, and pyrolysis-gas chromatography/ mass spectrometry study. Journal of Agricultural and Food Chemistry. 2007;**55**:3477-3490

[64] Evtuguin D, Neto CP, Silva AMS, Domingues PM, Amado FML, Robert D, et al. Comprehensive study on the chemical structure of dioxane lignin from plantation *Eucalyptus globulus* wood. Journal of Agricultural and Food Chemistry. 2001;**49**:4252-4261

[65] Genuit W, Boon JJ, Faix O. Characterization of beech milled wood lignin by pyrolysis-gas chromatography-photoionization mass spectrometry. Analytical Chemistry. 1987;**59**:508-513

[66] Choi JW, Faix O, Meier D. Characterization of residual lignins from chemical pulps of spruce (*Picea abies* L.) and beech (*Fagus sylvatica* L.) by analytical pyrolysis-gas chromatography/mass spectrometry. Holzforschung. 2001;**55**:185-192

[67] Rencoret J, Marques G, Gutiérrez A, Nieto L, Jiménez-Barbero J, Martínez AT, et al. Isolation and structural characterization of the milled-wood lignin from *Paulownia fortunei* wood. Industrial Crops and Products. 2009;**30**:137-143

[68] Lourenço A, Rencoret J, Chematova C, Gominho J, Gutiérrez A, del Río JC, et al. Lignin composition and structure differs between xylem, phloem and phellem in *Quercus suber* L. Frontiers in Plant Science. 2016;**7**:1612. DOI: 10.3389/fpls.2016.01612

[69] Lourenço A, Neiva D, Gominho J, Marques AV, Pereira H. Characterization of lignin in heartwood, sapwood and bark from *Tectona grandis* using Py-GC-MS/ FID. Wood Science and Technology.

2015;**49**(1):159-175. DOI: 10.1007/ s00226-014-0684-6

[70] Ghalibaf M, Lehto J, Alén R. Fast pyrolysis of hot-water-extracted and delignified silver birch (*Betula pendula*) sawdust by Py-GC/MS. Journal of Analytical and Applied Pyrolysis. 2017;**127**:17-22

[71] Lourenço A, Neiva DM, Gominho J, Curt MD, Fernández J, Marques AV, et al. Biomass production of four *Cynara cardunculus* clones and lignin composition analysis. Biomass and Bioenergy. 2015;**76**:86-95. DOI: 10.1016/j.biombioe.2015.03.009

[72] Lourenço A, Rencoret J, Chemetova C, Gominho J, Gutiérrez A, Pereira H, et al. Isolation and structural characterization of lignin from cardoon (*Cynara cardunculus* L.) stalks. Bioenergy Research. 2015;**8**(4):1946-1955. DOI: 10.1007/s12155-015-9647-5

[73] del Río JC, Rencoret J, Gutiérrez A, Nieto L, Jiménez-Barbero J, Martínez AT. Structural characterization of guaiacyl-rich lignins in flax (*Linum usitatissimum*) fibers and shives. Journal of Agricultural and Food Chemistry. 2011;**59**:11088-11099

[74] Hodgson EM, Nowakowski DJ, Shield I, Riche A, Bridgwater AV, Clifton-Brown JC, et al. Variation in *Miscanthus* chemical composition and implications for conversion by pyrolysis and thermos-chemical bio-refining for fuels and chemicals. Bioresource Technology. 2011;**102**:3411-3418

[75] Marques AV, Pereira H, Meier D, Faix O. Quantitative analysis of cork (*Quercus suber* L.) and milled cork lignin by FTIR spectroscopy, analytical pyrolysis and total hydrolysis. Holzforschung. 1994;**48**(Suppl):43-50

[76] del Río JC, Lino AG, Colodette JL, Lima CF, Gutiérrez A, Martínez AT, et al. Differences in the chemical structure

of the lignin from sugarcane bagasse and straw. Biomass and Bioenergy. 2015;**81**:322-338

[77] Berhanu H, Kiflie Z, Miranda I, Lourenço A, Ferreira J, Feleke S, et al. Characterization of crop residues from false banana/*Enset ventricosum*/ in Ethiopia in view of full-resource valorization. PLoS One. 2018;**13**(7):e0199422

[78] Sen A, Pereira H, Olivella MA, Villaescusa I. Heavy metals removal in aqueous environments using bark as a biosorbent. International Journal of Environmental Science and Technology. 2015;**12**:391-404

[79] Leite C, Pereira H. Cork-containing barks—A review. Frontiers in Materials. 2017;**3**:63

[80] Marques AV, Pereira H, Rodrigues J, Meier D, Faix O. Isolation and comparative characterisation of a Björkman lignin from the saponified cork of Douglas-fir bark. Journal of Analytical and Applied Pyrolysis. 2006;**77**:169-176

[81] Ohra-aho T, Tenkanen M, Tamminen T. Direct analysis of lignin and lignin-like components from softwood kraft pulp by Py-GC/MS techniques. Journal of Analytical and Applied Pyrolysis. 2005;**74**:123-128

[82] Lourenço A, Gominho J, Marques AV, Pereira H. Reactivity of syringyl and guaiacyl lignin units and delignification kinetics in the kraft pulping of *Eucalyptus globulus* wood using Py-GC-MS/FID. Bioresource Technology. 2012;**123**:296-302

Section 2

Thermal Degradation Study

Chapter 3

Release Profile of Nitrogen during Thermal Treatment of Waste Wooden Packaging Materials

Liuming Song, Xiao Ge, Xueyong Ren, Wenliang Wang, Jianmin Chang and Jinsheng Gou

Abstract

In this paper, the fast pyrolysis experiment of particle board was carried out on a fixed bed reactor and a Py-GC/MS equipment. The effects of temperature and gas phase residence time on the product yields and its components distribution were investigated. The effect of components of particle board on product yields and its components distribution was also investigated. The results showed that the temperature has a great influence on the yields of fast pyrolysis products, and the yield of pyrolysis oil reached the highest at 550°C. The urea-formaldehyde resin would prevent the pyrolysis of particle board. Compared with the bio-oil from fast pyrolysis of wood, the major components of the bio-oil from fast pyrolysis of particle board did not change much.

Keywords: pyrolysis, fixed bed, Py-GC/MS, particle board, bio-oil

1. Introduction

The world concerns about environmental pollution caused by fossil fuel combustion and exhaustion of energy resources have drawn significant attention to researchers. Biomass can be converted into various fuels and chemicals by different methods to replace petrochemical fuels [1–3]. Fast pyrolysis of biomass is one of the most promising and fast developing biomass thermochemical conversion technologies, which can turn organic materials into high value products such as chemical products or liquid fuels. And this technology has been widely used in the field of biomass renewable utilization in recent years [4–6]. This transformation into an environment-friendly renewable energy sources can replace the fossil fuels consumed and reduce greenhouse gas emissions. Among the biomass, the large amount of waste wood has attracted increasing attention because it can be used as an energy and reduce the waste of timber [7–9].

Particle boards occupy a large proportion of waste wood, so how to effectively convert it into high value chemical products has attracted the attention of researchers. Choi et al. [3] conducted fast pyrolysis of particle board over three types of zeolite catalysts, the results showed that the bio-oil yield and gas yield in catalytic pyrolysis was lower and higher than those in non-catalytic pyrolysis, respectively. Park et al. [10] also examined the catalytic pyrolysis of particle board using a nanoporous catalyst and showed that bio-oil is composed mainly of

oxygenates, phenolics and acids, with smaller amounts of aromatics and hydrocarbons. Lee et al. [11] investigated the co-pyrolysis of waste particle board and polypropylene over four types of catalysts, they found that catalytic co-pyrolysis suppressed the formation of PAHs, and the quality of bio-oil has improved. When the particle board was combined with other materials for co-pyrolysis, or when the particle board was pyrolyzed over different catalysts, high quality bio-oil or aromatic products could be obtained [8, 11–13].

When only the particle board was pyrolyzed, many researchers have found that temperature was the most important factor to determine the yields of bio-oil and gas products. Most scholars have only studied the influence of temperature on the pyrolysis characteristics of wood and particleboard, and there are few literatures concerning the influence of other conditions on the pyrolysis characteristics of wood and particle board. In this paper, fast pyrolysis experiments were carried out in fixed bed reactor and a Py-GC/MS equipment, and the effects of temperature and gas phase residence time on the product yields and its components distribution were investigated. The effect of components of particle board on product yields and its components distribution was also investigated.

2. Materials and methods

2.1 Experimental materials and characteristics analysis

2.1.1 Experimental materials

The experimental samples selected for this study included two types of solid wood, a wood adhesive, and six types of particle board.

Two types of solid wood, Larch wood (*Larix gmelinii* (Rupr.) Rupr.) and Poplar wood (*Populus deltoides*), which are the most commonly used for the production of wood based panel, were selected. Larch wood and Poplar wood were obtained from the north of Daxinganling, Inner Mongolia, the age of the trees was around 30 and 10 years respectively. Larch wood and Poplar wood were marked with "Larch" and "Poplar" respectively.

Urea formaldehyde (UF) is the most commonly used adhesive in the wood based panel industry. Provided by Beijing Taier Chemical Co., Ltd., its F/U molar ratio is 1.1 and the solids content is 53%.

PBL: Larch Particle Board and PBP: Poplar Particle Board. The adhesive levels used for preparing particle boards were 5%, 10%, and 20%, respectively.

The particle board was made in our laboratory (width: 400 × 400 mm, thickness: 10mm). There was a certain difference between self-made particle board and actual waste particle board, but there were uncertainties in the waste time, wood types, adhesive types and content, etc., which were actually unfavorable for research and analysis of results. Therefore, the particle board was placed in a room under controlled environment for 6 months after preparation to simulate the waste particle board in nature.

2.1.2 Characteristic analysis

The materials of solid wood and particle board were crushed, sieved and dried before the experiment. After the adhesive was dried and solidified in the oven, it was crushed and sieved, all materials have a particle size of about 1 mm. Elemental analysis, industrial analysis and component analysis of raw materials are shown in **Tables 1–3**, respectively.

Sample[a]	C%	H%	O%[b]	N%
Larch	46.15	6.31	47.36	0.12
Poplar	45.24	6.30	48.36	0.10
UF	33.45	5.02	29.31	32.22
PBL (10% sizing amount)	44.15	6.11	46.28	3.46
PBP (10% sizing amount)	43.35	5.96	47.55	3.14

[a]*The test result was an air-drying base.*
[b]*The oxygen value was obtained by subtraction.*

Table 1.
Element analysis of samples (wt%).

Sample[a]	M%	A%	V%	FC%
Larch	7.26	1.78	73.12	17.84
Poplar	6.79	1.81	72.51	18.89
UF	2.18	0.53	95.98	1.31
PBL	6.04	1.68	73.43	18.85
PBP	6.37	1.57	73.01	19.05

[a]*The test result was an air-drying base.*

Table 2.
Proximate analysis of samples (wt%).

Sample[a]	Cellulose %	Hemicellulose %[b]	Holocellulose %	Lignin %	pH	Ash %	Benzol extractive %
Larch	42.76	20.79	63.55	24.03	4.90	0.905	3.26
Poplar	45.87	28.44	74.31	19.12	5.01	1.169	5.89

[a]*The test result was an air-drying base*
[b]*The hemicellulose value was obtained by subtraction.*

Table 3.
Component analysis of samples.

Elemental analysis of raw materials was performed using the VarioEL elemental analyzer at the Analytical Center of Changchun Institute of Chemicals, Chinese Academy of Sciences. The analysis was conducted in accordance with the International "Method for Analysis of Carbon, Hydrogen, and Oxygen in Rock Organic Matter" (GB/T 19143-2003), where C, H, and N elements were tested experimentally and the final results were averaged twice for the experiment. The O element content was obtained by subtraction.

The industrial analysis was completed at the Chemical Laboratory of Beijing Forestry University, and conducted according to the national standard "Test Methods for Charcoal and Charcoal" (GB/T17664-1999). From **Table 2**, it can be concluded that the ash content of Poplar was larger than that of Larch, and the volatile content of particle board and solid wood was equivalent, while the volatile content of UF resin was much higher than that of solid wood and particle board, but the fixed carbon of particle board was higher than solid wood and UF resin.

The chemical composition analysis was performed in the Bio-oil Adhesives Laboratory at Beijing Forestry University. The raw material preparation was performed in accordance with the national standard, "Analysis of Samples for Papermaking Raw Material Analysis" (GB/T 2677.1-93). The lignin content was determined according to the national standard "Determination of Acid-insoluble Lignin in Papermaking Raw Materials" (GB/T 2677.8-94), the cellulose content was extracted by nitric acid ethanol method, and the holocellulose content was determined according to the national standard "Determination of Holocellulose Content of Papermaking Raw Materials" (GB/T 2677.10-1995). The lignin content of Larch was higher than that of Poplar from **Table 3**, while the Poplar content of cellulose and hemicellulose was higher than that of Larch.

2.2 Experimental devices and methods

In this article, two devices were used to discuss the fast pyrolysis characteristics of waste particle board. One was a fixed bed fast pyrolysis device (fixed-bed reactor), and the other was a Py-GC/MS equipment. The yields of product were obtained from the fast pyrolysis experiments which were carried out on the fixed bed reactor. The distribution of components in the liquid phase products and the distribution of nitrogen were analyzed by Py-GC/MS equipment.

2.2.1 Fixed bed reactor and experimental method

In this paper, a set of experimental apparatus for fast pyrolysis of small gas entrainment fixed bed was designed, precise automatic temperature control and extremely short gas phase residence time could be achieved through the device. The whole device consisted of gas supply system, sampling system, pyrolysis system, product absorption and measurement system. The schematic diagram of the experimental device is shown in **Figure 1**.

The gas supply system consisted of nitrogen cylinder, flow meter and three-way valve, etc. Nitrogen cylinder was equipped with safety valve and the nitrogen gas purity was 99.999%. The sampling system consisted of a feeding pipeline and a vibrating feeding device, which allows the continuous and
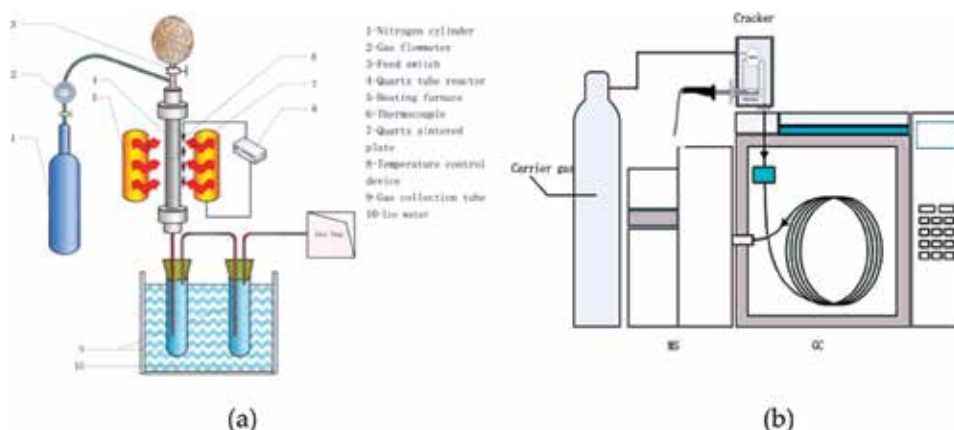

Figure 1.
Schematic of (a) fixed bed fast pyrolysis reactor with carry gas feeding module, and (b) Py-GC/MS.

uniform feeding of small amount of materials (less than 5 g). The pyrolysis system consisted of an automatic temperature-controlled electric heating furnace, a quartz tube reactor and a pipe end interface. The fixed-bed reactor was a quartz tube with an inner diameter of 20mm and a length of 500 mm, a quartz sintered plate was set in the middle of the tube to filter pyrolytic carbon produced by pyrolysis, both ends of the quartz tube were special metal quick connectors for convenient installation and removal, connected with stainless steel pipe through quick connector. The product absorption system consisted of a two-stage ice-water bath condensing tube, and an exhaust gas collection bag coupled with a volume flow meter.

The requirement of temperature for fast pyrolysis is 400∼600°C [1, 14–15]. In this paper, in order to explore the pyrolysis characteristics of temperature and the nitrogen release mechanism of the particle board, four pyrolysis temperatures were selected, which were 450, 500, 550 and 600°C, respectively.

The requirement for the gas phase residence time of the fast pyrolysis process is 3–0.1 s [1, 14, 15], in order to investigate the influence of gas-phase residence time on the pyrolysis characteristics and nitrogen release mechanism of particle board, three gas-phase residence time were set in the research process, which were 3, 1 and 0.5 s respectively. Considering that the gas phase residence time was controlled by the flow rate of the carrier gas during the actual experiment, the relationship between the gas flow rate and the gas phase residence time at different pyrolysis temperatures was calculated before the formal experiment, the corresponding carrier gas flow rate was 0.1, 0.16, and 0.3 m^3/h, respectively.

The temperature of the heating furnace was first determined during the experiment, and the pyrolysis system will stably maintained at the pyrolysis temperatures; then, the prepared feedstock was loaded into the feeding bag; open the intake system valve at a predetermined flow rate and began to purge the entire experimental pipeline with high-purity nitrogen to obtain the inert environment. After the temperature of the pyrolysis system was stabilized to the pyrolysis temperature, the feedstock particle slowly entered the injection line through the vibration feed tube, the material which fell into the injection line entrained by the carrier gas into the quartz tube reactor for fast pyrolysis reactions. The pyrolysis-generated volatiles and pyrolytic carbons entered the gas absorption and metering system with the carrier gas after being filtered by the sintered plate in the center of the quartz tube and the filter quartz wool placed at the end of the reactor pipeline. Pyrolytic carbon remaining in the reactor was collected after pyrolysis was completed.

The calculation of fast pyrolysis gas yield was converted into weight fraction after metering volume by flowmeter, the fast pyrolysis carbon yield was calculated by direct weighing, and the fast pyrolysis oil yield was obtained by subtraction method. In a typical experiment run, the feeding amount was 3 g, and the reaction temperatures of the fixed-bed quartz tube were 450, 500, 550, and 600°C respectively, the carrier gas flow rates were 0.1, 0.16, and 0.3 m^3/h respectively, and the pyrolysis time was 5 min.

2.2.2 Pyrolysis gas chromatography combined experimental device and method

The Py-GC/MS equipment included a cracking system and a gas chromatography coupled with mass spectrometry analysis system. The cracking system consisted of a CDS5150 fast thermal cracker, which was equipped with injection and gas loading supply system manufactured by CDS, USA. The gas chromatography

mass spectrometry analysis system consisted of a Shimadzu GCMS-QP2010Plus GC/MS analysis manufactured by Shimadzu Corporation of Japan. The pyrolysis system and the gas chromatograph mass spectrometry system were connected by a special insulation connecting pipeline, the chromatographic column was M-5 (60 m × 0.25 mm × 0.25 μm). The schematic diagram of the experimental device is shown in **Figure 1**.

During the experiment, accurately weighed raw materials and a little amount of quartz fiber were placed in the quartz tube of the CDS5150 cracker. The pyrolyzer was purged with high-purity nitrogen as the carrier gas, pyrolyzed at the determined heating rate, pyrolysis time, and pyrolysis temperature, and the product was analyzed online by GC/MS. The spectra obtained for each test were analyzed using the system's software. The NIST library was used to record the product's absolute peak area and relative peak area.

When using the NIST library for analysis, most of the peaks could be identified and confirmed, but there were also a small number of peaks that could not be determined (the degree of similarity between the library and the standard material provided by the library was too low). Therefore, the sum of the relative peak area content determined by GC/MS in the relevant experimental results was less than 100%. The part where the sum did not reach 100% was the unknown product, but this part was very small and was represented by other classes in the result analysis.

The Py-GC/MS experimental conditions and instrument parameter settings are shown in **Table 4**.

Parameter name		Setting value
Cracking conditions	Heating rate	20°C/ms
	Pyrolysis temperature	400, 500, 600°C
	Cracking time	15 s
	Gas flow	100, 50, 10 ml/min
Gas chromatographic conditions	Inlet temperature	280°C
	Gas loading	He
	Gas flow rate	1.0 ml/min
	Split ratio	100:1
	Heating program	50°C constant temperature 5 min, warm up to 280°C at 10°C/min, constant temperature 15 min
	Interface temperature	280°C
	Ion source temperature	250°C
Mass spectrometry conditions	EI source electron energy	70 eV
	Scanning method	SCAN
	Scan range	(20–450) u

Table 4.
Conditions and parameters for Py-GC/MS experiments.

3. Results and discussion

3.1 Influence of pyrolysis conditions on the yields of fast pyrolysis product of waste particle board

3.1.1 Effect of temperature on yields of fast pyrolysis product

Figure 2 shows the yields of fast pyrolysis products of UF resin, two types of wood and particle board at different temperatures. As can be seen from the figure, the effect of temperature on the pyrolysis products of raw materials was basically the same in the experimental temperature range. Wood mainly consists of cellulose, hemicellulose and lignin, and therefore its pyrolysis behavior can be considered to be the sum of the behaviors of these three components [16]. The pyrolysis products contain such substances as CO, CO_2, H_2, CH_4, C_2H_4, amine, alcohol, phenol, acid, ketone, sugar, aldehyde, ester, ether, hydrocarbon and heterocyclic. As the temperature rise, the yields of gas product gradually increased, and the rising tendency became more pronounced when the temperature exceeded 550°C. The yields of pyrolytic carbon gradually decreased with the increase of temperature, when the temperature exceeded 550°C, the downward trend tended to be gentle. The yields of pyrolysis oil increased and then decreased with the increase of temperature, which reached a maximum at 550°C. During the pyrolysis process, the carbonization reaction dominated at a lower temperature, and the volatilization was insufficient. At a higher temperature condition, the cracking reaction intensified, a large number of condensable volatiles precipitated, the yield of pyrolysis oil increased subsequently, and the output of pyrolytic carbon decreased. At 600°C, the secondary cracking in the reaction system will gradually strengthen while the components in the condensable volatiles undergo secondary cracking, resulting in the formation of small molecules of non-condensable gases. The sugars, alcohols, ketones and acids in tar contain functional groups such as hydroxyl
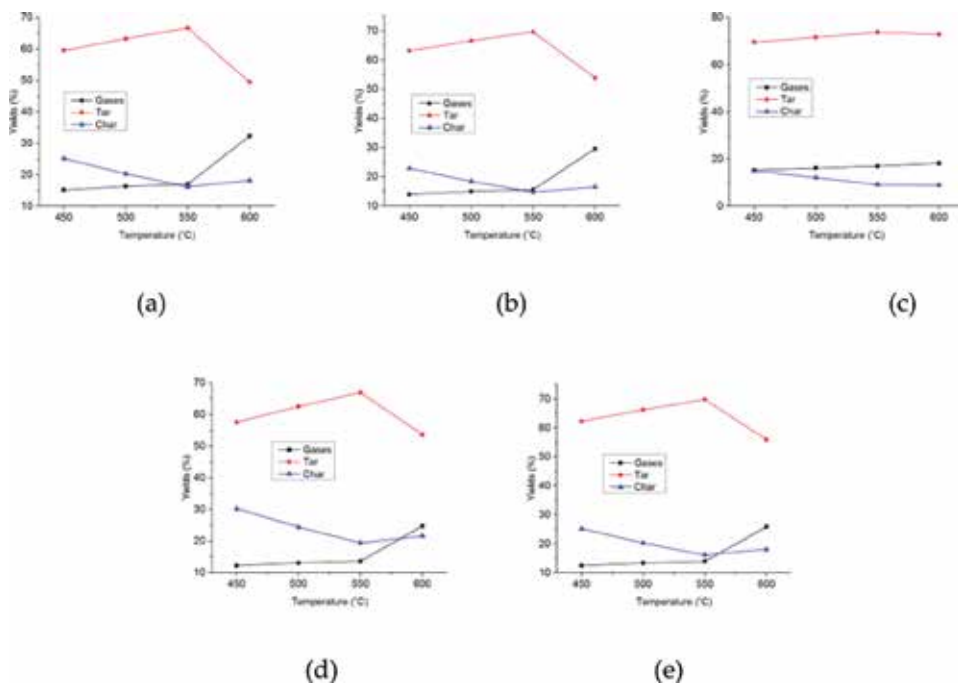
Figure 2.
Yields of products from fast pyrolysis at different temperature of (a) Larch, (b) Poplar, (c) UF, (d) PBL, and (e) PBP.

and carboxyl groups, with the increase of temperature, these functional groups will decompose and produce gases such as CO and CO_2, resulting in the increase of gas phase products, which in turn reduced the yield of pyrolysis oil. During wood pyrolysis, lignin produces more fixed carbon than cellulose and hemicellulose, so the char yield of Larch and Poplar is higher than that of UF resin. Because the structure of UF resin is not complicated with wood, the yield change of UF resin in the pyrolysis process is not as obvious as that of wood and particle board, and the products are relatively few, mainly ester and amine substances [16].

Figures 3 and **4** show the cumulative histogram of the yield distribution from fast pyrolysis products of PBL and PBP and their components at different temperatures. From **Figure 3**, it can be seen that due to the effect of UF resin, the yield of fast
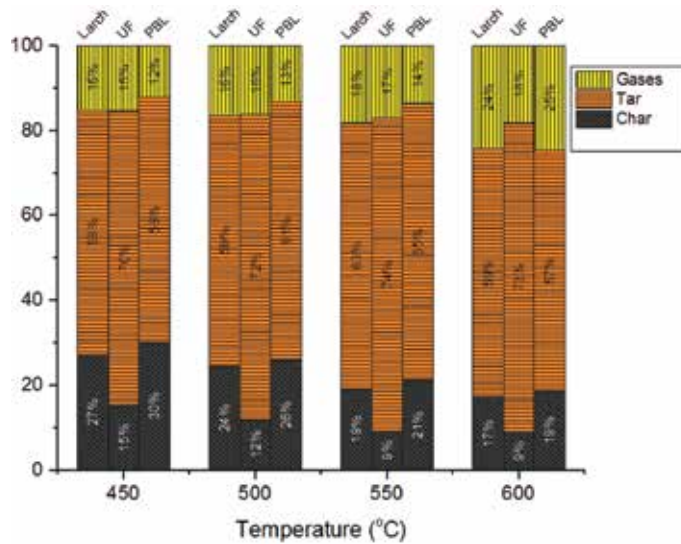
Figure 3.
Distribution of products from fast pyrolysis of PBL at different temperatures.
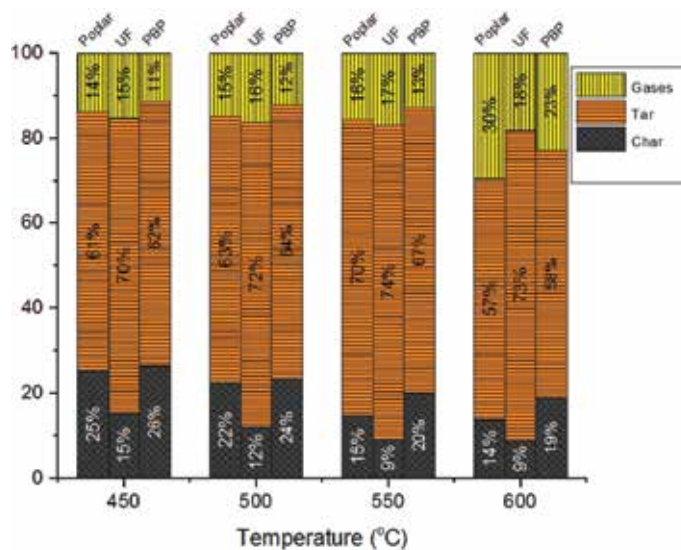
Figure 4.
Distribution of products from fast pyrolysis of PBP at different temperatures.

pyrolysis carbon of PBL is higher than that of Larch, and it can be inferred that UF resin will prevent the pyrolysis of the particle board at high temperatures. As the temperature rises, this inhibition slows down, at 450°C, particle board fast pyrolysis carbon is 3% higher than Larch, while the pyrolytic carbon from particle board is only 1% higher than that from Larch when the temperature reaches 600°C. The yield of pyrolysis oil from fast pyrolysis of particle board is basically the same as the yield from Larch at 450°C, and the former is less than later when the temperature setting at 500 and 550°C. However, when the temperature exceeds 600°C, the yield of pyrolysis oil from fast pyrolysis of particle board is less than that from Larch. This is because the yield of pyrolysis oil of UF resin is high than that of wood, which resulted in the superposition effect; and on the other hand, it also shows that the introduction of UF resin has an impact on the yield of pyrolysis oil, which is more sensitive to temperature. From **Figure 4**, it can be seen that the effect of UF resin on the yield of fast pyrolysis products of PBP is similar to that of PBL, which has an inhibitory effect on the pyrolysis process of the particle board, and increases the yield of pyrolytic carbon of the particle board, along with the temperature increased this inhibition slows down.

Figure 5 shows the content comparison diagram of Tar and Char in the fast pyrolysis products from different materials. As can be seen from the figure, the Tar yield of the UF resin is significantly higher than that of other raw materials, and the Tar yield is higher at 550°C than at other temperatures. At 600°C, the decrease in Tar yield of other raw materials is more obvious with increasing temperature except UF resin. The Char yield of all raw materials decreased with the increase of temperature, but the Char yield of UF resin is significantly lower than other raw materials. The fast pyrolysis of wood and particle board yields of Tar and Char are basically the same, indicating that the addition of UF resin has little effect on the fast pyrolysis products Tar and Char.

3.1.2 Effect of carrier gas flow on yields of fast pyrolysis products

Figure 6 shows the yields of fast pyrolysis products of raw materials at different carrier gas flows. As can be seen from the figure, the increase in carrier gas flow rate can effectively prevent secondary cracking in the system, therefore, the yields of fast pyrolysis oil has been greatly improved with the increase of gas flow rate, and the production of pyrolytic carbon and gaseous has gradually decreased. When the flow rate of the carrier gas continues to increase, the secondary reaction has been at a relatively low level, and therefore, the effect on the product is relatively small. Compared with temperature, the influence of carrier gas flow rate on the distribution of fast pyrolysis products is relatively low, therefore, as long as gas phase residence time of less than 3 s can be ensured, a higher pyrolysis oil yield can be
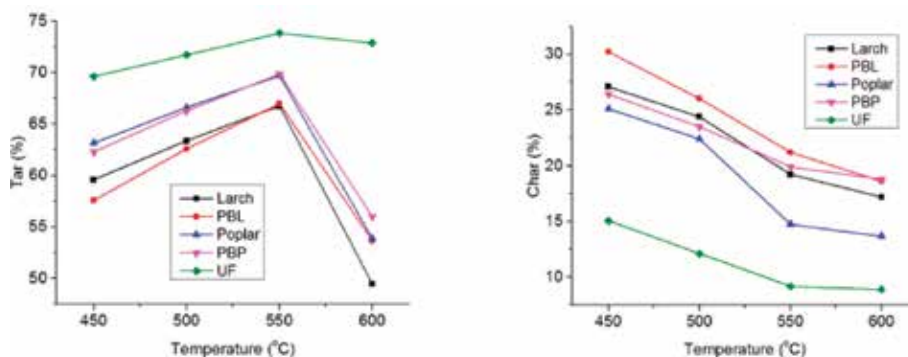
Figure 5.
Tar and char yields from fast pyrolysis of different raw materials at different temperatures.
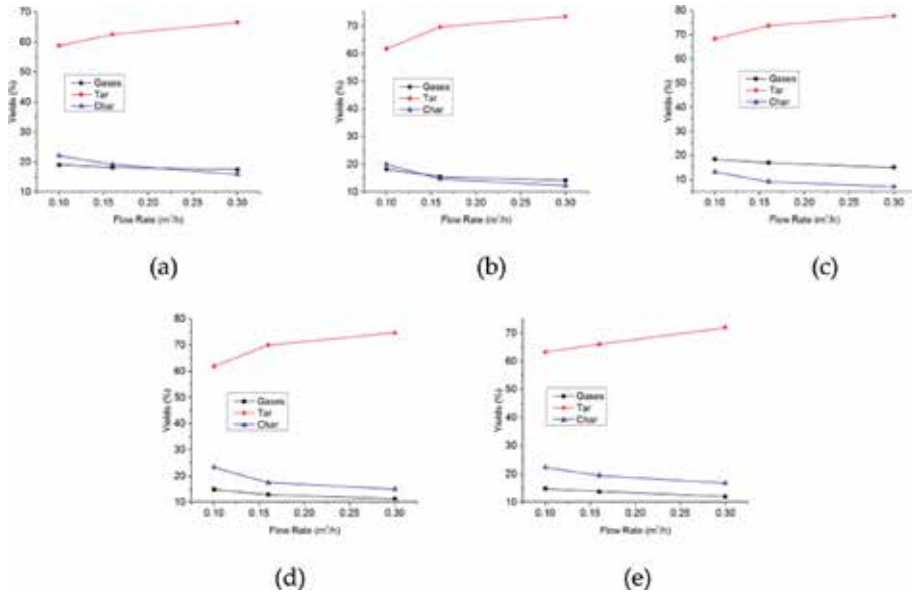
Figure 6.
Yields of fast pyrolysis products at different carrier gas flow rate of (a) Larch, (b) Poplar, (c) UF, (d) PBL, and (e) PBP.
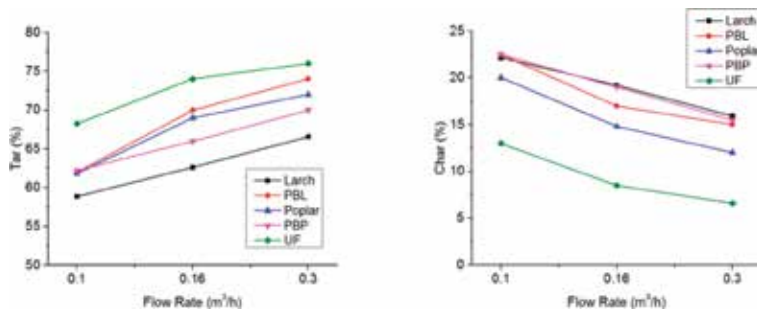
Figure 7.
Tar and char yields from fast pyrolysis of different raw materials at different flow rates.

obtained. Of course, increasing the flow rate of the carrier gas will contributes to the increase of pyrolysis oil yield, where other conditions permit.

Figure 7 shows the comparison of Tar and Char contents in fast pyrolysis products of different raw materials. From the figure, we can see that the Tar yield of UF resin increases with the increase of the carrier gas flow rate, which is basically the same as other raw materials, indicating that the degree of secondary pyrolysis of UF resin is equivalent to that of other raw materials. It shows that under the condition of fast pyrolysis, the addition of UF resin has no obvious effect on the wood and particle board product.

3.2 Influence of pyrolysis conditions on composition of fast pyrolysis products of waste particle board

3.2.1 Influence of pyrolysis conditions on distribution of gas product composition

Figure 8 changes of the gas composition in fast pyrolysis of raw materials at different temperatures. As can be seen from the figure, at different temperatures,
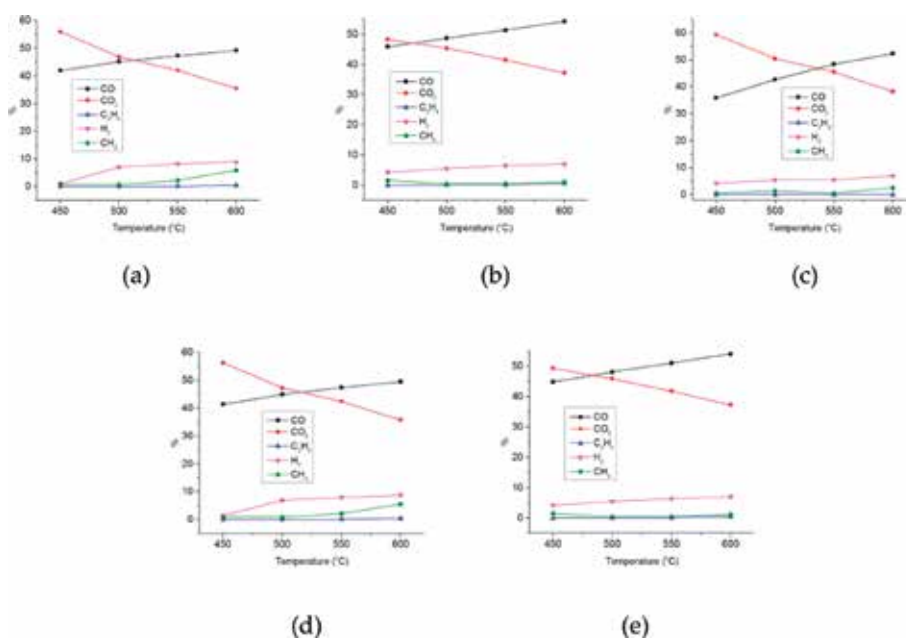
Figure 8.
Gaseous products distribution from fast pyrolysis at different temperature of (a) Larch, (b) Poplar, (c) UF, (d) PBL, and (e) PBP.

the fast pyrolysis gases of various raw materials are mainly CO and CO_2. With the increase of temperature, the CO content increased while the CO_2 content decreased, crossover occurred within the experimental temperature range, the temperature at this intersection varies depending on the composition of the raw materials. This aspect shows that the competitive reaction of the gas generated during the fast pyrolysis process is beneficial to the production of CO_2 at low temperatures, and is more conducive to the production of CO at high temperatures. It shows that the CO and CO_2 generation mode and mechanism are different during the fast pyrolysis process, and the effect of temperature on them is opposite. On the other hand, the cracking of the raw material in the fast pyrolysis process is accompanied by the secondary cracking of the primary volatiles, which means that the secondary cracking of the volatiles will generate more CO at high temperature, but it will not contribute much to the generation of CO_2, analysis shows that the CO is mainly produced by the cleavage of organic acids and aldehydes containing carbonyl groups and carboxyl groups. In addition, CO_2 reacts with the pyrolytic carbon in the reaction system to convert to CO at higher temperatures. The experimental results are similar to the fast pyrolysis experiments performed on different biomass in the literature.

As can be seen from **Figure 8**, the yield of several other gases is very small, with a relatively high H_2 content of about 5–10%, while the amount of CH_4 and C_2H_4 is less than 2%. With the increase of temperature, the amount of these gases has increased to some extent, and the overall calorific value of the fast pyrolysis gas has increased. The main reasons for the increase of H_2 yield are: the condensation of char; secondary reaction of tar, such as the polycondensation of aldehyde and ketone compounds; cracking of alkanes and alkenes. With the increase of temperature, the polycondensation reaction is enhanced. Some compounds in tar undergo polycondensation reaction to form benzene ring and other structures, and form H·, which eventually leads to the increase of H_2 content. For hydrocarbons, the C-H bond and the stability of C-C bond in the order: C≡C > C=C > C-H > C-C, however,

at high temperatures alkane content in tar is less, and alkenes, alkynes and aromatic compounds content is higher, compared with the C-H, C-C bond in tar is less, resulting in high temperature tar cracking process of CH_4 is less than the H_2. The variation pattern of CH_4 and C_2H_4 is similar to that of CO. In the study of biomass thermal cracking, the generation of CH_4 is mostly derived from the methoxy group in lignin structure, and the secondary decomposition of the volatile component of cellulose polymer can also produce CH_4. The detected unsaturated hydrocarbons are mainly C_2H_4, the yield of C_2H_4 is similar to that of CH_4, and the content in the gas is also very low. The analysis of its formation may be obtained from the thermal decomposition of unsaturated fatty acids.

Figure 9 shows the comparison of CO and CO_2 contents in fast pyrolysis gases of different raw materials. From the figure, we can see that the CO yield of UF with temperature rise is more obvious than that of wood and particle board, but the trend of CO_2 falling with temperature is basically the same. It shows that the UF contains a large amount of carbonyl groups which will be pyrolyzed to generate more CO during the fast pyrolysis process. Compared with two types of wood, the amount of CO and CO_2 produced from Larch is higher than that produced from Poplar, this is caused by the difference in the composition of the two types of wood. The yields of CO and CO_2 produced by pyrolysis of wood and particle board are basically the same, indicating that the addition of UF resin has no obvious effect on the fast pyrolysis of gas products.

Figure 10 is the variation diagram of the components of gaseous products from fast pyrolysis at different carrier gas flow rates. From this figure, it can be seen that under different carrier gas flow rates, CO and CO_2 are predominant in the fast pyrolysis gas composition of various raw materials. With the increase of flow rate, the content of CO and other gases have decreased to varying degrees, while the CO_2 content has increased. An increase in the flow rate of the carrier gas leads to a reduction in the retention time of the gas phase, thereby reducing the secondary cracking of the primary volatiles, so that the overall production of the gas product will decrease. The decrease of CO content and the increase of CO_2 content indicate that the secondary cracking of volatiles is more likely to produce CO, but has little effect on CO_2. Therefore, the percentage of CO_2 will increase as the total amount of gas decreases.

Figure 11 shows the comparison of CO and CO_2 contents in fast pyrolysis gases of different raw materials. From the figure, we can see that the CO yield of UF resin decreases with the increase of the carrier gas flow rate, which is basically the same as other raw materials, indicating that the degree of secondary pyrolysis of UF resin is equivalent to that of other raw materials. It shows that under the condition of fast pyrolysis, the addition of UF resin has no obvious effect on the wood gas product.
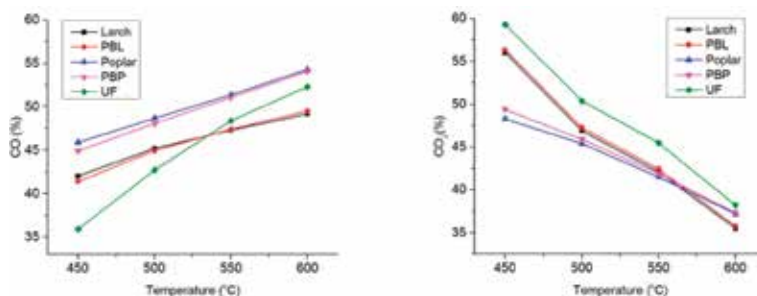
Figure 9.
CO and CO_2 yields from fast pyrolysis of different raw materials at different temperatures.
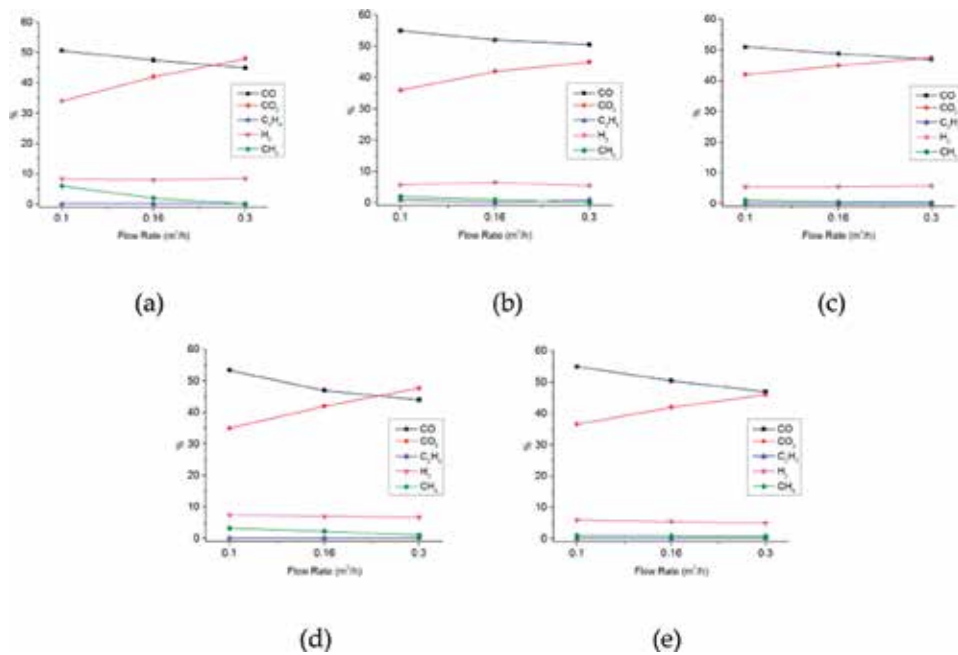
Figure 10.
Gaseous products distribution from fast pyrolysis at different carrier gas flow rates of raw materials: (a) Larch, (b) Poplar, (c) UF, (d) PBL, and (e) PBP.
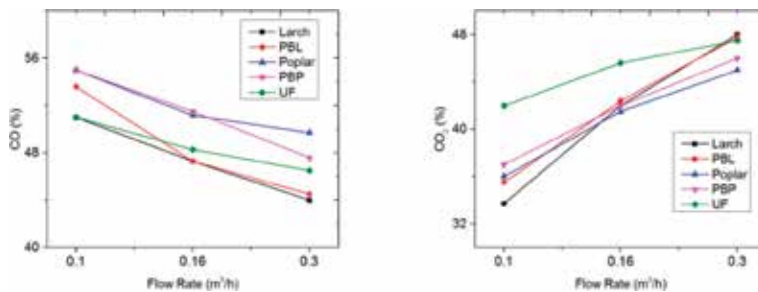
Figure 11.
CO and CO_2 contents fast pyrolysis products at different carrier gas flow rates.

3.2.2 Influence of pyrolysis conditions on the distribution of liquid product components

Figure 12 is a GC/MS total ion chromatogram (TIC) of the liquid product from fast pyrolysis of Larch, UF, and PBL, at 500°C. Due to the relatively simple structure of the UF resin, the TIC peak of the products from fast pyrolysis of UF resin is significantly lower than the TIC peak of the products from pyrolysis of wood and particle board, and no product peak appears after more than 30 minutes of retention time. When using the NIST library search, about 90 substances can be detected for the pyrolysis liquid phase products of particle board and wood raw materials under different conditions. The UF resin produced the most substances when it was pyrolyzed at 500°C, and only 37 products were found. The main components and relative content of liquid phase products of Larch, UF resin and PBL are shown in the appendix table. The spectral peaks of the PBL are very similar to those of the Larch, indicating that the main components of the pyrolysis products of the waste particle board are the same as the Larch.
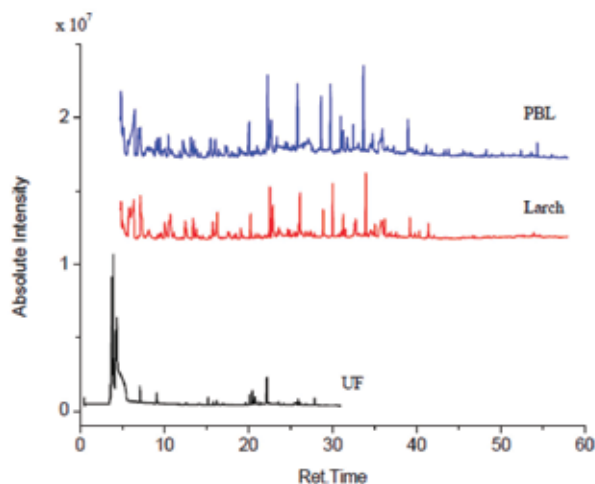
Figure 12.
TIC spectra of liquid products from fast pyrolysis of Larch, UF and PBL.

By classifying and comparing the pyrolysis liquid product components, the effect of pyrolysis conditions on the main categories of fast pyrolysis products can be analyzed. The products detected by GC/MS are classified into 13 categories, which are amines, alcohols, phenols, aldehydes, acids, ketones, esters, ethers, sugars, hydrocarbons, heterocyclic-N, other-N and others. From the appendix table, it can be seen that nitrogenous substances are the main components of UF resin pyrolysis liquid. UF resin contains amino, carbonyl, methylene and other groups, during the pyrolysis of UF resin, a group of hydroxyl methyl groups first split into formaldehyde and then produce nitrogen-containing volatile components with C-N bond breaking. The relative content of methyl isocyanate reaches up to 39.25%, in addition, other nitrogenous substances, such as ethyleneimine (13.68%), ethyl pyruvate (10.67%), 2,3-diazabicyclo [2.2.1]-hept-2-ene decanols (5.13%), l-alanine ethylamide, (S)-(3.91%), can also be detected in the pyrolysis liquid of UF resin. Compared with the composition of UF resin, the pyrolytic liquid products of Larch and PBL are very complicated. The products of wood mainly include alcohols, ketones, aldehydes, ketone derivatives and carbohydrates. The major con-stituent is hydroxyacetone and the relative content is 7.43%, other ketone deriva-tives, such as 1,3-cyclopentadione (3.12%) and 2,3-glutaric ketone (2.53%) can also be detected in the pyrolysis liquid of Larch, these ketone derivatives are generated by the pyrolysis of holocellulose. Lignin structure is rich in methoxy, and most phenolic compounds in the pyrolysis solution have the methoxyl chain. During the pyrolysis, the lignin molecular chain is cracked and the fragments are rearranged. The relative content of cis-isoeugenol and 2-methoxyl-4-vinyl phenol in Larch liquid phase products can reach 4.96 and 3.08%, respectively. In addition, phenolic compounds such as 4-ethyl guaiacol (1.38%), guaiacol (2.76%), 4-methyl guaiacol (2.53%), eugenol (1.32%) and phenol (0.33%) can also be detected. Particle board pyrolysis liquid product variety is one of the most in the three kinds of raw mate-rials, main components of acetic acid (13.04%), (E)-iso-eugenol (5.22%), guaiacol (5.07%), cyclopropylmethyl alcohol (4.81%), 4-methyl hydroxyacetone (4.24%), guaiacol (3.97%), 4-hydroxy-3-methyl acetophenone (3.48%), 3-methyl-1, 2-ring glutaric ketone (2.98%) and furfuryl alcohol (2.75%), and other substances phenols, alcohols and ketones. Compared with Larch pyrolysis liquid phase, more Larch and
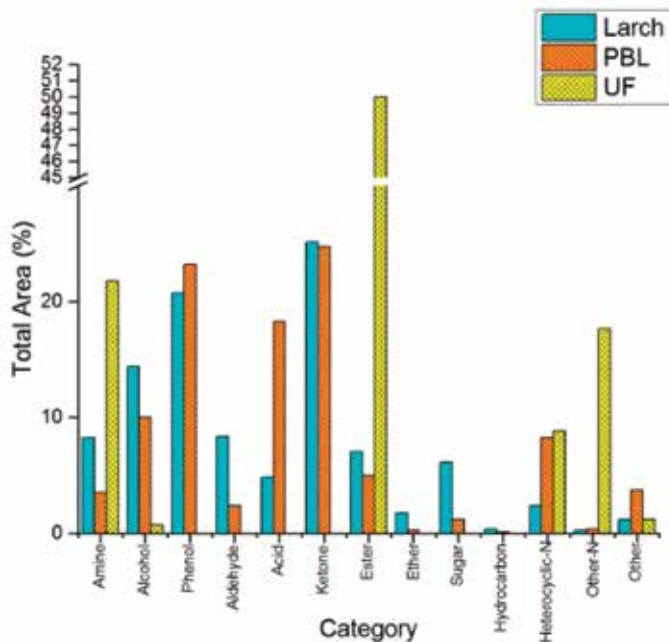
Figure 13.
Subtotal amount of different categories of fast pyrolysis liquid products (T = 500°C).

UF resin synergistic reaction products, such as 1,3,4-trimethyl-1,7-dihydro-6h-pyrazole and [3,4-b] pyridine 6-ketone, were obtained in the pyrolysis liquid phase products of particle board [16].

Figure 13 is a summary of the main components of the fast pyrolysis liquid of Larch, UF and PBL at 500°C. As can be seen from the figure, the type of fast pyrolysis liquid product of PBL is the same as that of Larch, and is mainly based on alcohol, phenol, acid, and ketone, the maximum content of esters in the urea-formaldehyde resin pyrolysis liquid phase product is nearly 50%, which together with amines, nitrogen heterocycles and other nitrogen-containing compounds form the main liquid phase products. Due to the effect of UF resin, the product of PBL has a greater change than Larch, and the nitrogen heterocyclic compound in the PBL has been greatly improved compared to wood. In addition, acid and phenolic substances have also been improved to varying degrees, while amines, alcohols, aldehydes, esters, sugars and other components have been reduced to varying degrees. The change of these components is due to the fact that the introduced UF resin itself is produced during the fast pyrolysis process, for example, the nitrogen heterocyclic compounds are mainly formed by the cyclization of the amide nitrogen from fast pyrolysis of UF resin. However, more compositional changes should result from the complex chemical reactions that occurred between the UF resin and wood components during the fast pyrolysis process, for example, amines and esters are the main products of UF resin, but the content of PBL products is lower than that of wood products. Phenolics and acids were not detected in the UF resin pyrolysis liquid phase product, but the content of PBL products was higher than that of wood. Therefore, during the fast pyrolysis of the particle board, a strong interaction occurs between the wood components and the UF resin component, in other words, chemical reactions occurred between the derivatives from UF resin and wood during fast pyrolysis.
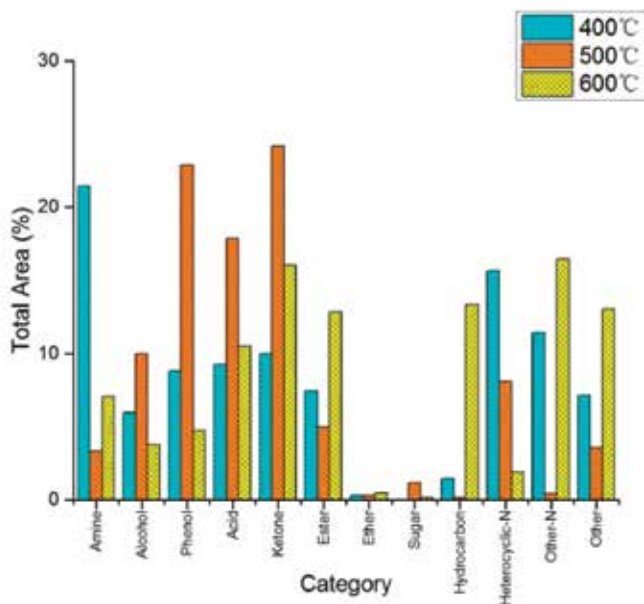
Figure 14.
Subtotal amounts of different categories of liquid products from fast pyrolysis of PBL at different temperatures.

Temperature is one of the main factors affecting fast pyrolysis. **Figure 14** is a summary of the main components of liquid products from fast pyrolysis of PBL at different temperatures. From the figure, it can be seen that the content of liquid products from fast pyrolysis of the PBL at 500°C is generally higher than that at 400 and 600°C, such as alcohol, phenol, acid, ketone, etc., this is consistent with the trend of maximum yield of pyrolysis oil obtained at a fixed bed fast pyrolysis experiment at 500°C. When the temperature is lower, the cracking of raw materials is incomplete and the yield of volatiles is low, when the temperature is higher, more secondary cracking occurs in the volatiles and they are converted into small molecules. The effect of temperature on the specific components of the product and its mechanism remain to be further studied.

It can also be seen from **Figure 14** that the nitrogen-containing compounds account for the most part in liquid phase products from fast pyrolysis of particle board at a lower temperature of 400°C, mainly amines, nitrogen heterocyclic, etc., indicating that at low temperatures UF resin already be decomposed to produce liquid products. When the temperature rises to 500°C, the amines, nitrogen heterocycles and other liquid nitrogen compounds in the product have been significantly reduced, indicating that some low-stability substances undergo secondary cracking to generate small-molecule gas-phase compounds, while the secondary cleavage of nitrogen heterocycles with higher stability is still not obvious. When the temperature continues to increase to 600°C, the nitrogen heterocyclic ring in the product is significantly reduced, indicating that at higher temperatures, a large number of nitrogen heterocycles also undergo cracking reactions. As a result, amines, nitrogen-containing esters, and other nitrogen-containing compounds are produced, making the amount of these substances significantly higher than at 500°C. These changes are similar to the effects of temperature on pyrolysis yields. Therefore, in the fast pyrolysis process, the temperature has a decisive effect on the product yield and composition.

Figure 15 is a summary of the main components of the liquid phase product of the PBL at different carrier gas flow rates. The flow rates were set to 100, 50 and

10 ml/min. It can be seen from the figure that with the decrease of the carrier gas flow rates, the gas phase residence time is prolonged and the secondary cracking of the volatiles is enhanced, more small molecules are produced. From the liquid product search results, it was found that the product types did not change, the content of the higher molecular weight material decreased, and the content of the
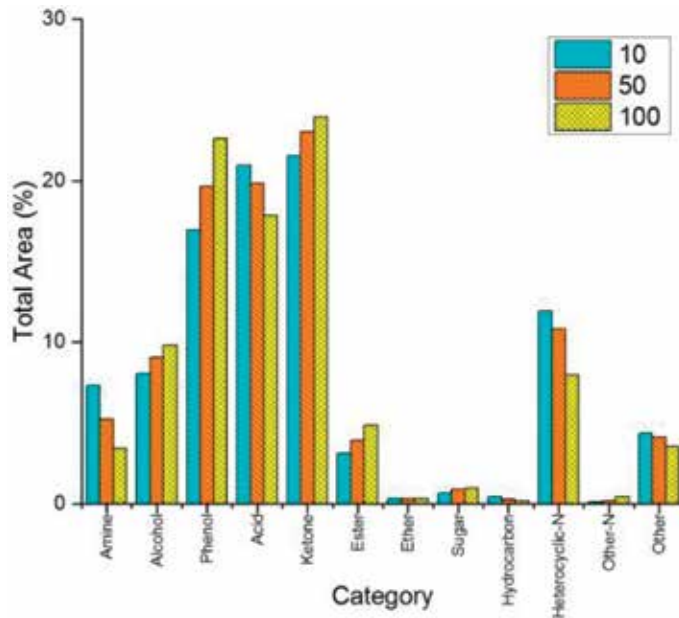
Figure 15.
Subtotal amounts of different categories of PBL fast pyrolysis liquid products at different carry gas flow rates.
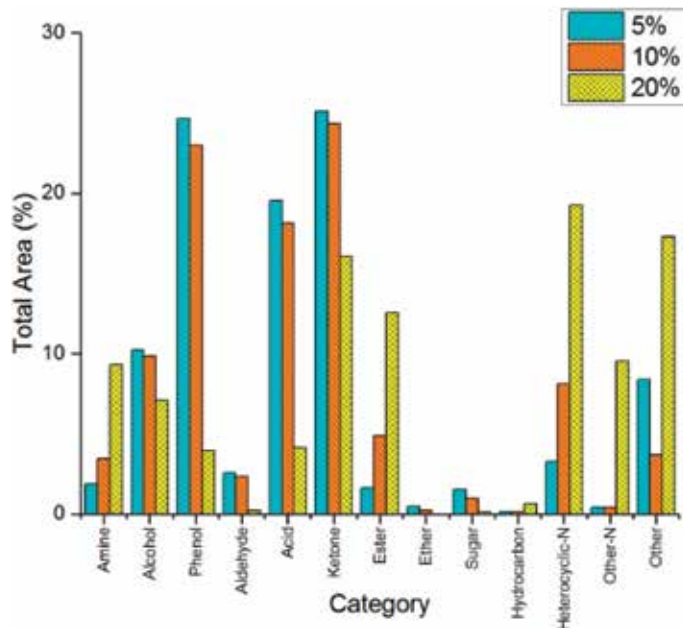
Figure 16.
Subtotal amounts of different categories liquid products from fast pyrolysis of PBL with different adhesive amounts.

lower molecular weight material increased. Under different temperature conditions, the yield of the same product is not much different, which indicates that the carrier gas flow rates has little influence on the product quantity, and the overall influence degree is not as obvious as the temperature.

Figure 16 is a summary of the main components of the liquid phase products from fast pyrolysis of PBL with different adhesive amount.

As can be seen from **Figure 16**, the increase in adhesive amount directly results in an increase in all nitrogenous products in the product, including amines, nitrogen heterocycles, and other nitrogen-containing compounds. In addition, the amount of ester products has also been significantly increased, the reason is that many esters contain nitrogen, which means that the amide nitrogen in the raw material is involved in a large number of esterification reactions. When the amount of adhesive is at a little level, UF resin has a promoting effect on the formation of phenol in wood, and plays a similar catalyst effect; when the amount of adhesive increases, the phenolics in the particle board begin to drop; when the amount of adhesive is 20%, it even drops to 4%, which is less than a quarter of the phenol content (20.5%) in fast pyrolysis products of wood. It is speculated that in a fast pyrolysis system, too much UF resin will compete with the phenol-forming reaction, generating more amine and nitrogen heterocyclic structures. In comparison, the effects of UF resin on acid substances are similar to those on phenolic substances, less adhesive amounts contribute to the formation of acids, while an increase in the amount of sizing inhibits acid production and appears to decrease.

4. Conclusions

Fast pyrolysis experiments of Larch and Poplar, UF, PBL and PBP were carried out, and the yields of pyrolysis products and its composition were analyzed. The results show that when the pyrolysis temperature is between 400 and 600°C, the gas yield steadily increase as the temperature increases, and the pyrolysis carbon yield continues to decrease, while the yield of pyrolysis oil increased at first and then decreased afterwards, and reached a maximum at 550°C. The carbon yield from fast pyrolysis of particle board is higher than that of wood, indicating that UF resin will prevent particle board decomposing, and this impact goes weak with increasing of temperature.

Compared with temperature, the influence of the carrier gas flow rates on the yields of products and its distribution is relatively low. Increasing of carrier gas flow rate can effectively prevent the occurrence of secondary cracking in the system and increase the pyrolysis oil yield. The gas products from fast pyrolysis of waste particle board are mainly CO and CO_2, as well as relatively small amounts of CH_4, C_2H_4, H_2, etc. With the increase of temperature, the content of CO_2 decreased and the contents of other gases increased. Among them, the tendency of CO obviously rose, and the calorific value of gas has increased. Under the conditions of fast pyrolysis, the effect of UF resin on the gas composition of particle board is not obvious.

Compared with wood, the main components of pyrolysis liquid phase products of waste particle board have not changed much, while the nitrogenous substances such as amines and nitrogen heterocycles are mainly increased, which promoted the formation of phenols and acids and prevented the formation of aldehydes, sugars, and alcohols. The temperature has little effect on the product type, but has a great influence on the yields. The carrier gas flow rate has little effect on the product composition. The effect of adhesive amount on the composition of the product is unclear.

Acknowledgements

A. Main compounds of fast pyrolysis liquid products of Larch, UF and PBL

No.	Name	Molecular formula	Molecular weight	Larch	Area % PBL	UF
1	Ethyleneimine	C_2H_5N	43	\	\	13.68
2	Formamide	CH_3NO	45	0.27	1.61	0.11
3	Aminoacetonitrile	$C_2H_4N_2$	56	\	\	0.03
4	Methyl isocyanate	C_2H_3NO	57	\	1.23	39.25
5	Acetamide	C_2H_5NO	59	6.53	0.57	\
6	N-Methylformamide	C_2H_5NO	59	\	0.64	\
7	Trimethylamine	C_3H_9N	59	\	\	2.56
8	Acetic acid	$C_2H_4O_2$	60	2.25	13.04	\
9	Ethylene glycol	$C_2H_6O_2$	62	\	0.68	\
10	Pyrrole	C_4H_5N	67	0.42	1.83	\
11	Allyl cyanide	C_4H_5N	67	\	\	0.05
12	2,5-Dihydrofuran	C_4H_6O	70	0.3	0.13	\
13	Cyclopropylmethanol	C_4H_8O	72	3.34	4.81	\
14	N-Methylacetamide	C_3H_7NO	73	\	0.52	\
15	Hydroxyacetone	$C_3H_6O_2$	74	7.43	4.24	\
16	Methyl acetate	$C_3H_6O_2$	74	\	1.41	\
17	Methylurea	$C_2H_6N_2O$	74	\	\	0.09
18	Methyl carbamate	$C_2H_5NO_2$	75	\	\	0.14
19	Pyridine	C_5H_5N	79	0.14	\	\
20	Pyrimidine	$C_4H_4N_2$	80	\	0.47	\
21	N-methylpyrrole	C_5H_7N	81	0.32	1.39	\
22	3-Methylpyrrole	C_5H_7N	81	\	0.33	\
23	1,3,5-Triazine	$C_3H_3N_3$	81	\	\	1.21
24	1,4-Pentadien-3-one	C_5H_6O	82	0.39	\	\
25	N-methylimidazole	$C_4H_6N_2$	82	\	0.56	0.06
26	2(5H)-Furanone	$C_4H_4O_2$	84	1.92	2.19	\
27	N,N-Dimethylaminoacetonitrile	$C_4H_8N_2$	84	\	1.12	0.66
28	Succinaldehyde	$C_4H_6O_2$	86	2.01	\	\
29	2,3-Butanedione	$C_4H_6O_2$	86	\	1.05	\
30	Beta-butyrolactone	$C_4H_6O_2$	86	\	\	0.21
31	1-Hydroxy-2-butanone	$C_4H_8O_2$	88	\	0.98	\
32	N,N-Dimethylurea	$C_3H_8N_2O$	88	\	\	0.56

No.	Name	Molecular formula	Molecular weight	Larch	Area % PBL	UF
33	Carbohydrazide	CH_6N_4O	90	\	\	0.2
34	Methyl hydroxyacetate	$C_3H_6O_3$	90	0.51	0.47	\
35	Phenol	C_6H_6O	94	0.33	\	\
36	3-Methylpyridazine	$C_5H_6N_2$	94	0.17	\	\
37	N-Vinylimidazole	$C_5H_6N_2$	94	\	\	0.1
38	2,3-Dimethyl-1H-pyrrole	C_6H_9N	95	0.25	\	\
39	3-Hydroxypyridine	C_5H_5NO	95	0.56	\	\
40	2,5-Lutidine	C_6H_9N	95	\	0.57	\
41	Furfural	$C_5H_4O_2$	96	2.21	1.34	\
42	4-Imidazole formaldehyde	$C_4H_4N_2O$	96	0.16	\	\
43	4-Cyclopentene-1,3-dione	$C_5H_4O_2$	96	0.29	0.22	\
44	3-Methyl-2-cycloalkenone	C_6H_8O	96	\	0.3	\
45	2,5-Dimethylfuran	C_6H_8O	96	\	1.24	\
46	2-Amino-1,3,5-triazine	$C_3H_4N_4$	96	\	\	0.27
47	2,3-Diazabicyclo[2.2.1]-hept-2-ene decanols	$C_5H_8N_2$	96	\	\	5.13
48	Furfuryl alcohol	$C_5H_6O_2$	98	2.55	2.75	\
49	1,3-Cyclopentadione	$C_5H_6O_2$	98	3.12	\	\
50	1,2-Cyclopentadione	$C_5H_6O_2$	98	\	1.51	\
51	2-Ethylene-3-vinyl epoxy-ethane	$C_6H_{10}O$	98	0.41	\	\
52	Ethyl cyanoformate	$C_4H_5NO_2$	99	\	0.21	\
53	3-Amino-5-hydroxypyrazole	$C_3H_5N_3O$	99	\	0.22	\
54	2-Methyl-2-pentene-1-alcohol	$C_6H_{12}O$	100	0.5	\	\
55	2,3-Glutaric ketone	$C_5H_8O_2$	100	2.53	0.27	\
56	2-Methyl-3-pentone	$C_6H_{12}O$	100	0.29	0.54	\
57	Tetrahydro-2H-pyran-3-ketone	$C_5H_8O_2$	100	0.47	0.52	\
58	Succinic anhydride	$C_4H_4O_3$	100	\	\	0.05
59	2, 2-Dimethyl-1-butanol	$C_6H_{14}O$	102	\	0.37	\
60	Methyl pyruvate	$C_4H_6O_3$	102	2.68	\	\
61	Acetic anhydride	$C_4H_6O_3$	102	0.78	\	\
62	M-Cresol	C_7H_8O	108	0.22	0.21	\
63	2-Acetylpyrrole	C_6H_7NO	109	0.18	0.25	\
64	2, 3-Diaminopyridine	$C_5H_7N_3$	109	\	\	0.24
65	2H-Tetrazole-2-ethyl acetonitrile	$C_3H_3N_5$	109	\	0.41	\
66	5-Methylfurfural	$C_6H_6O_2$	110	0.61	0.86	\
67	2,3-Dimethyl-2-cyclopentene-1-ketone	$C_7H_{10}O$	110	\	0.16	\
68	2-Acetylfuran	$C_6H_6O_2$	110	\	0.19	\
69	2-Amino-3-hydroxypyridine	$C_5H_6N_2O$	110	\	\	0.07
70	Isocytosine	$C_4H_5N_3O$	111	0.23	\	\
71	3-Hydroxypyridine-N-oxide	$C_5H_5NO_2$	111	\	\	0.39
72	N-Ethylidene-1-pyrrolidine	$C_6H_{12}N_2$	112	\	\	0.83

No.	Name	Molecular formula	Molecular weight	Larch	Area % PBL	UF
73	3-Methyl-1,2-cyclopentanedione	$C_6H_8O_2$	112	1.72	2.98	\
74	3-Methyl-1,2-cyclopentanedione	$C_6H_8O_2$	112	1.2	\	\
75	Cyclopentyl ethanone	$C_7H_{12}O$	112	\	0.14	\
76	3-Isopropoxypropionitrile	$C_6H_{11}NO$	113	\	0.11	\
77	2,3-Dimethylene-1,4-butanediol	$C_6H_{10}O_2$	114	\	0.51	\
78	Trans-2-hexenoic acid	$C_6H_{10}O_2$	114	0.28	\	\
79	2,5-Dione piperazine	$C_4H_6N_2O_2$	114	\	\	0.25
80	5,6-Dihydrouracil	$C_4H_6N_2O_2$	114	\	\	0.09
81	2,6-Dimethylpiperazine	$C_6H_{14}N_2$	114	\	\	0.56
82	l-Alanine ethylamide, (S)-	$C_5H_{12}N_2O$	116	\	\	3.91
83	Acetylacetone peroxide	$C_5H_8O_3$	116	0.68	1.02	\
84	Ethyl pyruvate	$C_5H_8O_3$	116	\	\	10.67
85	1,4-Dioxane-2,5-diol	$C_4H_8O_4$	120	5.66	\	\
86	1-Methyl-2-pyrrolethane cyanide	$C_7H_8N_2$	120	\	\	0.11
87	(Ethyleneoxy)benzene	C_8H_8O	120	0.34	\	\
88	Guaiacol	$C_7H_8O_2$	124	2.76	5.07	\
89	N-(S-triazolyl)acetamide	$C_4H_6N_4O$	126	\	0.08	\
90	2-Methyl-1,5-heptadiene-4-alcohol	$C_8H_{14}O$	126	0.14	\	\
91	Maltol	$C_6H_6O_3$	126	0.34	0.36	\
92	5-Hydroxymethylfurfural	$C_6H_6O_3$	126	0.67	\	\
93	Imidazol-4-acetic acid	$C_5H_6N_2O_2$	126	\	2.65	\
94	3-Ethyl-4-methyl-3-pentene-2-ketone	$C_8H_{14}O$	126	0.39	\	\
95	2-Methyl cycloheptanone	$C_8H_{14}O$	126	0.6	\	\
96	Ethyl cyclopentenolone	$C_7H_{10}O_2$	126	\	0.53	\
97	1-Methyluracil	$C_5H_6N_2O_2$	126	\	0.12	\
98	2-(1,1-Dimethylethyl)-1,3-dimethylnitrogen propidine	$C_8H_{17}N$	127	\	\	1.46
99	2,3-Dimethylcyclohexanol	$C_8H_{16}O$	128	0.26	\	\
100	1-Cyclopropyl-1-pentyl alcohol	$C_8H_{16}O$	128	\	0.17	\
101	6-Heptanoic acid	$C_7H_{12}O_2$	128	0.38	\	\
102	3-Symplectic ketone	$C_8H_{16}O$	128	\	0.43	\
103	1-Methyl-hydrouracil	$C_5H_8N_2O_2$	128	\	1.53	0.35
104	1,3,5-Trimethyl-hexamethyl-1,3,5-triazine	$C_6H_{15}N_3$	129	\	\	3.16
105	L-Ornithine	$C_5H_{12}N_2O_2$	132	\	\	0.1
106	4-Methyl guaiacol	$C_8H_{10}O_2$	138	2.53	3.97	\
107	Hexamethylenetetramine	$C_6H_{12}N_4$	140	\	\	0.03
108	3-Oxy-1-cyclopentene-1-acetate	$C_7H_8O_3$	140	0.63	\	\
109	Dipropylene aminoacetonitrile	$C_8H_{16}N_2$	140	\	\	0.14
110	Heptyl isocyanate	$C_8H_{15}NO$	141	0.43	\	\
111	(1Z)-2-Ethylcyclohexanone oxime	$C_8H_{15}NO$	141	0.28	\	\
112	4-Octyne-3,6-diol	$C_8H_{14}O_2$	142	0.27	\	\

No.	Name	Molecular formula	Molecular weight	Larch	Area % PBL	UF
113	Nonyl aldehyde	$C_9H_{18}O$	142	1.02	\	\
114	4-Ethyl-2,2-dimethylhexane	$C_{10}H_{22}$	142	0.32	\	\
115	4-Amino-N-hydroxy-1,2, 5-oxadiazole-3-carboxyamide	$C_3H_5N_5O_2$	143	0.94	\	\
116	N-(2-Hydroxyethyl) hexahydrogen-1H-acheptylamine	$C_8H_{17}NO$	143	\	\	0.89
117	2-Methoxy-4-vinyl phenol	$C_9H_{10}O_2$	150	3.08	\	\
118	4-Hydroxy-3-methyl acetophenone	$C_9H_{10}O_2$	150	\	3.48	\
119	4-Ethyl guaiacol	$C_9H_{12}O_2$	152	1.38	2.43	\
120	Vanillin	$C_8H_8O_3$	152	1.02	\	\
121	Isoflavin/isovanillin	$C_8H_8O_3$	152	\	0.11	\
122	2,6-Dimethoxyphenol	$C_8H_{10}O_3$	154	0.46	\	\
123	3,4-Dimethoxyphenol	$C_8H_{10}O_3$	154	\	0.21	\
124	Ethyl 2-heptynoate	$C_9H_{14}O_2$	154	\	0.64	\
125	Valdetamide	$C_9H_{17}NO$	155	0.55	\	\
126	Decanal	$C_{10}H_{20}O$	156	0.2	\	\
127	Ethyl-2-piperidine formate	$C_8H_{15}NO_2$	157	0.85	\	\
128	4-Butyryl morpholine	$C_8H_{15}NO_2$	157	\	0.54	\
129	2-Hydroxy cyclohexyl ester	$C_8H_{14}O_3$	158	0.26	\	\
130	1,6-Anhydride-B-D-pyran glucose	$C_6H_{10}O_5$	162	6.05	1.05	\
131	1-[(1E)-1-Butenyl]-4-methoxybenzene	$C_{11}H_{14}O$	162	0.2	\	\
132	4-Methyl-5-(5-methyl-1H-pyrazol-3-base)-1H-1,2,3-triazole	$C_7H_9N_5$	163	\	0.25	\
133	Eugenol	$C_{10}H_{12}O_2$	164	1.32	1.81	\
134	Cis-isoeugenol	$C_{10}H_{12}O_2$	164	4.96	1.15	\
135	2,3-Dihydro-2,2-dimethyl-7-benzofuranol	$C_{10}H_{12}O_2$	164	0.15	\	\
136	(E)-Isoeugenol	$C_{10}H_{12}O_2$	164	\	5.22	\
137	3-Allyl-6-methoxyphenol	$C_{10}H_{12}O_2$	164	\	0.19	\
138	3,4-Dimethoxystyrene	$C_{10}H_{12}O_2$	164	\	0.1	\
139	Dihydroeugenol	$C_{10}H_{14}O_2$	166	0.41	1.04	\
140	Vanilla ethyl ketone	$C_9H_{10}O_3$	166	0.72	1.08	\
141	4-Methoxy-3-hydroxyacetophenone	$C_9H_{10}O_3$	166	0.33	\	\
142	High vanillin alcohol	$C_9H_{12}O_3$	168	0.44	\	\
143	3-Hydroxyl-4-methoxybenzoic acid	$C_8H_8O_4$	168	0.18	\	\
144	Vanillic acid	$C_8H_8O_4$	168	0.33	\	\
145	6-Hydroxy 5-decanone	$C_{10}H_{20}O_2$	172	0.42	\	\
146	2-Heptyl-1,3-dioxy-amyl ring	$C_{10}H_{20}O_2$	172	\	\	0.29
147	1,3,4-Trimethyl-1,7-dihydrogen-6H-pyrazole and pyridine-6-ketone [3,4-b]	$C_9H_{11}N_3O$	177	\	0.31	\
148	Coniferyl alcohol	$C_{10}H_{12}O_3$	180	1.96	1	\
149	2,5-Dimethoxyl-4-toluene formaldehyde	$C_{10}H_{12}O_3$	180	0.4	\	\

No.	Name	Molecular formula	Molecular weight	Larch	Area % PBL	UF
150	4-Hydroxyl-3-methoxyphenylacetone	$C_{10}H_{12}O_3$	180	1.07	0.77	\
151	2′,4′-Dihydroxyl-3′-methylphenylacetone	$C_{10}H_{12}O_3$	180	\	0.29	\
152	Homovanillic acid	$C_9H_{10}O_4$	182	\	2.15	\
153	Vanillin ethyl ether	$C_{10}H_{14}O_3$	182	1.72	\	\
154	1-Tridecene	$C_{13}H_{26}$	182	\	0.09	\
155	γ-Dodecane acid lactone	$C_{11}H_{20}O_2$	184	0.71	\	\
156	6-Dodecyl alcohol	$C_{12}H_{26}O$	186	\	0.09	\
157	Tetraethylene glycol	$C_8H_{18}O_5$	194	\	\	0.05
158	4-Allyl-2,6-dimethoxyphenol	$C_{11}H_{14}O_3$	194	0.57	0.16	\
159	α-Methyl glucoside	$C_7H_{14}O_6$	194	\	0.21	\
160	2,3-Dimethyl-2-(3-oxobutyl)cyclohexanone	$C_{12}H_{20}O_2$	196	\	0.48	\
161	Ethyl-4-(acetylamino)-1,2,5-oxadiazole-3-carboxylate	$C_7H_9N_3O_4$	199	0.53	\	\
162	11-Methyl-12-methylene-tricyclic [5.3.1.1 (2,6)]-dodecane-11-alcohol	$C_{14}H_{22}O$	206	0.47	\	\
163	Eugenol acetate	$C_{12}H_{14}O_3$	206	0.34	\	\
164	2,5,5,8a-Tetramethylmethyl-4-methylene-4a,5,6,7,8,8a-hexahydrogen-4h-chromene	$C_{14}H_{22}O$	206	0.17	\	\
165	Ethyl oxalate	$C_{11}H_{14}O_4$	210	\	0.17	\
166	Tetradecyl alcohol	$C_{14}H_{30}O$	214	\	\	0.16
167	10-Oxo-dodecane acid	$C_{12}H_{22}O_3$	214	0.16	\	\
168	3,5-Dimethyl-1-phenyl-1H-pyrazol-4-carboxylic acid	$C_{12}H_{12}N_2O_2$	216	0.15	\	\
169	8-Methoxy[1]benzofuran and [3,2-d] pyrimidine −4(3H)-ketone	$C_{11}H_8N_2O_3$	216	0.15	0.12	\
170	3,3,4-Trimethyl-4-(4-methylphenyl) cyclopentyl alcohol	$C_{15}H_{22}O$	218	0.38	\	\
171	Cubenol	$C_{15}H_{26}O$	222	0.28	\	\
172	7-Pentadecanone	$C_{15}H_{30}O$	226	\	0.29	\
173	Pentaethylene glycol	$C_{10}H_{22}O_6$	238	\	\	0.52
174	2-(1,3-Dihydrogen-2h-indene-2-subunit)-2,3-dihydrogen-1h-indene-1-ketone	$C_{18}H_{14}O$	246	0.18	\	\
175	(Z)-14-Methyl-8-hexadecene-1-acetal	$C_{17}H_{32}O$	252	\	0.08	\
176	Palmitic acid	$C_{16}H_{32}O_2$	256	\	0.22	\
177	Dibutyl phthalate	$C_{16}H_{22}O_4$	278	\	0.11	\
178	(13R)-8a,13:9a,13-Diepoxy-15,16-dinorlabdane	$C_{18}H_{30}O_2$	278	0.14	\	\
179	3,4,8-Trimethoxy-6H-benzophenol[c] benzopyran-6-ketone	$C_{16}H_{14}O_5$	286	0.18	\	\
180	1-Naphthalenepropanol,.alpha.-ethenyldecahydro-.alpha.,5,5,8a-tetramethyl-2-methylene-,[1S-[1.alpha.(R*),4a.beta.,8a.alpha.]]-	$C_{20}H_{34}O$	290	\	0.29	\
181	12-Hydroxyandrostane-17-ketone	$C_{19}H_{30}O_2$	290	0.31	\	\

No.	Name	Molecular formula	Molecular weight	Larch	Area % PBL	UF
182	5,8-Diethoxy-3-(methoxy carbonyl)-2-quinoline carboxylic acid	$C_{15}H_{16}N_2O_6$	296	0.36	\	\
183	Di-N-decyl ether	$C_{20}H_{42}O$	298	\	0.27	\
184	Vitamin A acetate	$C_{22}H_{32}O_2$	328	\	0.73	\
185	Tetracosane	$C_{24}H_{50}$	338	\	0.1	\
186	14-Heptacosanone	$C_{27}H_{54}O$	394	0.25	\	\
187	Lanosterol	$C_{30}H_{50}O$	426	\	0.28	\
188	3′,8,8′-Trimethoxy-3-piperidinyl-2,2′-binaphthalene-1,1′,4,4′-tetraone	$C_{28}H_{25}NO_7$	487	\	0.34	\

Author details

Liuming Song, Xiao Ge, Xueyong Ren, Wenliang Wang, Jianmin Chang and Jinsheng Gou*
Key Laboratory of Wooden Material Science and Application, College of Materials Science and Technology, Beijing Forestry University, Ministry of Education, Beijing, China

*Address all correspondence to: jinsheng@bjfu.edu.cn

IntechOpen

References

[1] Bridgwater AV, Peacocke GVC. Fast pyrolysis processes for biomass. Renewable & Sustainable Energy Reviews. 2000;**4**:1-73. DOI: 10.1016/S1364-0321(99)00007-6

[2] Mohan D, Pittman CU, Steele PH. Pyrolysis of wood/biomass for bio-oil: A critical review. Energy & Fuels. 2006;**20**:848-889. DOI: 10.1021/ef0502397

[3] Choi SJ, Park SH, Jeon J-K, Lee IG, Ryu C, Suh DJ, et al. Catalytic conversion of particle board over microporous catalysts. Renewable Energy. 2013;**54**:105-110. DOI: 10.1016/j.renene.2012.08.050

[4] Yanik J, Kornmayer C, Saglam M, Yüksel M. Fast pyrolysis of agricultural wastes: Characterization of pyrolysis products. Fuel Processing Technology. 2007;**88**:942-947. DOI: 10.1016/j.fuproc.2007.05.002

[5] Deng N, Zhang Y-F, Wang Y. Thermogravimetric analysis and kinetic study on pyrolysis of representative medical waste composition. Waste Management. 2008;**28**:1572-1580. DOI: 10.1016/j.wasman.2007.05.024

[6] López A, de MI, Caballero BM, Laresgoiti MF, Adrados A. Pyrolysis of municipal plastic wastes: Influence of raw material composition. Waste Management. 2010;**30**:620-627. DOI: 10.1016/j.wasman.2009.10.014

[7] Manzano-Agugliaro F, Alcayde A, Montoya FG, Zapata-Sierra A, Gil C. Scientific production of renewable energies worldwide: An overview. Renewable and Sustainable Energy Reviews. 2013;**18**:134-143. DOI: 10.1016/j.rser.2012.10.020

[8] Han TU, Kim Y-M, Watanabe C, Teramae N, Park Y-K, Kim S, et al. Analytical pyrolysis properties of waste medium-density fiberboard and particle board. Journal of Industrial and Engineering Chemistry. 2015;**32**:345-352. DOI: 10.1016/j.jiec.2015.09.008

[9] Sheldona RA, Sanders JPM. Toward concise metrics for the production of chemicals from renewable biomass. Catalysis Today. 2015;**239**:3-6. DOI: 10.1016/j.cattod.2014.03.032

[10] Park Y-K, Choi SJ, Jeon J-K, Park SH, Ryoo R, Kim J, et al. Catalytic conversion of waste particle board to bio-oil using nanoporous catalyst. Journal of Nanoscience and Nanotechnology. 2012;**12**:5367-5372. DOI: 10.1166/jnn.2012.6412

[11] Lee HW, Choi SJ, Jeon J-K, Park SH, Jung S-C, Park Y-K. Catalytic conversion of waste particle board and polypropylene over H-beta and HY zeolites. Renewable Energy. 2015;**79**:9-13. DOI: 10.1016/j.renene.2014.07.040

[12] Kim H, Choi SJ, Kim JM, Jeon J-K, Park SH, Jung S-C, et al. Catalytic copyrolysis of particle board and polypropylene over Al-MCM-48. Materials Research Bulletin. 2016;**82**:61-66. DOI: 10.1016/j.materresbull.2016.03.009

[13] Jin B-B, Heo HS, Ryu C, Kim S-S, Jeon J-K, Park Y-K. The copyrolysis of block polypropylene with particle board and medium density fiber. Energy Sources, Part A: Recovery, Utilization, and Environmental Effects. 2014;**36**:958-965. DOI: 10.1080/15567036.2010.551263

[14] Bridgwater AV. Principles and practice of biomass fast pyrolysis processes for liquids. Journal of Analytical and Applied Pyrolysis. 1999;**51**:3-22. DOI: 10.1016/S0165-2370(99)00005-4

[15] Babu BV. Biomass pyrolysis: A state-of-the-art review. Biofuels, Bioproducts and Biorefining: Innovation for a Sustainable Economy. 2008;**2**:393-414. DOI: 10.1002/bbb

[16] Zhang Y, He ZB, Xue L, Chu DM, Mu J. Influence of a urea-formaldehyde resin adhesive on pyrolysis characteristics and volatiles emission of poplar particleboard. RSC Advances. 2016;**6**:12850-12861. DOI: 10.1039/c5ra18068f

Hydrocarbonization. Does It Worth to Be Called a Pretreatment?

Silvia Román, Beatriz Ledesma, Andrés Álvarez-Murillo,
Eduardo Sabio, J. F. González, Mara Olivares-Marín
and Mouzaina Boutieb

Abstract

In this work, we aim to evaluate the potential of hydrothermal carbonization (also known as wet pyrolysis) as a pretreatment, by evaluating the changes induced in the raw material (cellulose) under varying experimental conditions. Hydrocarbonization processes were performed under different temperature, time and biomass/water ratios following a response surface methodology. The hydrochars obtained were characterized in terms of proximate analysis, behavior towards pyrolysis and combustion, heating value and surface textural and chemical features. The presence of typical hydrocarbonization reactions (dehydration, hydrolysis, decarboxylation, decarbonylation, recondensation, etc.) was only possible if a limit temperature (200°C) was used. Under these conditions, proximate analyses changed, the surface chemistry was modified, and the formation of a second lignite-type solid fraction was observed.

Keywords: hydrocarbonization, wet pyrolysis, cellulose, drying, energy efficiency, biomass

1. Introduction

As the consequences of the massive use of fossil fuels are more and more worrying, national and international strategies are pointing out the clear and immediate need of shifting the current energy supply infrastructures towards more environmental friendly and sustainable models. Geopolitical conflicts due to dependency relations between countries, next depletion and climate change issues involve a severe reality that is at the moment causing wars, increasing human inequality, jeopardizing food security and triggering human relocation processes, which cause more and more international conflicts [1].

One purposeful renewable energy source with proven potential to provide heat or biofuels is biomass. Estimates conclude that a shift to biological raw materials could save up to 2.5 billion tons of CO_2 equivalent per year by 2030, increasing markets for bio-based raw materials and new consumer products several-fold [2].

Regarding biomass sources, their abundance and availability, decentralization, ease to extract and handle and heating value are very precious features. There are, however, some issues that limit the use of some biomass resources, as for

example, their high moisture content, which involves the implementation of cost-intensive drying pretreatments before classical thermochemical processes such as pyrolysis, combustion or gasification.

One pretreatment that has recently gained prominence is hydrocarbonization (HTC) or wet pyrolysis, that is, the thermochemical conversion of biomass in hot compressed water under relatively low temperature and self-generated pressure. In this way, biomass moisture is not a downside, but takes a role in the reaction both as solvent and as catalyst, triggering the reaction. Because of this important advantage as well as other additional features related to the final product quality, ease, low cost or process energy efficiency, this technique has gained relevance during last years. Because of the abovementioned advantages, HTC processes have been more and more used during last years and researchers have mainly focused their attention on (a) studying it as a previous reactions step for other processes, or (b) investigating HTC as a process to yield a material suitable for specific applications such as biofuel, adsorbent, soil amendment or catalyst [3].

In previous works, we studied the potential of HTC processes to upgrade tomato peel, olive pomace and orange peel [4–6]. Other authors have addressed the HTC of other humid materials such as waste streams [7], grape pomace [8] or potato peel [9]. In this work, we aim to evaluate the changes induced by HTC on pure cellulose that can affect to their further use in other thermochemical processes. Based on the experimental results obtained by HTC under varying experimental conditions, as well as the results found in the bibliography, we aim to offer insight about the chemical and structural changes induced as a result of the process, and their potential influence in further processing of the raw material.

2. Experimental

2.1 Hydrocarbonization experiments

Microcrystalline cellulose (Sigma-Aldrich) was dried at 105°C until constant weight and then stored in closed flasks placed in desiccators for further analysis.

The HTC processes were performed in a stainless steel autoclave (Berghof, Germany). In a 0.2 L Teflon vessel (unstirred), an appropriate amount of sample (5–18.4 g) and 150 mL of deionized water at room temperature were added, in order to obtain the targeted biomass/water ratio, R (1.1–12.3%). Then, the Teflon vessel was sealed and placed into the autoclave and the system remained overnight at room temperature. Thereafter, the system was heated up in an electric furnace at selected temperatures (150–250°C), during a chosen processing time (3.2–36.8 h). The experimental conditions were designed according to the response surface methodology, as described elsewhere [5]. Following this procedure, 18 runs were performed (15 under different conditions, and 3 additional runs at one particular condition to test experimental variability, as stated by the method).

The reactor pressure was always at or slightly above the water vapor pressure. After the reaction, the system was cooled down using an ice bath and then the autoclave was opened and the solid product (Hydrochar, HC) was obtained by vacuum filtration (Whatman filter paper number 3). Then, the HCs were dried for 24 h and stored in a desiccator for further analysis.

2.2 Characterization of hydrochars

Both pure cellulose and derived HCs were characterized in terms of their proximate analysis (% wt./wt.) following the technical specifications CEN/TS 1474–2,

CEN/TS 15148 and CEN/TS 14775 for moisture (M), volatile matter (VM) and ash (A), respectively. Fixed carbon was determined by difference (100-M-VM-A).

The thermogravimetric behavior of the raw material and the derived HCs was studied under both air and nitrogen atmospheres, using a thermobalance (TA Instruments) using a heating rate of 10°C min^{-1} and a gas flow of 100 mL min^{-1} in both cases, as described elsewhere [10]. In order to get further knowledge on the thermal degradation profiles, selected samples were analyzed by coupled thermo-gravimetric and mass spectrometry analysis (TG/MS, thermogravimetric system, TA Instruments; Mass Spectrometer, Pfeiffer Tecnovac Thermostar GDS301 T3). The gas line between the TG and MS was heated to 200°C in order to avoid cold points and thus preventing the condensation of some of the gaseous products. The mass/charge ratios (m/z) 44 and 16 were assigned, respectively, to CO_2 and CH_4, respectively.

The higher heating value (HHV) of solid samples was measured in a Parr 1241 adiabatic oxygen bomb calorimeter (Moline, IL) fitted with continuous tempera-ture recording. HTC biochar samples of 0.4–0.5 g were dried at 105°C for 24 h prior to analysis. Results are reported on a dry, ash-free (daf) basis.

Surface morphology studies were carried out by scanning electron microscopy with coupled X-Ray Electron dispersion (SEM–EDX, Quanta 3D FEG, FEI). The samples were prepared by depositing about 50 mg of sample on an aluminum stud covered with conductive adhesive carbon tapes, and then coated with Rh-Pd for 1 min to prevent charging during observations. Imaging was done in the high vacuum mode at an accelerating voltage of 30 kV, using secondary electrons under high vacuum conditions.

The surface chemistry of the hydrochars was studied by FTIR spectroscopy. FTIR spectra were recorded with a PerkinElmer model Paragon 1000 PC spectro-photometer, using the KBr disc method, with a resolution of 4 cm^{-1} and 100 scans.

3. Discussion of results

3.1 HC characterization and thermal degradation study

Table 1 lists the elemental and proximate analysis of the HCs, as well as the corresponding SY and HHV values.

Two dissimilar HC behaviors were identified from the immediate analyses. On the one hand, one can find HCs with volatile content higher than 85%, indicative of negligible HTC and, on the other hand, samples in which the process readily took place and brought up a clear decrease on volatile matter, with fixed carbon values higher than 50%. Dehydration and decarboxylation are well-known HTC mecha-nisms, bringing up an expected decrease in moisture and volatile matter content. From our results, both effects are clear although the prominence of them is clearly affected by the experimental conditions; as previously suggested, it seems that there is a cutting point that delimitates when HTC is really taking place. Moreover, it seems that this cutting point is determined by the temperature, whereas time has a slight influence and the biomass/water ratio does not have an effect on its location.

According to the bibliography, biomass starts its decomposition in the pres-ence of water, only when particular subcritical conditions are reached, and water behaves as a non-polar solvent and can therefore make biomass constituents become soluble [11]. Under these conditions, the properties of water such as the ionic constant readily change (it has been reported as being nearly two orders of magnitude higher than at room temperature) [12]. The temperature and pressure defining these conditions is controversial and has been reported as low as 170°C [13] or as high as 220°C [14].

No. run	Ratio % (g/100 ml)	T (°C)	t (h)	SY (%)	Moisture (%)	Vol. (%)	Fixed carbon (%)	Ash (%)	HHV (MJ/kg)
Raw	—	—	—	—	8.9	88.72	1.75	0.63	17.0
1	11.7	200	0.9	93.96	1.62	91.77	5.44	1.17	16.99
2	3.3	230	15.0	29.89	3.51	43.5	52.4	0.57	27.06
3	20.0	170	4.5	95.63	6.91	88.31	4.32	0.46	16.99
4	11.7	150	9.8	93.45	7.6	90.02	1.81	0.57	17.34
5	3.3	170	4.5	94.98	4.84	91.9	1.69	1.57	17.04
6	3.3	230	4.5	21.72	3.31	49.42	49.96	3.31	25.89
7	3.3	170	15.0	59.73	2.61	86.18	6.91	4.31	17.30
8	20.0	170	15.0	83.08	2.88	89.54	7.09	0.49	16.99
9	25.7	200	9.8	49.47	1.92	47.50	52.5	0.49	26.13
10	11.7	200	9.8	44.25	0.22	46.36	51.43	1.99	26.42
11	20.0	230	4.5	46.99	2.59	49.03	44.78	3.74	26.25
12	20.0	230	15.0	47.80	2.44	43.94	50.81	2.81	27.39
13	11.7	200	18.6	44.66	2.73	47.89	47.71	1.68	26.65
14	11.7	200	9.8	44.29	1.57	49.91	44.78	3.74	26.72
15	1.5	200	9.8	42.02	1.65	46.52	51.83	1.65	26.38

Table 1.
Values for solid yield (SY, %), proximate analysis (%) and high heating value (HHV) (kJ/kg), for reactions made under different Ratio (%), temperature (T), time (t).

The interpretation of the results showed in **Table 1** can be facilitated by plotting 2D level curves for a fixed value of one variable. As an example, **Figure 1** shows these plots for fixed biomass/water ratios (a–c), fixed temperature values (d–f) and fixed time periods (g–i), when the output function is the solid yield (%). A glance to these figures can provide valuable information not only about the effect of the experimental variables but also on their interactions, as it is explained next.

First, it can be observed that for a fixed ratio, increasing temperature involves a lower SY, up to a cutting point for which the process is reversed; this suggests, in coherence with results reported by other researchers, that the presence of reactions responsible for the formation of aggregates from monomers in the liquid phase, that finally migrate to the solid phase might be only possible if a certain temperature is used. Funke et al. [15] identify this effect with the reach of a critical saturation concentration, by which the cellulose fragments (produced from dehydration or decarboxylation, both endothermal processes) react to form cross-linked hydrophobic polymer structures. It is also interesting to notice that this effect is mitigated when a greater ratio is used; probably because of diffusion restrictions. Dissimilarly, for a fixed ratio, time has a scant influence under these conditions.

On the other hand, one can see that for a fixed temperature increasing *R* brings out an increase on the solid yield. Besides, time has a positive influence on the solid yield only if the fixed temperature is low, whereas the tendency is inverted if a high temperature is employed.

If **t** is fixed, a higher **T** decreases the solid yield, up to a maximum value of SY; thereafter, if T is increased, the SY is also enhanced. This temperature value is always higher than 200°C, and decreases for longer treatments. The ratio has a scant influence on the SY for low temperatures and a positive effect on it a higher temperatures.
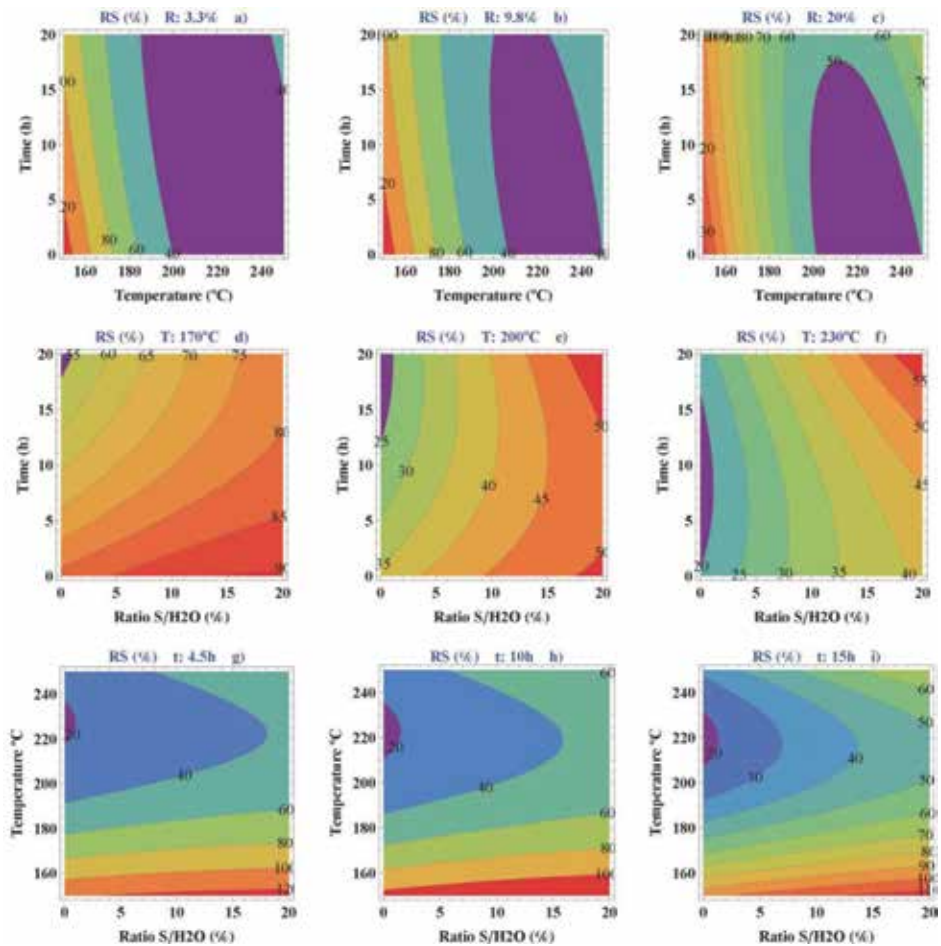
Figure 1.
Level curves for solid yield corresponding to HTC processes under varying experimental conditions.

Figure 2a and **b** depicts the results obtained from the thermal degradation studies under inert and oxidizing atmosphere, respectively. As it can be inferred from this figure, the first weight loss, associated to moisture, is in general less marked for samples that were hydrocarbonized under more aggressive conditions (and, in all cases, lower than for pure cellulose, see **Table 1**; moisture content of 8.9%), which confirms that HTC was effective as drying process. Hydrolysis and dehydration are, as previously reported, specially favored for higher temperatures. Further on, one can see that the slope of the thermogram step associated to the release of volatile matter is also markedly affected by the experimental conditions. While most of the volatile matter has been degraded for HCs prepared at T > 200°C, the runs made under soft conditions show TG profiles that almost overlap with that of pure cellulose. This behavior has a clear effect on the fixed carbon content, as explained above.

The breaking-up of volatile matter as a result of HTC has been associated to hydrolysis, dehydration, decarboxylation, decarbonylation or demethanation reactions. Besides, some other reactions responsible for the stabilization (and even further creation) of the solid phase have also been reported (namely condensation, polymerization, and aromatization). By having a look to DTG profiles obtained for biomass precursors [14], one could suggest that the higher proportion of lignin in the HCs prepared under more aggressive conditions is responsible for
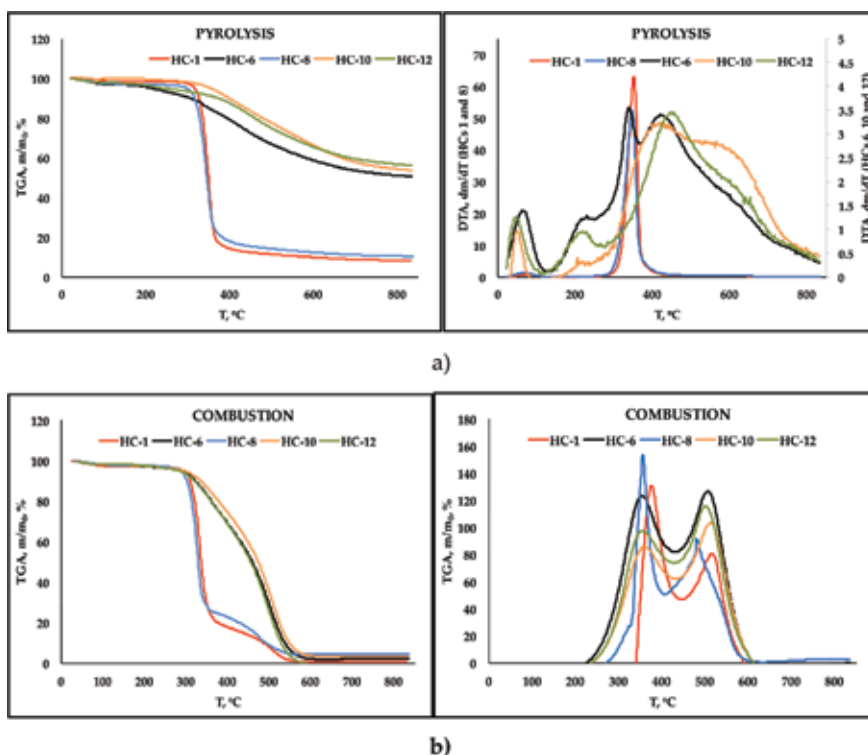
Figure 2.
Thermal degradation study (TG and DTA) under inert (a) and oxidizing (b) conditions.

the gradual mass release at high temperatures during TGA analyses. However, in the case of cellulose, the examination of DTA curves at temperatures higher than 400°C allows concluding that after effective HTC (samples 6, 10 and 12) a solid phase has been created on the HC, which is more resistant than the precursor. This new constituent is accounts approximately for 50% of the HC weight, and degrades in the range of temperature 400–750°C, a temperature range that is associated to *charring* processes [16]. The same trend can be observed from combustion profiles.

Monitorizing the emissions associated to thermal degradation processes can be very useful to confirm the prominence of particular reactions pathways. In this work, the emissions associated to the combustion of selected HCs were studied, and, as an example, **Figure 3** shows the ion intensity profiles found for sample 6, made under aggressive conditions (i.e., under which HTC readily took place). The analysis confirms the release of CO_2 along the temperature range associated to the removal of volatile matter, and also, although in a lower extent, at higher temperatures. This in turn is coherent to the existence a fraction of HC that is more resistant to degradation, even under oxidizing conditions, and is the consequence of the aromatization reactions and repolymerization of cellulose fragments, as described previously. CH_4 release is also found at temperatures higher than 500°C, supporting the previous behavior.

3.2 HC characterization and thermal degradation study

The surface morphology of the samples was examined by SEM micrography. For the sake of brevity, only some of them have been included in this work, and have been collected in **Figure 4**, classified in two groups in **Figure 4a–e**.
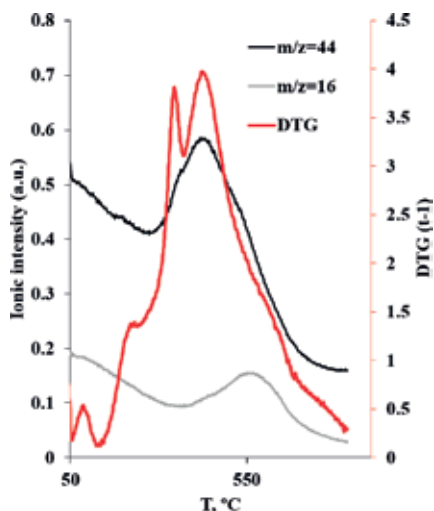
Figure 3.
Emissions associated to the thermal degradation of HC-6.

Firstly, one can observe that for sample 1 (a, representative of very mild conditions), the HC surface is smooth and there is presence of some irregular aggregates, which might be associated to the initial steps of cellulose dilution, although the precursor fibrous structure remains almost unchanged. Sample 8 (b), also prepared at low temperature, also exhibited these features.

In contrast, the appearance of samples prepared at temperatures higher than 200°C (such as 6, 10 and 12) is markedly different (**Figure 4c–e**). In these HCs, the surface appears heterogeneous and covered of microspheres of various sizes. The formation of these spheres has been traditionally associated to the breaking-up of cellulose molecules, as found in biomass materials. As a result of hydrolysis, cellulose breaks into small-chain polymers and monomers which further can polymerize as higher molecular weight compounds (is a second solid phase, as it was previously suggested from TG profiles). After hydrolysis (or simultaneously), dehydration is assumed to take place [14]; this process can be both physical (reject of water from the solid precursor) and chemical (removal of hydroxyl groups). The spherical configuration is related to their limited solubility and hydrophobicity, as it minimizes the interfacial surface HC-solvent [17].

The changes induced on the surface chemistry of the HCs were also dependent on the preparation conditions, and, as in the case of the previous analyses, two different trends were found, as a result of a less or more aggressive treatment. **Figure 5** collects the spectra obtained for selected HCs; the assignation of bands was made using suitable bibliography.

As inferred from **Figure 4**, the bands found for HCs 1 and 8 are significantly different in size and location to those found for samples 6, 10 and 12.

In the first place, the bands usually assigned to –OH groups (signals around 3400 and 2800 cm^{-1}) are significantly less intense for those samples hydrocarbonized at higher temperature, suggesting that hydrolysis and dehydration were more prominent in these cases.

Also, as the HTC temperature is increased there is a decrease on the oxygenated groups present on the HC surface; for instance, the vanishing of the spectral band at 1030 cm^{-1} suggests the removal of ether-type functional groups (C–O).

A peak at 1264 cm^{-1}, corresponding to the C–O–C bond of cellulose, is clearly found in samples 1 and 8, and remains, also slighter, for the remaining samples, indicating that part of the cellulose was degraded, but there is still a fraction of it that did not react.

On the other hand, the bands around 600 cm^{-1} are also less intense. Likewise, other bands appear or become more intense, such as the one located at 1700 cm^{-1}, suggesting a larger presence of carbonyl groups. Also, the presence of the band at 1600 cm^{-1} can be associated to a greater aromatization degree (vibration C=C) on the hydrochars.
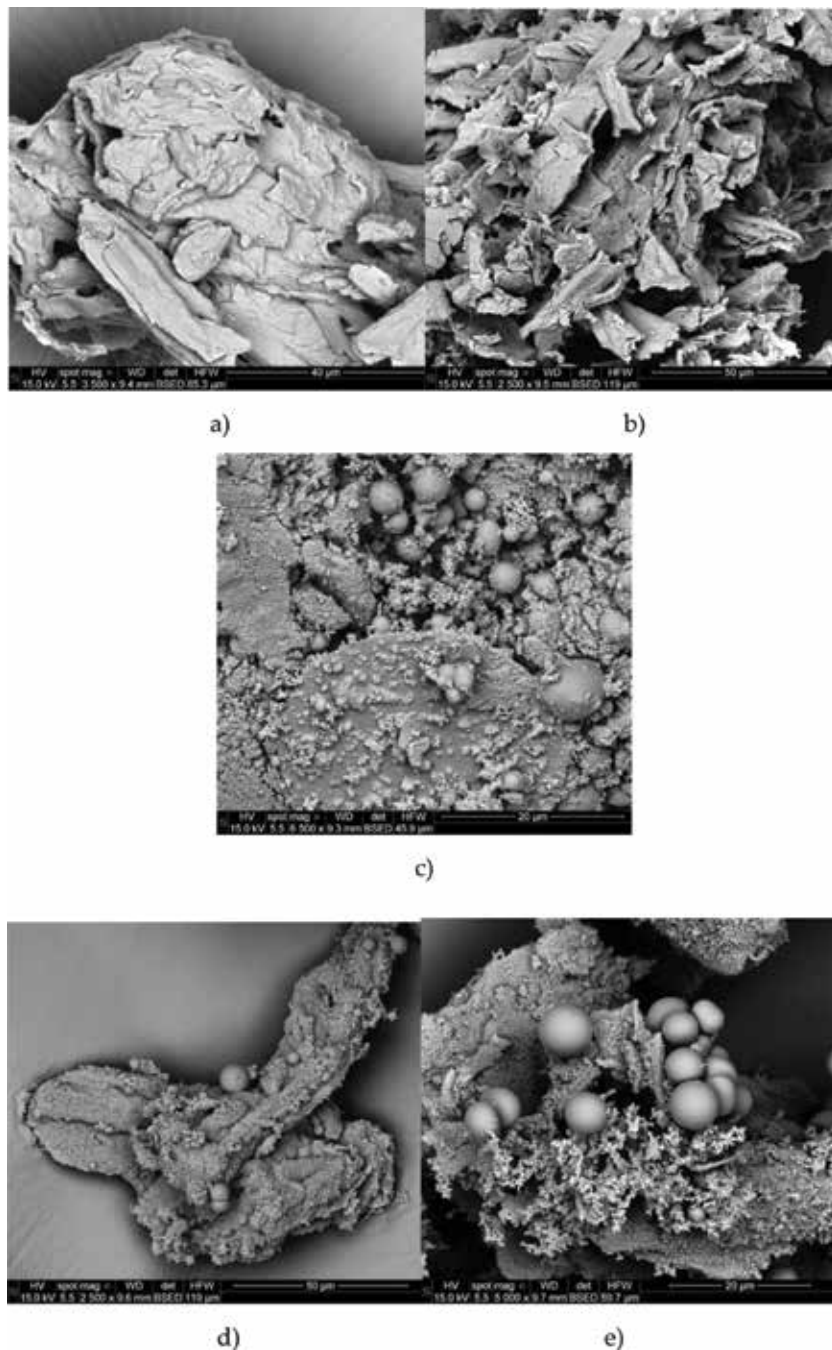

Figure 4.
SEM micrographs of selected HCs: (a) 1 (magnification: 3500; (b) 8 (magnification: 2500); (c) 6 (magnification: 6500); (d) 10 (magnification: 2500); and (e) 12 (magnification: 5000).
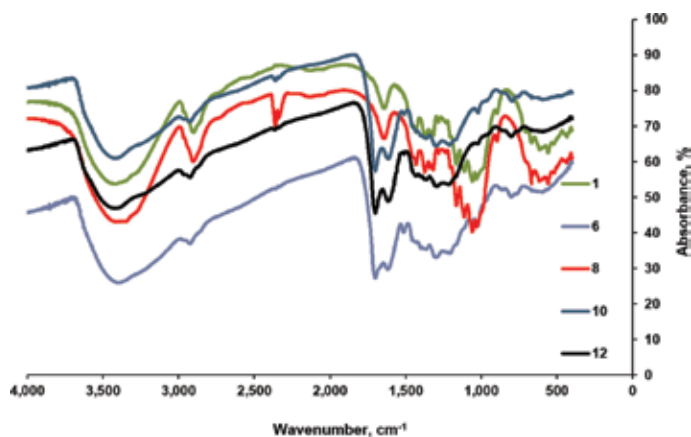
Figure 5.
FT-IR spectra of selected hydrochars.

4. Concluding remarks

The HTC of cellulose brings out a significant amount on the physical and chemical features of the material, that, depending on the experimental conditions used, can be determinant for its further use.

It was found that there is a lower limit in the experimental reaction conditions that has to be attained in order to guarantee that HTC takes place and that, in the case of cellulose, this point is associated to the use of temperatures higher than 200°C. Once these conditions are reached, the prominence of a complex combination of reactions takes place (hydrolysis, dehydration, decarboxylation, decarbonylation, repolymerization, condensation, aromatization…), whose occurrence gives rise to significant changes on the HC chemical composition, morphology, and surface functional groups.

Apart from the increase in fixed carbon and decrease in volatile matter and moisture (and, in consequence, enhanced energy densification), the behavior towards pyrolysis and combustion is clearly modified after HTC. In this way, it is confirmed that the fragments resultant from cellulose breaking are combined and a new solid is formed, with lignite-type features, and enhanced resistance to thermal degradation. The release of CO_2 during combustion can confirm this effect, since it was present upon degradation up to temperatures as high as 700°C.

Other important features brought up by HTC are related to the different surface morphology, increase in aromaticity, hydrophobicity and development of oxygen surface groups, whose abundancy can also be modeled as a result of the experimental conditions.

These changes justify the use of HTC as sustainable and straightforward method to produce materials suitable for many applications, and also as pretreatment for other processes. The lower moisture is advantageous for improving storage conditions, and also to avoid cost-intensive drying processes prior to combustion processes. Also, the enhanced heating value and hydrophobicity is positive for the use of HCs as biofuels.

The greater porosity and stability provide a better behavior towards applications related to soil remediation and adsorption processes. Besides, the availability of π electrons related to greater aromaticity is very interesting if the HC is to be used to produce supercapacitors or other energy storage devices.

Finally, the variety and abundancy of oxygenated functional groups is related to an enhanced reactivity towards activation and improved adsorption performance towards particular adsorbates.

Acknowledgements

Author details

Silvia Román[1]*, Beatriz Ledesma[1], Andrés Álvarez-Murillo[1], Eduardo Sabio[1], J. F. González[1], Mara Olivares-Marín[2] and Mouzaina Boutieb[3]

1 Department of Applied Physics, University of Extremadura, Badajoz, Spain

2 Mechanical, Energetic and Materials Engineering Department, University of Extremadura, Badajoz, Spain

3 Laboratory of Process Engineering and Industrial Systems (LR11ES54), National School of Engineering, University of Gabès, Tunisia

*Address all correspondence to: sroman@unex.es

IntechOpen

References

[1] Global Trends 2016: Figures at a Glance. The UN Refugees Agency. Available from: http://www.unhcr.org/figures-at-a-glance.html [Accessed: May 2018]

[2] Biobased Industries. European Comission Report. Horizon 2020: The EU Framework Programme for Research and Innovation. Available from: https://ec.europa.eu/programmes/horizon2020/en/area/bio-based-industries [Accessed: October 2017]

[3] Román S, Libra J, Berge N, Sabio E, Ro K, Liang L, Ledesma B, Álvarez A, Bae S. Hydrothermal carbonization: Modeling, final properties design and applications: A review. Energies. 2018;**11**:216. DOI: 10.3390/en11010216

[4] Fernandez ME, Ledesma B, Román S, Bonelli PR, Cukierman AL. Development and characterization of activated hydrochars from orange peels as potential adsorbents for emerging organic contaminants. Bioresource Technology. 2015;**183**:221-228

[5] Sabio E, Álvarez-Murillo A, Román S, Ledesma B. Conversion of tomato-peel waste into solid fuel by hydrothermal carbonization: Influence of the processing variables. Waste Management. 2016;**47**:122-132

[6] Álvarez-Murillo A, Sabio E, Ledesma B, Román S, González-García CM. Generation of biofuel from hydrothermal carbonization of cellulose. Kinetics modelling. Energy. 2016;**94**:600-608

[7] Berge ND, Ro KS, Mao J, Flora JRV, Chappell MA, Bae S. Hydrothermal carbonization of municipal waste streams. Environmental Science and Technology. 2011;**45**(13):5696-5703

[8] Pala M, Kantarli IC, Buyukisik HB, Yanik J. Hydrothermal carbonization and torrefaction of grape pomace: A comparative evaluation. Bioresource Technology. 2014;**161**:255-262

[9] Pham TPT, Kaushik R, Parshetti GK, Mahmood R, Balasubramanian R. Food waste-to-energy conversion technologies: Current status and future directions. Waste Management. 2015;**38**:399-408

[10] Álvarez-Murillo A, Ledesma B, Román S, Sabio E, Gañán J. Biomass pyrolysis toward hydrocarbonization. Influence on subsequent steam gasification processes. Journal of Analytical and Applied Pyrolysis. 2015;**113**:380-389. DOI: 10.1016/j.jaap. 2015.02.030

[11] Peterson AA, Vogel F, Lachance RP, Fröling M, Antal J, Tester JW. Thermochemical biofuel production in hydrothermal media: A review of sub- and supercritical water technologies. Energy & Environmental Science. 2008;**1**(1):32-65. DOI: 10.1039/B810100K

[12] Bandura A, Lvov A. The ionization constant of water over wide range of temperature and density. Journal of Physical and Chemical Reference Data. 2006;**35**(1):793-800

[13] Román S, Nabais JMV, Laginhas C, Ledesma B, González JF. Hydrothermal carbonization as an effective way of densifying the energy content of biomass. Fuel Processing Technology. 2012;**103**:78-83. DOI: 10.1016/j.fuproc.2011.11.009

[14] Reza MT, Uddin MH, Lynam JG, Hoekman SK, Coronella CJ. Hydrothermal carbonization of loblolly pine: Reaction chemistry and water balance. Biomass Conversion and Biorefinery. 2014;**4**:311-321

[15] Funke A, Ziegler F. Hydrothermal carbonization of biomass: A summary and discussion of chemical mechanisms for process engineering. Biofuels, Bioprodunts Biorefinery. 2010;**4**:160-177

[16] Skodras G, Palladas A, Kaldis SP, Sakellaropoulos GP. Cleaner co-combustion of lignite-biomass-waste blends by utilising inhibiting compounds of toxic emissions. Chemosphere. 2007;**67**:191-197

[17] Falcó C. Sustainable biomass-derived hydrothermal carbons for energy applications [doctoral Phd]. Postdam: Max Planck Institut für Kolloid und Grenzflächenforschung; 2012

Chapter 5

Estimation of Energy Potential for Solid Pyrolysis By-Products Using Analytical Methods

Gabriela Ionescu and Cora Bulmău

Abstract

Waste can be converted into energy and value-added products by thermo-chemical processes. Pyrolysis represents the thermal degradation of the material under a non-oxidant atmosphere leading to generation of three products: char—solid, oil—liquid and pyrolysis gas. Pyrolysis process means a complex mechanism of reactions, endothermic and/or exothermic chemical reactions that occurs simultaneously and/or subsequently. The use of lignocellulosic and plastic waste for energy purposes leads to the production of solids that could replace much of the conventional fuels once energy conversion technologies will prove profitable. In this chapter the authors proposed to describe, analyze and apply analytical methods for the heating value estimation of the solid products generated by pyrolysis of different wood and plastic materials. Our results obtained by experimental studies and empirical formulas will be evaluated and compared. The impact of the thermo-chemical process operational conditions on the variation of chars and biochars heating value will be also discussed in this chapter.

Keywords: analytical pyrolysis, heating value, biomass, plastic

1. Introduction

Today, the society concentrates on technological forces to switch the energy generation from conventional sources to renewables. This global tendency evolved due to the use of more clean, alternate and reusable energy sources. Denmark has already produced 44% of its electricity needs with renewable wind power and it intends to require at least 50% of its energy needs to come from renewable sources by 2030 [1]. The Scottish Government aims to generate 100% of Scotland's electrical power from renewable energy by 2020. Also, India plans nearly 60% of electricity capacity from non-fossil fuels by 2027. Waste and biomass are inevitable products of society. The main challenge for the future generations is to investigate how to manage large quantities of these fuels in a sustainable way. The energy content (heating value) represents a key factor of the waste, which determines how much energy can be extracted from it. Wood, cardboard or plastic waste is one of the main components of the municipal solid wastes (MSW), residential types respectively. These energy resources could be exploited by thermal processes to produce solids fuels with valuable energy content. Cellulosic and plastic residues, despite others exhaustible or expensive materials, could be used to produce fuels with valuable energy content.

The impact of biomass properties and operational conditions of pyrolysis processes on physical and chemical properties of the biochar has been already discussed [2–4], but insufficient materials are published concerning the relation between biomass and plastic based waste types and the energy content of chars and biochars. The present work brings contributions with critical analytical data regarding this correlation. This could help to identify optimum types of waste to be treated to produce chars valuable for their energy potential in a variety of pyrolysis units. Therefore, the research concentrates on theoretical and experimental studies that could give more clues about the heating value of the chars generated from five types of waste. So, we proposed to obtain viable experimental results applicative at industrial level and give some ideas how use the chars obtained or how to replace some materials with these lignocellulosic/plastic wastes. These could solve environmental problems that affect in the present the entire world.

2. Calorimetry: instrumentation and analysis

Calorimetry is the science dedicated to the measuring of heat. This represents the amount of energy exchanged within a given time interval in the form of a heat flow [5]. Since its foundation in 1780, the calorimetry meets variated and successful uses in many fields. The modern calorimetry has some targeted fields: material science, life science (biology, medicine and biochemistry), pharmacy and food science, environmental control analysis, safety investigations and determinations of energy content of fuels, search of new alternative energy sources.

During the past century, the classical methods of calorimetry have not known many changes, only microelectronic and computer science get progress allowing to develop new types of calorimeters and open new fields of application.

Each calorimetric experiment has three stages very well defined:

- The calorimetric part assumes the accurate determination of the energy generated in the reaction.

- The chemical part involves the characterization of the initial and final states.

- The transformation of the results obtained in the calorimetric experiment to a standard-state combustion energy at 298.15 K, from which a standard enthalpy of formation can be calculated [6].

2.1 Units

Heat cannot be measured by a direct method. Consequently, heat must be determined by means of its effects. The oldest unit quantity of heat is the calorie. This was defined in terms of the heating of water. A traditional definition specifies that 1 calorie is the amount of heat required to raise the temperature of 1 gram of water by 1°C, from 14.5 to 15.5°C (American Physical Society). Conversion relation between calorie and joule:

$$1 \text{ cal } = 4.184 \text{ J}$$

$$1 \text{ J } = 0.2388459 \text{ cal}$$

Nowadays, the International System of Unit recommend joule as unit for heat. Another common unit for heat is British thermal unit (Btu), that is the English system analog of the calorie.

$$1 \text{ Btu } = 251.9958 \text{ cal}$$

The last unit is the International Table (IT) calorie that has been adopted in the publications of the Energy Information Administration of the U.S. Department of Energy (DOE/EIA) [7] and of the International Energy Agency of the Organization for Economic Co-operation and Development (OECD/IEA) [8].

2.2 Calorimeters

The calorimeter represents an instrument used in calorimetric testing (calorimetry) that allows to measure the amount of heat released or absorbed in chemical or physical reactions. It can determine heat content, latent heat, specific heat, and other thermal properties of substances. The design of a calorimeter is based on a container with a temperature thermocouple through which the thermal phenomenon is investigated. The container communicates with the environment by its insulating walls that have some thermal resistance.

There are many types of calorimeters used for measurement of the heat. The most common are:

- *Bomb calorimeters*—they are isolated devices with a constant volume. Since the volume does not changed, the instruments measure the heat evolved under constant volume, q_v,

$$q_v = C \times dT \ [J], \tag{1}$$

where dT is the temperature increase. The q_v so measured is also called the change in internal energy, dE. Note that.

$$dE = q_v = C \times dT \ [J] \tag{2}$$

- *Differential scanning calorimeters*—represent an important tool in thermal analysis. If a calorimeter measures the heat into or out of a sample, a differential calorimeter measures the heat of sample relative to a reference. The difference in the quantity of heat necessary to increase the temperature of the sample starting from the reference temperature is measured as a function of temperature. In the last years, the methods of thermal analysis have been widely accepted in analytical chemistry. Differential scanning calorimeters are often used in many industries—from pharmaceuticals and polymers, to nanomaterials and food products.

- Isothermal titration calorimeters—they are based on a technique (isothermal titration calorimetry—ITC) used in quantitative studies of an extensive variety of biomolecular interactions. They directly measure the heat that is either released or absorbed during a biomolecular binding event. Isothermal titration calorimetry (ITC) is a valid method to investigate biological reactions with high sensitivity and accuracy at a constant temperature [9].

- *Calvet-type calorimeters*—they are not so often used. They can measure the enthalpy change during sublimation reactions and the behavior of a material. In case of these calorimeters, the detection is based on a three-dimensional flux meter sensor. There is no calibration and standard methods required for this type of calorimeters. The calibration can be achieved at a constant temperature, in heating and cooling modes, while the system can manage temperatures up to 1600°C. Calvet microcalorimeter is one of the most known type of

heat conduction calorimeter [10], SETARAM Instrumentation being the only producer of these categories instruments.

During this chapter we focused on oxygen bomb calorimeters. These type of calorimeters have a wide range of uses, but their mainly applicability are in the coal industry, i.e., coal fired power stations, iron and steel plants, cement plants and other users of coal. Also, they are often used in other non-coal related industries. Some examples for this case are:

- animal feeds—to determine their nutritional value,

- animal digestion of feeds, dairy products and other foods to measure the caloric value,

- ammunition propellants are analyzed for their effectiveness,

- liquid fuels can also be analyzed in a similar way to coal.

Other important applicability of the bomb calorimeters is the use in colleges, universities or research institutes, where these instruments could bring a contribution to teaching or to experimental and development research that is performed in many departments. But the main applications for oxygen bomb calorimeters are:

- Solid and liquid fuel testing,

- Waste and refuse disposal,

- Food and metabolic studies,

- Propellant and explosive testing,

- Fundamental thermodynamic studies,

- Educational training.

3. High heating value

The heating value or calorific value defines the energy content of a fuel. It is one of the most important properties to evaluate the fuel quality and a key parameter in the development of any energetic application. The heating value is the amount of heat released during the complete combustion of a specific fuel quantity at standard conditions, pressure 1 atm and temperature 25°C. Generally, it is measured in energy content (Joule, Calorie, British Thermal Unit- Btu or Watt-hours-Wh) per specific quantity (mass or volume) of the combusted fuel. The specific quantity is given by the fuel physical state: molar, gram or kilogram for solid fuels, liter for liquid fuels and cubic meter for gaseous fuels.

The fuel heating value can be classified as Higher or Lower Heating Value (LHV). The High Heating Value (HHV) otherwise known as heat of combustion or Higher Calorific Value or Gross Calorific Value (GCV) or Gross Energy or Upper Heating Value is the total amount of energy released during the fuel complete combustion per fuel specific quantity. The LHV, also known as Net

Heating Value or Net Calorific Value, is determined by subtracting the latent heat of vaporization produced during the complete combustion of the fuel from the HHV [11].

The heating value can be estimated theoretically based on the proximate, ultimate and chemical analysis composition of the fuel by using dedicated empirical formulas or experimentally by employing an adiabatic calorimetric bomb, which measures the enthalpy change between reactants and products [12–14].

3.1 Theoretical estimation of the heating value

Although the calorimeter instrument is easy to use and relatively accurate, it might not always be accessible to researchers. The earliest and most used empirical correlation for the HHV estimation was developed by Dulong by in end of nineteenth century, based on the ultimate analysis of coal [15]. One century later, Tillman [16] developed the simplest heating value prediction formula for woody biomass based on the fuel carbon content.

Up to now, various empirical formulas, models and correlations have been improved or developed for the predication of the HHV using the proximate or ultimate analysis of the fuel such as: fossil fuels/waste [17], biomass [18, 19], refused derived-fuels [20], commingled wastes [21, 22]. However, sometimes the models can have their limitations, due to their wide variety on fuels applications, that can be homogeneous (e.g., fossil fuels and biomass) or heterogenous (refused derived fuels, solid recovered fuels, municipal solid waste) such as:

- the equations based on the elemental analysis are generally more accurate than those based on proximate analysis [12];

- usually, the weight of the moisture or ash free basis or both, is undefined in the equation, limiting its accuracy;

- for precise values, even for homogenous wastes, like biomass, Özyuğuran and Yaman, show the necessity to create models for each subclasses (e.g., herbaceous, woody or agricultural waste) [23];

- sometimes the same model can be reproduced based on different units (i.e., kcal/kg, kJ/kg, Btu/lb, etc.) leading to confusion [24].

- some studies suggest the creation of personalized models, based on the fuel derivation/application, country/region, to avoid the over or under prediction [25, 26].

3.2 Estimation of the high heating value from ultimate or proximate analysis

In the absence of calorimeter instrument, the HHV can be estimated based on the elemental, proximate or physical analysis of the fuel.

Based on a comprehensive literature review the most common equations for the appropriate estimation of the HHV of biomass, commingled biomass-plastic waste, municipal solid waste (MSW), coal and char are summarized in **Table 1**. Ten correlations for each type of analysis (ultimate and proximate) were studied in order to establish the wide applicability and versatility of the formulas by considering cellulose, hemicellulose, lignocellulose and plastic polymers-based waste.

Eq no.	Name of the author/source	Original equation	U.M.	Recommend fuel type	Ref.
Estimation of the high heating value from ultimate analysis					
1	Sheng and Azevedo	$HHV = 0.3259C + 3.4597$	MJ/kg	Biomass	[12]
2	Tillman	$HHV = 0.4373C - 1.6701$	J/kg	Biomass	[27]
3	REM model	$HHV = 36C + 120H - 16O$	MJ/kg	Biomass-plastic	[21]
4	Friedl et al.	$HHV = 3.55C^2 - 232C - 2230H + 51.2C \times H + 131N + 20{,}600$	kJ/kg	Biomass	[28]
5	Dulong	$HHV = 7831C + 35{,}932H - O/8 + 1187O + 578N$	kcal/kg	Waste	[29]
6	Yacio	$HHV = 0.336C + 1.418H - 0.0145O + 0.0941S$	MJ/kg	Coal/refuse	[30]
7	Dermirbas	$HHV = 0.335C + 1.423H - 0.154 * O - 0.145N$	J/kg	Waste/biomass	[31]
8	Dulong	$HHV = 144.5C + 609.6H - 76.2O + 40S + 10N$	Btu/lb	Waste/coal	[32]
9	Boie	$HHV = 35.2C + 116.2H + 6.3N + 10.5S + 11.1O$	MJ/kg	Waste/biomass	[21]
10	Scheurer-Kestner	$HHV = 81(C - 3O/4) + 342.5H + 22.5S + 171O/4 - 6(9H + W)$	kcal/kg	Waste	[25]
Estimation of the high heating value from proximate analysis					
11	García et al.	$HHV = 18{,}300 - 3.98A^2 - 112.10A$	kJ/kg	Biomass	[32]
12	Yin	$HHV = 0.1905VM + 0.2521FC$	MJ/kg	Biomass	[19]
13	Cordero et al.,	$HHV = 354.3FC + 170.8VM$	kJ/kg	Biomass	[33]
14	Phichai et al.	$HHV = 157234(VM + FC) + 4243.97$	kJ/kg	Biomass	[34]
15	Bento	$HHV = 44.75VM - 5.85W + 21.2$	kcal/kg	Refuse/char	[25]
16	Kathiravale et al	$HHV = 356.047VM - 118.035FC - 5600.613$	kJ/kg	MSW	[35]
17	Soponpongpipat et al.	$HHV = 354879 - 0.3023A - 0.1905VM$	MJ/kg	Chars/coal	[36]
18	Özyuğuran, et al.	$HHV = 1672 - 1.449VM - 1.562FC - 1.846A$	MJ/kg	Biomass	[23]
19	Kieseler et al.	$HHV = 0.4108FC + 0.1934VM - 0.0211A$	MJ/kg	Chars	[37]
20	Parikh et al.	$HHV = 0.3536FC + 0.1559VM - 0.0078A$	MJ/kg	Biomass	[38]

HHV, high heating value; U.M., unit measure; C,H,N,S,O, wt% of carbon, hydrogen, nitrogen, sulphur, oxygen content; W, wt% total moisture content; A, wt% of ash, dry basis; VM, wt% volatile matter; FC, wt% of fixed carbon.

Table 1.
Most common equations used for high heating value prediction.

As seen from **Table 1**, most empirical formulas are linear regression models, build based on the mass fractions (weight) or percent of the fuel principal elements and constant coefficients. The simplest equations for the HHV prediction from the ultimate or proximate analysis consider only the carbon (C) fuel content (Eqs. (1, 2)), or ash (A) (Eq. (11)), respectively. Besides these two elements, the reliability of the results increases with the augmentation of the chemical or physical elements used partly or fully in the formulas: hydrogen (H), oxygen (O), nitrogen (N), sulfur (S), chlorine (Cl) or fixed carbon (FC), volatile matter (VM) and moisture (W). Over more Eqs. (2, 5, 8, 16) represent one of the most known and used equations in the exact science area, while the rest have been proposed, adjusted or improved in the last in several decades [15, 19].

It is worth noting in order to use or create dedicated empirical formulas, the experimental determination of the chemical–physical characteristic of the fuel is need. In this case dedicated laboratory instruments are necessary. The proximate analysis could be established by using a thermogravimetric analyzer (TG), following the ASTM D7582-12. In the absence of the TG analyzer, the drying oven and the calcination furnace can be used. Thus, for woody-biomass the content of moisture is determined according to ASTM standard method 871-82, for volatile matter (VM) with ASTM D5832-98 (2014) and ash with ASTM D1102-84 (2013). The fixed carbon content (FC) is always determined by difference considering the sum of total moisture (if available), volatile matter and ash. The elementar analyzer is used for the ultimate analysis determination adopting ASTM D5373 – 08. Usually the oxygen (O) is obtained by subtracting the rest of the determined chemical elements carbon (C), hydrogen (H), nitrogen (N), sulfur (S) and chlorine (Cl) from the total content (O = 100 − C − H − N − S − Cl) or by subtracting the carbon (C), hydrogen (H) and ash from the matter (O = C − H − Ash).

3.3 Proximate and ultimate analyses data on biomass and plastic waste

The validation of the HHV predication models presented in the preceding section was made by using the characterization of three biomass-based waste (cherry wood, cardboard and newspaper waste) and two types of plastic waste, polypropylene (PP) and high-density polyethylene (HDPE) waste. The waste sampling, along with the analytical and empirical procedure for the ultimate and proximate analysis of the newspaper, cardboard, PP and HDPE resulted from the selective collection of the municipal solid waste were former presented in previews researches made by the authors [39, 40]. The cherry wood waste elemental and proximate composition was obtained after a generic review of the former literature [41, 42]. The summaries of the ultimate and proximate analysis are presented in **Table 2**.

	Ultimate analysis [wt%]						Proximate analysis [wt%]			
Sample	C	H	N	S	O	Total	V.M.	F.C.	Ash	Total
Newspaper	47.00	7.00	2.00	1.00	43.00	100.00	88.4	3.5	8.1	100.00
Cardboard	48.00	8.00	2.00	1.00	41.00	100.00	87.5	6.6	5.9	100.00
Cherry wood waste	49.52	5.81	0.31	0.02	44.34	100.00	84.9	15	0.1	100.00
PP	85.50	12.50	1.20	0.10	0.70	100.00	99.13	0.27	0.6	100.00
HDPE	84.70	14.47	0.11	0.12	0.60	100.00	99.74	0.06	0.2	100.00

Table 2.
Summaries of ultimate and proximate analysis [39, 43].

4. Experimental determinations

The experimental research was developed adopting a bench scale pyrolysis system and an oxygen bomb calorimeter with the purpose to investigate alternative energy sources from residue material as light packaging waste and wooden biomass.

Calorimetry experiments were performed for the solid products (chars) generated by biomass and light packaging waste (LPW) pyrolysis processes and with a calorimetric bomb IKA C200. Testing were completed for five types of chars resulted from waste pyrolysis: biochars produced from woody biomass and mixers of biomass and plastic based material.

4.1 Collection and preparation of the samples

Five types of materials were considered and analyzed in the present chapter. Cherry sawdust was the wooden biomass used to produce biochar samples and it was collected from furniture industry. The configuration, the procedure to get the reduced dimensions and characterization of the cherry wood and the others plastic based materials were previously detailed described in other works [43, 44]. Other four LPW mixtures representative for Eastern Europe, coming from the MSW selective collection were used: Mix 1 (paper and cardboard mixture—in equal proportion), Mix 2 (plastic solid waste mixture—HDPE, PP, PET—in equal proportion), Mix 3 (90% paper & cardboard waste mixture and 10% plastic solid waste mixture), Mix 4 (67% paper & cardboard waste and 33% plastic solid waste).

Pyrolysis processing was applied to cherry wood, resulting in a series of 12 samples of cherry biochars, 36 samples of LPW mixtures respectively. So, a total of 48 samples were prepared for measurements of high heating values by using the oxygen bomb calorimeter.

4.2 Processing for char samples production

To obtain the solid pyrolysis by-products that can be used as fuel with high calorific energy content, pyrolysis processes were completed through a laboratory scale pyrolyser. **Figure 1** explains the general schema of the reactor. The furnace temperature was very well controlled to achieve the desired heating rate and temperature for samples thermal-chemical treatment as the furnace is equipped with an automatic integrated control for heating. The tubular batch reactor worked in a discontinuous mode, so the waste sample was placed in a crucible of refractory steel W4541 with tubular parallelepiped form and then this was introduced in the furnace. Each sample of the cherry biomass was weighted trying to keep the mass constant at 25 g. The total amount of the mixture that entered in the crucible was in a range 25–30 g depending on the form and structure of the waste fractions.
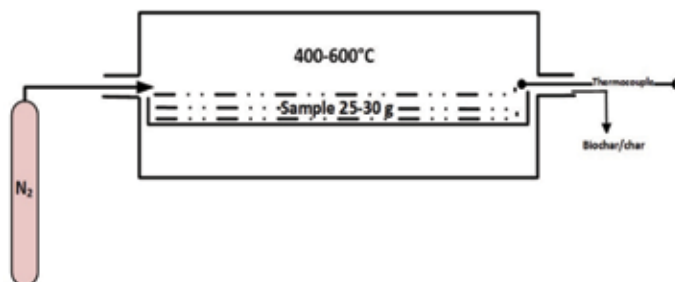

Figure 1.
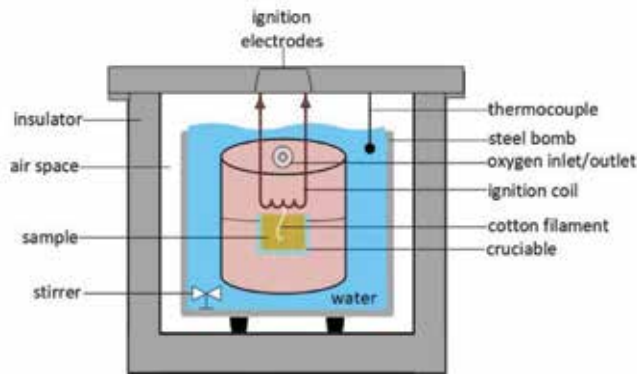*Simplified scheme of the pyrolysis batch reactor.*

Figure 2.
Calorimetric system.

The reactor was heated by electrical resistances until the temperature of the process has reached the desired value. At this moment the biomass waste sample was introduced in the reactor, where an inert atmosphere was maintained throughout the pyrolysis processing by inserting a nitrogen flow of about 1 l/min. For the types of the materials analyzed in this chapter, the pyrolysis processing was conducted in almost the same conditions: temperature: 400, 500 and 600°C, atmospheric pressure, inert gas: purified N_2 (99.9995%) at a gas pressure 50–100 kPa; only the process time was different: 30 min for cherry wood and 60 min for municipal solid waste types. Considering previously results of our experimental research [45] that demonstrated heating value is not very much influenced by the treatment time during the pyrolysis processes but depends more on the process temperature [46], it is valuable to discuss and compare here the actual experimental results. All pyrolysis experiments were done in triplicates.

4.3 Procedure for HHV measurement

Experimental determinations of the high heating value in case of the five types of pyrolysis chars were performed in the laboratory conditions: combustion of the sample under specific conditions in a C200 system according to ASTM D2015-96 standard (1998). C200 (**Figure 2**) can be used to determine the calorific value for solids or liquids samples by engagement an adiabatic bomb calorimeter that allows to measure the heat of reactions involving gases.

The measuring of the samples calorific power involves the following steps:

a. Melting the crucible and weighing the sample using a high precision electronic balance;

b. Inserting the sample into a small plastic bag;

c. Positioning the filament (a cotton yarn). It binds in the middle of the firing wire.

d. Place the crucible on the support and insert the filament into the crucible, over which the material sample is placed;

e. Turning of the bomb;

f. Transporting the bomb to the oxygen station. Insert oxygen for about 3 minutes into the bomb at a pressure of 30 bar.

g. Transporting the bomb to the calorimeter. Attaching the bomb to the ignition fitment, then insert it into the calorimeter. Fit it in its intended place and then close the calorimeter.

h. Fill the IKA C200 calorimeter tank with water until the level indicator indicates the water level at a position between the minimum level and the maximum level.

i. Digital operation with the device display. Enter the values corresponding to the sample mass and the lower calorific value of the bag into which the sample is introduced.

j. After the apparatus displays the value of the calorific value, the water tank is emptied.

k. Positioning the gas removal device on the top of the calorimeter bomb.

l. Press and the gases are exhausted.

m. Opening the sample, removing the filament and cleaning the crucible with alcohol.

All the calorimetric measurements for the determination of biochars and chars HHV were performed in triplicates.

4.4 Results, comparison, and discussions

4.4.1 Theoretical high heating value of pyrolysis chars

The HHVs of the biomass and polymer-based materials were predicted by using 20 equations presented in **Table 1**. The ultimate and proximate analysis for each type of material, presented in **Table 2** were used for the application of the formulas. **Table 3** shows the newspaper, cardboard, cherry wood, PP and HDPE waste HHV-predicted values obtained using the equations presented in **Table 1**. To avoid confusion and compare more easily the results, all the predicted values were normalized, by using the same reference unit measure [kJ/kg]. The comparison of the data was made based on: the HHV predicted mean value generated by the equations, standard deviation (STD) by analyzing all the equations from each type of determination (ultimate or proximate analysis), HHV of the material obtained with the calorimeter (HHV experimental) and STD by comparing the predicted and experimental results.

From the elemental analysis models, the HHVs predicted from biomass-based materials (newspaper, cardboard and cherry wood) varies between 21,273 and 23,034 kJ/kg, while the plastic-waste ranges between 44,111–46,017 kJ/kg with a STD of ≈6000–7000 kJ/kg. By comparing only, the data obtained using the equations, the trend lines plotted in **Figure 3** report homogenies correlation between the results for most equations. However there are some visible exceptions since for plastic based materials Eq. (3, 4) underestimate the predicted HHV with almost 30%, while Eq. (7) for plastic and Eqs. (7, 8, 11) for biomass-based waste overestimates it. For some correlations inconsistent results can be observed while comparing the mean HHV predicted v.s. HHV experimental. For a better evaluation of the correlation the mean absolute error (MAE) was determined. The MAE evaluates the accuracy of the HHV predicted to the experimental one. In this case, lower values tending to 0% indicate good accuracy of a specific correlation. The MAE negative values indicate the underestimation of the results, while the positive their

High heating value (HHV) [kJ/kg]

Estimation of the high heating value from ultimate analysis

Eq. no.	1	2	3	4	5	6	7	8	9	10		Data comparison		
Type of waste/ name of the author/s	Sheng and Azevedo	Tilman	REM model	Friedl et al.	Dulong 1	Yacio	Demirbas	Dulong 2	Boie	Scheurer-Kestner	HHV predicted mean value	STD all eq.	HHV experimental [39, 43]	STD (Predicted v.s. experimental)
Newspaper	18,777	18,883	18,440	19,035	28,107	25,189	18,794	18,117	29,682	21,328	21,635	4154	14,183	3726
Cardboard	19,103	19,320	20,320	19,726	29,810	26,972	20,860	20,226	30,974	23,025	23,034	4297	15,387	3823
Cherry wood waste	19,598	19,985	17,653	19,632	27,116	24,201	17,984	16,975	29,102	20,486	21,273	3926	17,500	1887
PP	31,324	35,719	45,668	53,718	46,825	46,452	46,148	46,347	44,785	44,125	44,111	5925	42,772	670
HDPE	31,063	35,369	47,760	56,915	49,491	48,980	48,857	48,887	46,715	46,137	46,017	7046	45,783	117

Estimation of the high heating value from proximate analysis

Eq. no.	1	2	3	4	5	6	7	8	9	10		Data comparison		
Type of waste/ name of the author/s	García et al.	Yin	Cordero et al.	Phichai et al.	Bento	Kathiravale et al	Soponpongpipat et al.	Özyuğuran, et al.	Kieseler et al.	Parikh et al.	HHV predicted mean value	STD all eq.	HHV experimental [39, 43]	STD (Predicted v.s. experimental)
Newspaper	17,131	17,723	16,339	18,704	25,422	25,461	16,199	16,571	18,363	14,956	18,687	3533	14,183	2252
Cardboard	17,500	18,333	17,283	19,050	25,253	24,774	17,036	16,572	19,509	15,929	18,931	3121	15,387	1772
Cherry wood waste	18,289	19,955	19,815	19,962	24,766	22,857	19,284	16,573	22,580	18,539	20,189	2328	17,500	1345
PP	18,231	18,952	17,027	19,884	27,431	29,662	16,422	16,575	19,270	15,545	19,731	4544	42,772	11,520
HDPE	18,277	19,016	17,057	19,947	27,545	29,904	16,427	16,575	19,310	15,569	19,797	4607	45,783	12,993

Table 3.
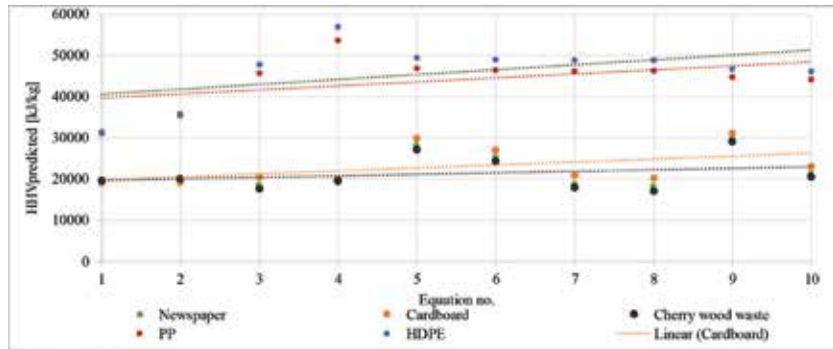*The HHVs prediction based on ultimate and proximate analysis.*

Figure 3.
Comparison of the HHV-predicted values based on ultimate analysis.

overestimation. Eqs. (5, 9, 10) and Eqs. (5, 7–12) can predict the HHVs for biomass-based wastes and plastics-based wastes respectively, with MAE lower than 10%, indicating their versatile applicability.

From the proximate analysis models, for all studied materials the HHVs predicted varies between ≈18,600 and 30,000 kJ/kg with a STD reaching to almost 12,000 kJ/kg for the plastic-based waste as shown in **Figure 4**. For plastic—based materials, the HHV predicated is different from HHV experimental, for all 10 studied equations. In all cases the predicted energetic value is underestimated. This is further strengthened by MAE that varies between −31 and −66%. In this case the validity of the correlations towards their universal usage on the defined type of materials is uncertain. Good correlation can be notice for cherry wood waste. The latter is confirmed by the mean percentage error that tends to zero and is lower than 15% for Eqs. (13–16), (19), (22). For the other biomass-based waste (newspaper and cardboard) adequate MAE varying between 4%–20% are registered for Eqs. (13–16, 19–22). Eqs. (17) and (18) are overestimating the predicted newspaper and cardboard HHV with 60–80%. By analysis the equations correlated with the number of elements considered, we can conclude that the heating value is mainly a function of ash content or volatile matter. The previews statement is support also by literature [25]. In conclusion the accuracy of the results increases with the numbers of elements correlated with ultimate and proximate analysis considered in the prediction formulas. Furthermore, higher correlations accuracies have been registered in the case of ultimate analysis usage. The current statement is supported by former investigations presented by Menikpura and Basnayake [47].

4.4.2 Experimentally determined high heating value of pyrolysis chars

The results concerning the caloric energy of the chars resulted from pyrolysis of the wood cherry and four PSW and PCW mixes (Mix 1, Mix 2, Mix 3, Mix 4) could be a support to provide energy fuels valuable for energy systems. From this point of view, it is evident to underline the energy content of the generated chars. So, a challenge for this experimental research was to discuss the way how type of waste marks changes on the high heating value of the pyrolysis chars. There were significant differences in the caloric value of the chars resulted from wood waste vs. light packaging wastes (LPW). These can be clearly observed in **Figure 5**.

In case of the cherry wood pyrolysis, the increase of process temperature leads to more energy valuable products. The maximum value of HHV (30,043 kJ/kg) was determined for the biochars obtained from pyrolysis at 600°C and marks these
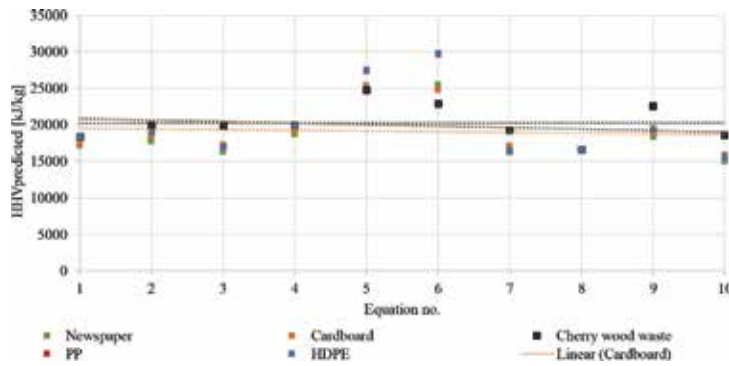
Figure 4.
Comparison of the HHV predicted values based on proximate analysis.
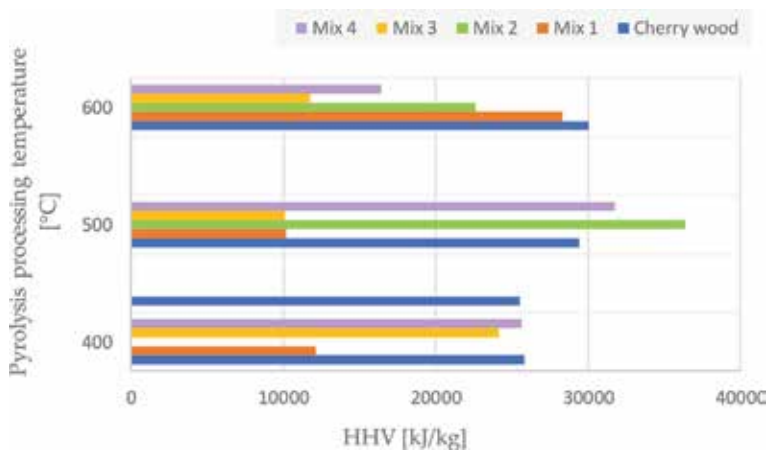

Figure 5.
HHV of chars and biochars depending on the pyrolysis process temperature.

as products comparable with a real coal (e.g., semi-anthracite coal—29,500 kJ/kg, bituminous coal—30,200 kJ/kg, anthracite coal—32,600 kJ/kg), while for plastic the maximum value of HHV was 31,378 kJ/kg, obtained at 500°C. If we consider the chars resulted from the LPW mixes, we can conclude there is not any linear increasing/decreasing of the HHV function of the pyrolysis process. Comparing the experimental determinations, it was revealed that for pyrolysis processing, 400°C produces chars with appropriated HHV as value in case of cherry wood, Mix 3 and Mix 4, 500°C in case of cherry biomass and Mix 4 and 600°C for case of cherry wood and Mix 1, respectively. It was already reported that heating value of lignocel-lulosic biomass type can greatly vary with climate and soil [48]. It is obviously that these factors strongly influence the HHV of wood and of the mixes analyzed in the present research. At lower process temperature of 400°C, for the plastic-based mix-tures (Mix 2, Mix 3, Mix 4) the agglutination rate of the char produced increases. At this process temperature, during the experiments, the recovery of the char was obstructed by its high agglutination level, due to plastic incomplete decomposition. In this case, at industrial level, in mixture with other wastes, the deposition of the melted char on the side of the reactor walls might overload it, limiting its recovery from the pyrolysis chamber. In conclusion, the minimal recommend pyrolysis process temperature in case of plastic waste presence should be 500°C.

The closest value of HHV registered for cherry wood and Mix 1 confirming that these two materials have a similar chemical structure and composition. Since all types of biomass have similar carbon mass fraction they have a comparable HHV, between 16,200 and 21,600 kJ/kg [49]. This rule could explain the same tendency for the biochars resulted from wood and Mix 1, respectively. Another aspect to be considered is the ash content that lead to variation of the HHV of the biochar. Experiments of Brewer [50] lead to biochars from corn stover, switchgrass, and hardwood treated by pyrolysis and gasification processes. The results showed that is an inversely proportional relation between biomass ash content and the heating potential of the biochar.

5. Conclusions

In this study analytical methods have been used for the HHV determination of different raw biomass, plastic waste and biomass-plastic waste mixtures and their by-products (biochar and char) resulted from the pyrolysis process. The main conclusion of the present research are listed:

- The comprehensive analysis of the scientific literature reveled that limited information is delivered in the regarding the energy potential of the chars and biochars produced by pyrolysis processing of the waste types analyzed in our research.

- The biomass and plastic wastes presented in this chapter store a significant quantity of energy that can be converted into different energy products depending on the correlation between feedstock properties, operational conditions of the available technology processes and the end use of the obtained products.

- The results generated by using the empirical equations mentioned in the present chapter demonstrates that their accuracy increases with the numbers of elements correlated with ultimate and proximate analysis considered in the prediction formulas.

- In the absence of instrumentation for HHV determination, empirical dedicated formulas can be used based on the ultimate and proximate analysis of the material. The experimental determination of the individual elements and substances is required for further application of the correlations. Twenty prediction formulas for HHV were analyzed. The elemental analysis represents the most essential parameter for determining the fuel heat of combustion. For a better accuracy of the results, the authors suggest the usage of at least three types of different dedicated correlations, considering the main fuel characteristic of the studied fuel.

- The experimental results reported that ash content is the main function in the energy content of biochars/chars. The latter is confirmed by the empirical results, where the heating value is strongly influenced by the ash content or volatile matter.

- Our experimental research revealed the following maximum values for the HHVs of the chars and biochars produced by pyrolysis processes: cherry wood 30,043 kJ/kg at 600°C, PCW 28,335 kJ/kg at 600°C, PSW 36,378 kJ/kg at 500°C, Mix 3 (PCW 90% & PSW 10%) 24,174 kJ/kg at 400°C and Mix 4 (PCW 67% & PSW 33%) 31,732 kJ/kg at 500°C.

Author details

Gabriela Ionescu and Cora Bulmău*
University Politehnica of Bucharest, Bucharest, Romania

*Address all correspondence to: cora4cora@gmail.com

IntechOpen

References

[1] https://www.windpowermonthly.com/article/1463710/denmark-moves-strengthen-renewable-energy-goals [Accessed: 2018-07-03]

[2] Antal MJ, Croiset E, Dai X, DeAlmeida C, Mok WSL, Norberg N, et al. High-yield biomass charcoal. Energy & Fuels. 1996;**10**(3):652-658. DOI: 10.1021/ef9501859

[3] Sun Y, Gao B, Yao Y, Fang J, Zhang M, Zhou Y, et al. Effects of feedstock type, production method, and pyrolysis temperature on biochar and hydrochar properties. Chemical Engineering Journal. 2014;**240**:574-578. DOI: 10.1016/J.CEJ.2013.10.081

[4] Demirbas A. Effects of temperature and particle size on bio-char yield from pyrolysis of agricultural residues. Journal of Analytical and Applied Pyrolysis. 2004;**72**(2):243-248. DOI: 10.1016/J.JAAP.2004.07.003

[5] Sarge SM, Hemminger W. Calorimetry Fundamentals, Instrumentation and Applications. John Wiley & Sons; 2014. p. 280. DOI: 10.1002/9783527649365

[6] Rodríguez AJA, Proupín CJ. Energy evaluation of materials by bomb calorimetry in thermal analysis. In: Fundamentals and Applications to Material Characterization. Universidade di Santiago; 2005. pp. 155-165

[7] U.S. Department of Energy. Annual Energy Review 1995, Energy Information Administration Report DOE/EIA-0384(95). Washington, D.C: U.S. DOE; 1996

[8] Organization for Economic Co-operation and Development, International Energy Agency. Energy Balances of OECD Countries, 1992-1993. Paris: OECD; 1995

[9] Subczynski WK, Markowska E, Sielewiesiuk J. Spin-label studies on phosphatidylcholine-polar carotenoid membranes: Effects of alkyl-chain length and unsaturation. Biochimica et Biophysica Acta. 1993;**1150**(2):173-181. DOI: 10.1016/0005-2736(93)90087-G

[10] James AM. Thermal and Energetic Studies of Cellular Biological Systems. Butterworth-Heinemann; 2016. 232 p. ISBN: 1483193551, 9781483193557

[11] Domalski ES, Jobe TL Jr, Milne TA. Thermodynamic Data for Biomass Conversion and Waste Incineration (No. SERI/SP-271-2839). Golden, CO (US)/Washington, DC (US): National Bureau of Standards/Solar Energy Research Inst.; 1986

[12] Sheng C, Azevedo JLT. Estimating the higher heating value of biomass fuels from basic analysis data. Biomass and Bioenergy. 2005;**28**(5):499-507. DOI: 10.1016/j.biombioe.2004.11.008

[13] Miranda R, Sosa C, Bustos D, Carrillo E, Rodríguez-Cantú M. Characterization of pyrolysis products obtained during the preparation of bio-oil and activated carbon. In: Lignocellulosic Precursors Used in the Synthesis of Activated Carbon-Characterization Techniques and Applications in the Wastewater Treatment. InTech; 2012. pp. 77-92

[14] Rada EC. Present and future of SRF. Waste Management. 2016;**47**(2):155-156. DOI: 10.1016/j.wasman.2015.11.035

[15] Channiwala SA, Parikh PP. A unified correlation for estimating HHV of solid, liquid and gaseous fuels. Fuel. 2002;**81**(8):1051-1063. DOI: 10.1016/S0016-2361(01)00131-4

[16] Tillman DA. Wood as an Energy Source. New York, NY, USA: Academic Press; 1978

[17] Vargas-Moreno JM, Callejón-Ferre AJ, Pérez-Alonso J, Velázquez-Martí B. A review of the mathematical models for predicting the heating value of biomass materials. Renewable and Sustainable Energy Reviews. 2012;**16**(5):3065-3083. DOI: 10.1016/j.rser.2012.02.054

[18] Demirbaş A. Calculation of higher heating values of biomass fuels. Fuel. 1997;**76**(5):431-434. DOI: 10.1016/S0016-2361(97)85520-2

[19] Yin CY. Prediction of higher heating values of biomass from proximate and ultimate analyses. Fuel. 2011;**90**(3):1128-1132. DOI: 10.1016/j.fuel.2010.11.031

[20] Dos Santos RG, Bordado JM. Design of simplified models for the estimation of higher heating value of refused derived fuels. Fuel. 2018;**212**:431-436. DOI: 10.1016/j.fuel.2017.10.062

[21] Han J, Yao X, Zhan Y, Oh SY, Kim LH, Kim HJ. A method for estimating higher heating value of biomass-plastic fuel. Journal of the Energy Institute. 2017;**90**(2):331-335. DOI: 10.1016/j.joei.2016.01.001

[22] Shi H, Mahinpey N, Aqsha A, Silbermann R. Characterization, thermochemical conversion studies, and heating value modeling of municipal solid waste. Waste Management. 2016;**48**:34-47. DOI: 10.1016/j.wasman.2015.09.036

[23] Özyuğuran A, Yaman S. Prediction of calorific value of biomass from proximate analysis. Energy Procedia. 2017;**107**:130-136. DOI: 10.1016/j.egypro.2016.12.149

[24] Kathiravale S, Yunus MNM, Sopian K, Samsuddin AH, Rahman RA. Modeling the heating value of municipal solid waste. Fuel. 2003;**82**(9):1119-1125. DOI: 10.1016/S0016-2361(03)00009-7

[25] Liu JI, Paode RD, Holsen TM. Modeling the energy content of municipal solid waste using multiple regression analysis. Journal of the Air & Waste Management Association. 1996;**46**(7):650-656. DOI: 10.1080/10473289.1996.10467499

[26] Wahid FRAA, Saleh S, Samad NAFA. Estimation of higher heating value of torrefied palm oil wastes from proximate analysis. Energy Procedia. 2017;**138**:307-312. DOI: 10.1016/j.egypro.2017.10.102

[27] Demirbaş A, Demirbaş AH. Estimating the calorific values of lignocellulosic fuels. Energy Exploration & Exploitation. 2004;**22**(2):135-143. DOI: 10.1080/00908319708908888

[28] Friedl A, Padouvas E, Rotter H, Varmuza K. Prediction of heating values of biomass fuel from elemental composition. Analytica Chimica Acta. 2005;**544**(1-2):191-198

[29] Khan MA, Abu-Ghararah ZH. New approach for estimating energy content of municipal solid waste. Journal of Environmental Engineering. 1991;**117**(3):376-380

[30] Yacio. Waste characteristics. In: Report submitted to the Ministry of Housing and Local Government, Malaysia. Kuala Lumpur: Ministry of Housing and Local Government; 2000

[31] Demirbaş A. Relationships between lignin contents and heating values of biomass. Energy Conversion and Management. 2001;**42**(2):183-188. DOI: 10.1016/S0196-8904(00)00050-9

[32] García R, Pizarro C, Lavín AG, Bueno JL. Spanish biofuels heating value estimation, Part II: Proximate analysis. Fuel. 2014;**117**:1139-1147. DOI: 10.1016/j.fuel.2013.08.049

[33] Cordero T, Marquez F, Rodriguez-Mirasol J, Rodriguez J. Predicting

heating values of lignocellulosics and carbonaceous materials from proximate analysis. Fuel. 2001;**80**:1567-1571. DOI: 10.1016/S0016-2361(01)00034-5

[34] Phichai K, Pragrobpondee P, Khumpart T, Hirunpraditkoon S. Prediction heating values of lignocellulosics from biomass characteristics. International Journal of Mining and Mineral Engineering. 2013;**7**:532-535. DOI: scholar.waset.org/1307-6892/16408

[35] Thipkhunthod P, Meeyoo V, Rangsunvigit P, Kitiyanan B, Siemanond K, Rirksomboon T. Predicting the heating value of sewage sludges in Thailand from proximate and ultimate analyses. Fuel. 2005;**84**:849-857. DOI: 10.1016/j.fuel.2005.01.003

[36] Soponpongpipat N, Sittikul D, Sae-Ueng U. Higher heating value prediction of torrefaction char produced from non-woody biomass. Frontiers in Energy. 2015;**9**(4):461-471. DOI: 10.1007/s11708-015-0377-3

[37] Kieseler S, Neubauer Y, Zobel N. Ultimate and proximate correlations for estimating the higher heating value of hydrothermal solids. Energy & Fuels. 2013;**27**:908-918. DOI: 10.1021/ef301752d

[38] Parikh J, Channiwala SA, Ghosal GK. A correlation for calculating HHV from proximate analysis of solid fuels. Fuel. 2005;**84**:487-494. DOI: 10.1016/j.fuel.2004.10.010

[39] Ionescu G, Marculescu C, Badea A. Alternative solutions for MSW to energy conversion. University Politehnica of Bucharest Scientific Bulletin. 2010;**73**:243-254. ISSN: 1454-234x

[40] Ionescu G, Rada EC, Ragazzi M, Dal Maschio R, Ischia M, Mărculescu C. Packaging waste thermal treatment and pyro-products characterization

for power conversion. In: Proceedings of the 4th International Conference on Engineering for Waste and Biomass Valorisation, WasteEng12, Porto, Portugal, 10-13 September 2012. France: Mines d''Albi; 2012. pp. 892-897

[41] BIOBIB a DataBase for Biofuels. https://www.vt.tuwien.ac.at/biobib [Accessed: 2018-05-22]

[42] Telmo C, Lousada J, Moreira N. Proximate analysis, backwards stepwise regression between gross calorific value, ultimate and chemical analysis of wood. Bioresource Technology. 2010;**101**(11):3808-3815. DOI: 10.1016/j.biortech.2010.01.021

[43] Gheorghe (Bulmău) C. Contributions concerning the biomass pyrolysis processes [thesis]. University Politehnica of Bucharest; 2009

[44] Ionescu G. Critical analysis of pyrolysis and gasification applied to waste fractions with growing energetic content [doctoral dissertation]. University of Trento; 2012

[45] Bulmău C, Mărculescu C, Badea A, Apostol T. Pyrolysis parameters influencing the bio-char generation from wooden biomass. University Politehnica of Bucharest Scientific Bulletin-Serie C: Electrical Engineering. 2010;**72**(1):29-38. ISSN: 1454-234x

[46] Gheorghe (Bulmău) C, Marculescu C, Badea A, Dincă C, Apostol T. Effect of pyrolysis conditions on bio-char production from biomass. In: Proceedings of the 3rd International Conference on Renewable Energy Sources, WSEAS. Tenerife, Canary Islands Spain: University of La Laguna; 2009. pp. 239-241

[47] Menikpura SNM, Basnayake BFA. New applications of 'Hess Law' and comparisons with models for determining calorific values of municipal solid wastes in the Sri

Lankan context. Renewable Energy. 2009;**34**(6):1587-1594. DOI: 10.1016/j. renene.2008.11.005

[48] Cai J, He Y, Yu X, Banks SW, Yang Y, Zhang X, et al. Review of physicochemical properties and analytical characterization of lignocellulosic biomass. Renewable and Sustainable Energy Reviews. 2017;**76**:309-322. DOI: 10.1016/j. rser.2017.03.072

[49] Dufour A. Thermochemical Conversion of Biomass for the Production of Energy and Chemicals. John Wiley & Sons; 2016. DOI: 10.1002/9781119137696

[50] Brewer CE. Biochar characterization and engineering [Graduate theses and dissertations]. Iowa State University; 2012

Edited by Peter Kusch

Analytical pyrolysis deals with the structural identification and quantitation of pyrolysis products with the ultimate aim of establishing the identity of the original material and the mechanisms of its thermal decomposition. The pyrolytic process is carried out in a pyrolyzer interfaced with analytical instrumentation such as gas chromatography (GC), mass spectrometry (MS), gas chromatography coupled with mass spectrometry (GC/MS), or with Fourier-transform infrared spectroscopy (GC/FTIR). By measurement and identification of pyrolysis products, the molecular composition of the original sample can often be reconstructed.This book is the outcome of contributions by experts in the field of pyrolysis and includes applications of the analytical pyrolysis-GC/MS to characterize the structure of synthetic organic polymers and lignocellulosic materials as well as cellulosic pulps and isolated lignins, solid wood, waste particle board, and bio-oil. The thermal degradation of cellulose and biomass is examined by scanning electron micrography, FTIR spectroscopy, thermogravimetry (TG), differential thermal analysis, and TG/MS. The calorimetric determination of high heating values of different raw biomass, plastic waste, and biomass/plastic waste mixtures and their by-products resulting from pyrolysis is described.

IntechOpen